

# Transverse spin effects in hard semi-inclusive collisions

M. Anselmino<sup>1</sup>, A. Mukherjee<sup>2</sup> and A. Vossen<sup>3,4</sup>

<sup>1</sup>Dipartimento di Fisica, Università di Torino and INFN Sezione di Torino,  
Via P. Giuria 1, I-10125 Torino, Italy

<sup>2</sup>Department of Physics, Indian Institute of Technology Bombay,  
Mumbai-400076, India

<sup>3</sup>Duke University, Durham, North Carolina 27708, USA

<sup>4</sup>Jefferson Lab, 12000 Jefferson Avenue, Newport News, VA 23606, USA

May 22, 2020

## Abstract

The nucleons (protons and neutrons) are by far the most abundant form of matter in our visible Universe; they are composite particles made of quarks and gluons, the fundamental quanta of Quantum Chromo Dynamics (QCD). The usual interpretation of the nucleon dynamics in high energy interactions is often limited to a simple one-dimensional picture of a fast moving nucleon as a collection of co-linearly moving quarks and gluons (partons), interacting accordingly to perturbative QCD rules. However, massive experimental evidence shows that, in particular when transverse spin dependent observables are involved, such a simple picture is not adequate. The intrinsic transverse motion of partons has to be taken into account; this opens the way to a new, truly 3-dimensional (3D) study of the nucleon structure. A review of the main experimental data, their interpretation and understanding in terms of new transverse momentum dependent partonic distributions, and the progress in building a 3D imaging of the nucleon is presented.

## Contents

<b>1</b>	<b>Introduction</b>	<b>2</b>
<b>2</b>	<b>Transverse spin effects and the parton transverse motion</b>	<b>4</b>
2.1	<i>Spin effects in SIDIS</i>	5
2.2	<i>Spin effects in hard <math>NN</math> collisions</i>	7
2.2.1	Transverse single spin asymmetries in $pN \rightarrow hX$ processes	11
2.2.2	Transverse single spin asymmetries in $\gamma^*, W/Z, \gamma$ production	11
2.2.3	Transverse single spin asymmetries in di-hadron production	15
2.2.4	Transverse single spin asymmetries of jets and hadrons in jets	15
2.3	<i>Spin effects in <math>e^+e^- \rightarrow h_1 h_2 X</math> and <math>e^+e^- \rightarrow \Lambda^\dagger X</math> processes</i>	18
<b>3</b>	<b>Phenomenology of spin phenomena</b>	<b>20</b>
3.1	<i>Transverse Momentum Dependent Parton Distributions (TMD-PDFs) and Fragmentation Functions (TMD-FFs)</i>	21
3.1.1	Quark TMD-PDFs	21
3.1.2	Gluon TMD-PDFs	24

3.1.3	TMD-FFs . . . . .	25
3.2	<i>How to interpret spin data in SIDIS</i> . . . . .	26
3.3	<i>How to interpret spin data in hard <math>NN</math> collisions</i> . . . . .	28
3.3.1	Asymmetries in $p^\uparrow N \rightarrow h X$ processes . . . . .	29
3.3.2	Asymmetries in $\gamma^*$ , $W/Z$ , $\gamma$ production . . . . .	31
3.3.3	Asymmetries in di-hadron production . . . . .	33
3.3.4	Asymmetries of jets and hadrons in jets . . . . .	34
3.4	<i>How to interpret azimuthal correlations of back-to-back hadrons and the <math>\Lambda</math> polarisation in semi-inclusive <math>e^+e^-</math> annihilations</i> . . . . .	35
3.5	<i>The Collins fragmentation function</i> . . . . .	37
<b>4</b>	<b>From data to the 3-dimensional imaging of the nucleon</b>	<b>38</b>
4.1	<i>The unpolarised TMD-PDFs</i> . . . . .	38
4.2	<i>The Sivers function</i> . . . . .	41
4.3	<i>The transversity distribution</i> . . . . .	43
<b>5</b>	<b>The ultimate goal: the nucleon Wigner functions</b>	<b>46</b>
5.1	<i>Introduction to Wigner distributions for quarks and gluons</i> . . . . .	46
5.2	<i>Wigner distributions and Generalized Transverse Momentum Dependent parton distribution functions (GTMDs)</i> . . . . .	48
5.3	<i>Definitions</i> . . . . .	50
5.3.1	Unpolarized target and different quark polarizations . . . . .	50
5.3.2	Longitudinally polarized target and different quark polarizations . . . . .	50
5.3.3	Transversely polarized target and different quark polarizations . . . . .	50
5.3.4	Properties: connection to GPDs and TMDs and orbital angular momentum . . . . .	51
5.4	<i>Model Calculations</i> . . . . .	53
5.5	<i>Experiments to access the Wigner Distributions and GTMDs</i> . . . . .	54
<b>6</b>	<b>Conclusions</b>	<b>54</b>

# 1 Introduction

The nucleons – protons and neutrons – form the almost totality of the visible matter in the Universe. We know that they are composite objects, made of quarks and gluons (collectively denoted as partons), which interact according to the strong interactions rules of Quantum Chromo Dynamics (QCD), a fundamental relativistic quantum field theory. However, the full partonic description of the nucleons is still a very mysterious and fascinating open issue. Because of this, the understanding of the internal structure of the nucleons, both in momentum and in coordinate space, is the ultimate goal of many ongoing or planned experiments and the focus of theoretical activities worldwide.

The experiments are mainly high energy scatterings of point-like leptons off protons and neutrons, in which the lepton scatters off a single parton, or inelastic collisions between nucleons, like Drell-Yan processes in which a quark and an antiquark annihilate into a pair of leptons. Also the production of a single hadron or two hadrons in the high energy collision of two nucleons can be related to QCD elementary interactions among partons. The outcome of these experiments, when correctly interpreted, gives information on the internal nucleon composition. The theoretical scheme in which these processes are studied is QCD, both in its perturbative and non-perturbative aspects.

The cross sections for the above processes are written, according to a factorisation theorem, as the convolution of elementary partonic interactions - known from perturbative calculations in the Standard Model of strong and electro-weak interactions - with Partonic Distribution and Fragmentation Functions

(PDFs and FFs). These are not calculable using perturbative methods, but their evolution with the large-scale  $Q^2$  of the process can be computed in QCD. By measuring the cross sections one learns about the PDFs and FFs at a certain scale, and can evolve them to other values of  $Q^2$ , thus achieving predicting power. Independent information on the FFs can be obtained from other processes, like the annihilation of  $e^+$  and  $e^-$  into pairs of hadrons.

For a long time, the PDFs and FFs were considered as collinear splitting processes, which corresponds to a 1-dimensional imaging of a fast nucleon as a simple set of co-linearly moving partons. Recently, it has become more and more clear that the understanding of many experimental results - in particular those involving spin degrees of freedom - must take into account the transverse degrees of freedom, that is the intrinsic motion of quarks and gluons inside the nucleons. This opens the way to the full study of the 3-dimensional (3D) structure of the nucleons.

The complete 3D information on the partonic momentum distributions has been encoded in Transverse Momentum Dependent Partonic Distribution Functions (TMD-PDFs). In experimental observables, they are often combined with Transverse Momentum Dependent Fragmentation Functions (TMD-FFs). Apart from perturbative QCD corrections, when integrated over transverse momentum the TMDs reduce to the collinear PDFs and FFs. A full knowledge of the partonic distributions must also include their dependence on hadronic and partonic spin, related to subtle spin-orbit correlations of the strong force.

At leading order in  $1/Q$  there are eight TMD-PDFs and, for spinless final hadrons, 2 TMD-FFs. Beside the TMD-PDFs and TMD-FFs, new objects - the Generalised Partonic Distributions, GPDs - offer information on the parton distribution in coordinate space. There are also eight leading order nucleon GPDs which give new information, like the correlation between the transverse position and the longitudinal momentum of partons, providing a 3D mapping of the nucleon. They are also related to the orbital momentum contribution of partons to the nucleon spin. The GPDs are off-diagonal matrix elements of quark and gluon operators between nucleon states and can be measured in hard exclusive processes such as the lepto-production of a photon or of a meson or the photo-production of a lepton pair. Like for the TMDs, the measured quantities are convolutions of GPDs with hard scattering amplitudes. In the diagonal limit the GPDs coincide with the PDFs.

Both the GPDs and the TMD-PDFs are particular limits of a vast class of functions, the so-called Wigner functions (or Generalised TMDs, GTMDs), which are the quantum mechanical version of the classical phase-space distributions. The really ultimate theoretical goal is that of reconstructing the nucleon Wigner functions; attempts to do that can be done, at the moment, by modelling the light-front nucleon wave functions.

In the last 10-15 years the first measurements of azimuthal asymmetries in Semi Inclusive Deep Inelastic Scattering (SIDIS, lepton + nucleon  $\rightarrow$  lepton + hadron + X,  $\ell N \rightarrow \ell h X$ ) processes by the HERMES (DESY, Germany), COMPASS (CERN) and Jefferson Laboratory (JLab, USA) Collaborations, together with the related theoretical analyses, have definitely revealed the role of the TMDs and allowed the first extraction of some of them. Similarly for the GPDs. Recent results by the Belle (KEK, Japan), BaBar (SLAC, USA) and BES-III (BEPC, China) Collaborations in  $e^+e^- \rightarrow h_1 h_2 X$  processes have definitely shown the role of TMD-FFs. Important data are expected soon from the Drell-Yan (D-Y) processes at COMPASS and possibly RHIC (BNL, USA), and from the 12 GeV upgrade of JLab. Great expectations are linked to the planned future Electron Ion Collider (EIC) in USA and the LHCb (polarised) fixed target experiment at CERN.

We have then reached a stage in which one should combine phenomenological studies of TMDs and GPDs with theoretical models of proton and neutron wave functions. It is the only way which may lead to a true 3D knowledge of the nucleon structure. The available data give the necessary (although not yet complete) information in modelling the 3D structure, while the soon expected new data will allow improvements of the models and tests of their predictions.

In this review paper we focus on TMDs and inclusive processes, that is on the 3D structure of

nucleons in momentum space. The plan of the paper is the following. In Section 2 we summarise the experimental results which show and lead to the necessity of taking into account the transverse motion of partons inside the nucleons and the transverse momentum of hadrons in a parton hadronisation process. These are typically, but not exclusively, polarised interactions. We consider separately three kinds of processes: SIDIS,  $\ell N \rightarrow \ell h X$ ; hard nucleon-nucleon interactions,  $NN \rightarrow \ell^+ \ell^- X$ ,  $NN \rightarrow h_1 h_2 X$  and  $NN \rightarrow h_1 X$ ; hadron production in  $e^+e^-$  annihilations,  $e^+e^- \rightarrow h_1 h_2 X$  and  $e^+e^- \rightarrow \Lambda^\dagger X$ . Although the formal definition and discussion of TMDs will be presented in Section 3, some TMDs will already be mentioned in Section 2, when illustrating the experimental evidence for transverse motion. In particular, the Sivers TMD-PDF, that is the distribution of unpolarised partons inside a transversely polarised proton, and the Collins TMD-FF, that is the transverse motion of a hadron within a jet generated by a transversely polarised quark.

In Section 3 we present and discuss the TMD phenomenology; that is, after introducing the TMD-PDFs and the TMD-FFs, we show how to relate them to physical observables, and how to extract TMD information from data, which is not a simple procedure. This is mainly and explicitly done at leading order, again separately for the three kinds of processes described above. Some comments and full references to QCD corrections and TMD evolution are also given.

In Section 4 we summarise our actual knowledge on some TMDs and their relevance towards a 3D imaging of the nucleon. Some specific issues, like the orbital motion of quarks inside a nucleon and the universality of the TMDs, will only be mentioned. The last part of this Section is amply devoted to the Wigner function, its importance and the ongoing attempts, mainly theoretical, to study it.

In the Conclusions we summarise the content and the purpose of the paper, indicating open problems and possible further developments. The importance of new results from the running COMPASS and RHIC D-Y measurements, and from the operating 12 GeV JLab upgrade is discussed. Crucial improvements expected from the planned EIC facility are emphasised.

Several excellent review papers related and complementary to the issues covered in this paper can be found in the literature [1, 2, 3, 4, 5, 6]. A collections of topical contributions dedicated to the 3-dimensional nucleon structure can be found in Ref. [7], while the physics case of the Electron Ion Collider, a planned future machine devoted to the exploration of the nucleon structure, is discussed in Ref. [8]. This paper is focused on the phenomenological features of transverse spin physics and most technical aspects and subtleties of QCD, like TMD evolution, will not be discussed: a complete and fundamental introduction to a correct QCD description of high energy processes can be found in Ref. [9].

## 2 Transverse spin effects and the parton transverse motion

In this Section we recall the experimental data which cannot be understood in the usual collinear QCD parton model scheme; they are mainly, but not uniquely, spin data. As usual, polarised experiments test a theory at a much deeper level than unpolarised quantities; in particular, Single Spin Asymmetries (SSAs) originate from subtle Quantum Mechanical interference effects, which do not affect the unpolarised observables. In addition, if we consider parity conserving strong and electromagnetic interactions, only transverse SSAs are allowed by parity invariance; thus, they are the ideal probe to explore the transverse (with respect to the direction of motion) internal structure of hadrons.

We consider high energy inclusive processes, which are usually described in terms of interactions among quarks and gluons. The relation between the measured hadronic quantities, the elementary QCD or QED partonic interactions, and the nucleon structure we wish to explore, is encoded in the factorisation scheme, which we shall use and on which we shall comment in the next Section. We simply discuss, in this Section, the available data for the three kinds of processes mentioned in the Introduction: SIDIS, hard  $NN$  collisions and  $e^+e^-$  annihilations.

## 2.1 Spin effects in SIDIS

Traditionally, since the end of the 60s, the exploration of the nucleon structure has been successfully performed via Deep Inelastic Scattering (DIS,  $\ell N \rightarrow \ell X$ ) in which a point-like lepton (typically electron, positron or muon) is scattered at high energy and large angle off a nucleon. The basic interpretation is that the lepton scatters off a quark, via one virtual photon exchange, and the measurement of the final lepton energy and direction allows to learn about the longitudinal momentum fraction ( $x$ ) of the nucleon carried by the quark. The QCD corrections induce a dependence on the 4-momentum transfer squared of the lepton (the 4-momentum squared of the virtual photon,  $q^2 = -Q^2$ ) which can be computed. Thus, one learns about the Parton Distribution Functions (PDFs),  $f_q(x, Q^2)$ , that is the number density of quarks  $q$ , carrying a fraction  $x$  of the parent nucleon momentum, as seen at a distance  $\sim 1/Q$ . The correct prediction of the  $Q^2$  dependence is one of the triumphs of perturbative QCD.

However, despite its great success, this study gives a one-dimensional (1D) picture of the nucleon, limited to the longitudinal degrees of freedom. This might be sufficient in many high energy experiments, where the transverse motion of partons inside the nucleon is negligible compared to the fast longitudinal motion; indeed, many high energy cross sections are correctly predicted in several experiments. When introducing spin degrees of freedom this 1D picture allows to obtain information on the parton helicity distributions, that is the difference between the density number of partons with the same and opposite helicity as the parent proton: again, only longitudinal features of the nucleon. The transversity distribution, that is the difference between the density number of partons with *transverse* spin parallel and antiparallel to the *transverse* spin of the parent proton, cannot be accessed in DIS. As it will be shown in the next Section, information on the transversity distributions can only be obtained by considering TMD effects.

In general, transverse SSAs in hadronic processes cannot be understood in the simple collinear partonic picture of the nucleon. This is related to the fact that QCD or QED massless and parity conserving partonic interactions, do not allow transverse SSAs and a collinear fragmentation process cannot build up a transverse polarisation. Although PDFs have provided much information to shape our physical picture of the nucleon, they cannot answer key questions for understanding the structure of the nucleon, namely how its spin is apportioned between the spin of its constituents and their orbital angular momentum. We definitely need a 3D imaging of the nucleon, if we want to understand its structure and to explain many experimental data.

So far, SIDIS processes ( $\ell N \rightarrow \ell h X$ ) are the main probe exploited to explore the 3D structure of the nucleon. In such processes, differently from the DIS case in which one only detects the final lepton, the point-like lepton scatters off a quark, which, subsequently, fragments into an observed hadron. By looking at the hadron distribution one can get further information on the quark which generated it, its intrinsic motion and possible correlations between its spin, its motion and the spin of the nucleon.

The kinematics of a typical SIDIS process, in the virtual photon-nucleon center of mass frame is shown in Fig. 1, where the relevant kinematical variables are defined. It is already clear from this figure that, in the simple leading order collinear parton model in which the  $\gamma^*$  hits a quark, which bounces back and fragments co-linearly, one could not have a final hadron with a transverse momentum  $\mathbf{P}_T$ . This could be generated by higher order QCD interactions, but, at leading order in the strong interaction coupling, a transverse momentum of the final hadron must be related to the intrinsic motion of the quark in the nucleon and the transverse momentum of the hadron  $h$  with respect to the momentum of the fragmenting quark.

The most general expression for the SIDIS cross section, with unpolarised leptons and fully transversely polarised nucleons, assuming a single virtual photon exchange and neglecting masses, can be

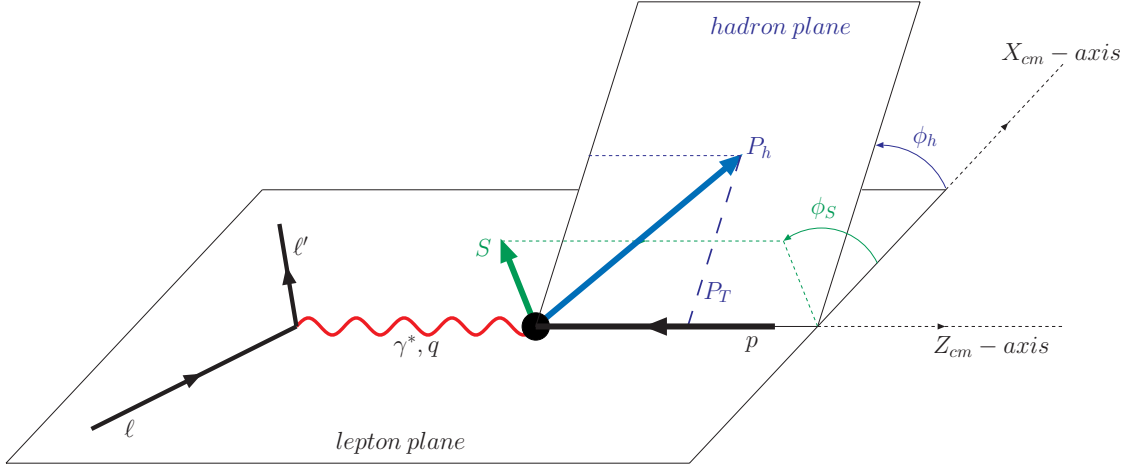


Figure 1: Kinematics and definition of the variables of SIDIS processes in the  $\gamma^* - N$  c.m. frame.

written as [10, 11, 12, 13, 14, 15, 16]:

$$\frac{d\sigma^{\ell+p(S_T)\rightarrow\ell'hX}}{dx_B dQ^2 dz_h d^2\mathbf{P}_T d\phi_S} = \frac{2\alpha^2}{Q^4} \times \quad (1)$$

$$\left\{ \frac{1+(1-y)^2}{2} F_{UU} + (2-y)\sqrt{1-y} \cos\phi_h F_{UU}^{\cos\phi_h} + (1-y) \cos 2\phi_h F_{UU}^{\cos 2\phi_h} \right.$$

$$+ \left[ \frac{1+(1-y)^2}{2} \sin(\phi_h - \phi_S) F_{UT}^{\sin(\phi_h - \phi_S)} + (1-y) \sin(\phi_h + \phi_S) F_{UT}^{\sin(\phi_h + \phi_S)} \right.$$

$$\left. \left. + (1-y) \sin(3\phi_h - \phi_S) F_{UT}^{\sin(3\phi_h - \phi_S)} + (2-y) \sqrt{1-y} \left( \sin\phi_S F_{UT}^{\sin\phi_S} + \sin(2\phi_h - \phi_S) F_{UT}^{\sin(2\phi_h - \phi_S)} \right) \right] \right\},$$

where we have used the usual SIDIS variables:

$$s = (\ell + p)^2 \quad Q^2 = -q^2 = -(\ell - \ell')^2 \quad x_B = \frac{Q^2}{2p \cdot q} \quad z_h = \frac{p \cdot P_h}{p \cdot q} \quad y = \frac{p \cdot q}{p \cdot \ell}. \quad (2)$$

The  $F_{UU}$  and the  $F_{UT}$  are structure functions which depend on the kinematical variables (2): the first index denotes the lepton polarisation state ( $U =$  unpolarised) while the second one denotes the nucleon polarisation state (either  $U =$  unpolarised or  $T =$  transversely polarised). The full structure of the SIDIS cross section, with all lepton and nucleon polarisations, can be found in Refs. [15, 16]; Eq. (1) is the main source for all phenomenological SIDIS studies we discuss here.

Obviously, the azimuthal modulations of the cross section require the detection of the transverse momentum  $\mathbf{P}_T$  of the final hadron; by integration over  $\phi_h$  all terms, except that containing  $F_{UU}$ , would vanish. Notice also that the above SIDIS cross section can originate several transverse SSAs: if one takes differences of cross sections with opposite nucleon transverse spins,  $d\sigma(\phi_S) - d\sigma(\pi + \phi_S)$ , many terms in Eq. (1) survive.

These asymmetries are often expressed through their azimuthal moments,

$$A_{UT}^{W(\phi_h, \phi_S)} = 2 \frac{\int d\phi_h d\phi_S [d\sigma^\uparrow - d\sigma^\downarrow] W(\phi_h, \phi_S)}{\int d\phi_h d\phi_S [d\sigma^\uparrow + d\sigma^\downarrow]}, \quad (3)$$

where  $W(\phi_h, \phi_S)$  is the appropriate azimuthal weight function required in order to isolate the specific contribution of interest and  $d\sigma^{\uparrow, \downarrow}$  is the differential cross section of Eq. (1) with  $S_T = \uparrow, \downarrow$  denoting, respectively, a transverse polarisation with azimuthal angle  $\phi_S$  and  $\phi_S + \pi$ .

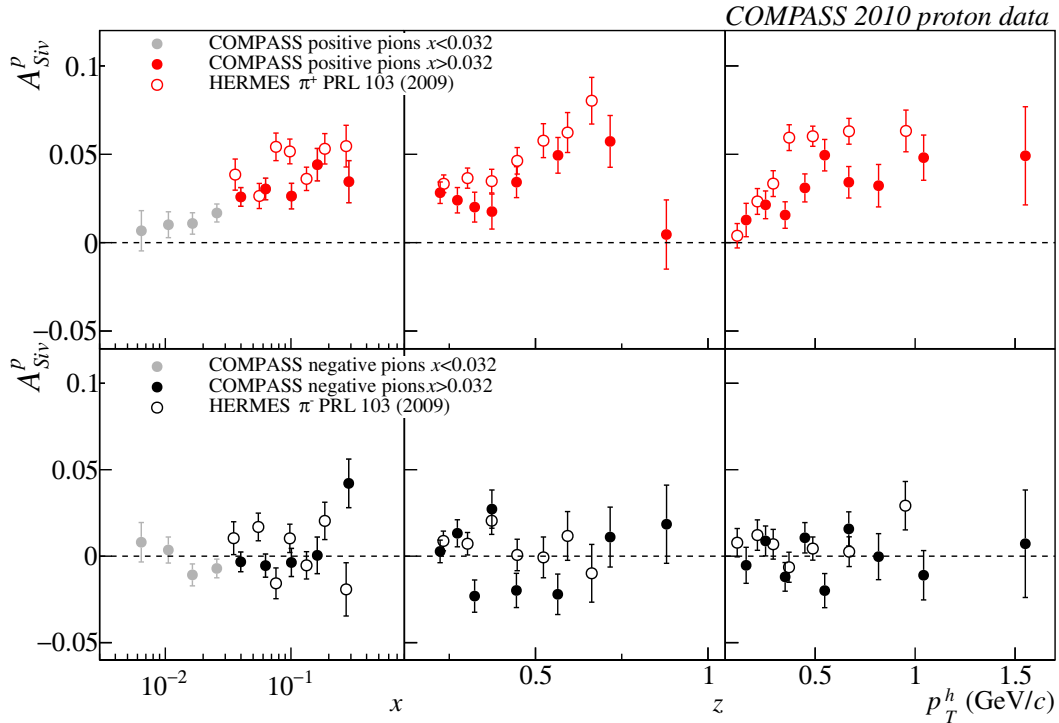


Figure 2: The weighted transverse SSA  $A_{UT}^{\sin(\phi_h - \phi_S)}$ , as measured by the COMPASS and Hermes Collaborations is shown as a function of its kinematical variables (notice that  $x = x_B$ ,  $z = z_h$  and  $p_T^h = P_T$ ). This asymmetry is also denoted as  $A_{Siv}^p$ , because it will be interpreted as related to a TMD-PDF introduced by Sivers. Figure reprinted from Ref. [6] with kind permission of Società Italiana di Fisica, ©Società Italiana di Fisica 2019.

For example, taking  $W(\phi_h, \phi_S) = \sin(\phi_h - \phi_S)$ , one obtains:

$$A_{UT}^{\sin(\phi_h - \phi_S)} \equiv A_{Siv}^p = \frac{F_{UT}^{\sin(\phi_h - \phi_S)}}{F_{UU}}, \quad (4)$$

while with  $W(\phi_h, \phi_S) = \sin(\phi_h + \phi_S)$  one has

$$A_{UT}^{\sin(\phi_h + \phi_S)} \equiv A_{Col}^p = \frac{2(1-y) F_{UT}^{\sin(\phi_h + \phi_S)}}{[1 + (1-y)^2] F_{UU}}. \quad (5)$$

These SSAs have been observed by several experimental Collaborations: HERMES at HERA [17, 18], COMPASS at CERN [19, 20, 21, 22], HALL A at JLab [23, 24]. Some results from COMPASS and HERMES are shown in Figs. 2 and 3.

In Section 3.2 we will interpret the SIDIS cross section, at least in limited kinematical regions, in terms of elementary lepton-quark interactions; at leading order in such interactions no SSAs is allowed and the spin effects must be originated by intrinsic non perturbative properties of the parton distributions and fragmentations, which will be encoded in the TMDs. Also the  $P_T$  distribution of the unpolarised cross section will be related to TMDs.

## 2.2 Spin effects in hard $NN$ collisions

The observation of transverse single spin asymmetries in hard  $NN$  collisions played a pioneering role in the field of transverse spin physics. Of special importance were the observation of a significant

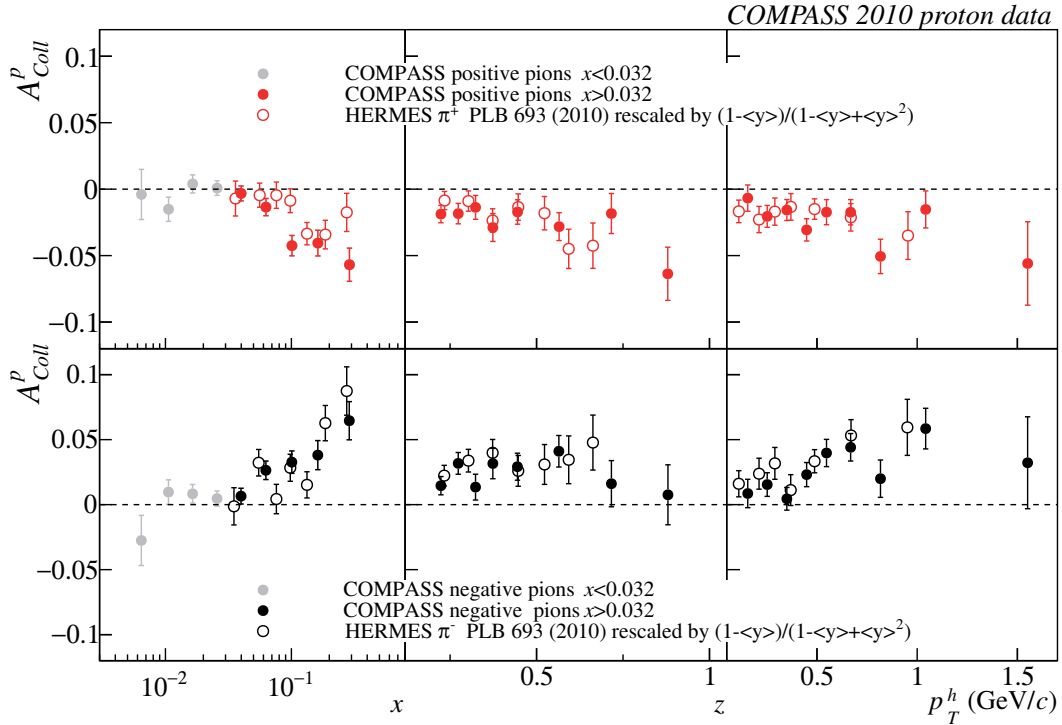


Figure 3: The weighted transverse SSA  $A_{UT}^{\sin(\phi_h + \phi_S)}$ , as measured by the COMPASS and Hermes Collaborations is shown as a function of its kinematical variables (notice that  $x = x_B$ ,  $z = z_h$  and  $p_T^h = P_T$ ). This asymmetry is also denoted as  $A_{Coll}^p$ , because it will be interpreted as related to a TMD-FF introduced by Collins. Figure reprinted from Ref. [6] with kind permission of Società Italiana di Fisica, ©Società Italiana di Fisica 2019.

transverse polarisation of hyperons produced in the collision of a 300 GeV unpolarised proton beam with a Berillium target at Fermilab [25, 26], as well as the observation of left-right asymmetries,  $A_N$ , for pions produced in the forward direction of a polarised proton beam impinging on an unpolarised nuclear or proton target, first at the ZGS at ANL [27, 28] and later at the AGS at BNL [29] and at the E704 experiment at Fermilab [30, 31], with beam energies ranging between 6 and 200 GeV. As noted in the introduction, these results were in contradiction to the expectation that transverse spin effects are suppressed at high scales [32] and therefore gave the first experimental hint of their importance in hard collisions. It can be argued that these early experiments did not reach high enough in the relevant momentum scale; however, recent data by the STAR experiment at the Relativistic Heavy Ion Collider (RHIC) shows that  $A_N$  persists up to transverse momenta  $p_T$  close to 10 GeV [33].

These results provided first tantalising evidence for the importance of transverse spin and intrinsic transverse momenta of partons. In particular, the first attempt to explain the surprising left-right asymmetries observed in  $p^\uparrow p \rightarrow \pi X$  processes prompted the first introduction of a TMD parton distribution (the Sivers distribution [34]), in the framework of a simple generalisation of the collinear factorisation scheme, subsequently denoted as the Generalised Parton Model (GPM). However, all these spin results in  $pp$  single inclusive interactions are difficult to interpret in a partonic picture. As will be discussed later in Sec. 3.3, since they are one-scale processes, a collinear twist-3 picture is applicable. The latter has non-trivial connections to the partonic TMD picture, *e.g.* via the Wandzura-Wilczek relations [35]; however, it includes additional degrees of freedom parameterised by non-perturbative functions that would have to be measured as well [36]. A significant recent development has been the experimental

process	framework	hard scale	soft scale
$pp \rightarrow h X$	twist-3	$p_{T,h}$	-
$pp \rightarrow h X$	TMD, GPM	$p_{T,h}$	-
$pp \rightarrow h_1 h_2 X$	collinear twist-2	$p_{T,(h_1+h_2)}$	-
$pp \rightarrow (jet + h) X$	TMD	$p_{T,jet}$	$k_{\perp h}$
$pp \rightarrow \ell \ell' X$	TMD	$M_{\ell-\ell'}$	$p_{T\gamma^*}$
$pp \rightarrow W/Z^0 X$	TMD	$M_{W/Z^0}$	$p_{T,W/Z^0}$
$pp \rightarrow \gamma X$	twist-3	$p_{T,\gamma}$	-

Table 1: List of different processes sensitive to TMDs in hadronic collisions. The table shows the relevant hard scale (for the TMD factorisation and the twist-3 framework) and the soft scale (TMD framework only). The di-hadron production process is an outlier, since it can be described in a collinear, twist-2 framework due to the additional degrees of freedom in the final state. The TMD framework for  $pp \rightarrow h X$  assumes the validity of the GPM. Symbols for the hard scales denote the hadron ( $p_{T,h}$ ), hadron-pair ( $p_{T,(h_1+h_2)}$ ), jet ( $p_{T,jet}$ ) and photon  $p_{T,\gamma}$  transverse momenta as well as the masses of the di-lepton system in D-Y ( $M_{\ell-\ell'}$ ) and the vector bosons in  $W/Z$  production. Soft scales are given by the hadron transverse momentum within a jet,  $k_{\perp h}$ , for hadron in jet measurements and by the transverse momenta of the virtual photon and vector boson in D-Y and  $W/Z^0$  production respectively. These quantities will be defined in more details when discussing the single processes in the following Sections.

and theoretical effort put into observables where TMDs can be accessed directly such as di-hadron final states and two scale processes, like the production of hadrons in jets and the  $W/Z$  production [37, 38, 39].

To give an overview of the observables characterising the hadronic collisions discussed here, Table 1 shows, for each process, the applicable framework and the large and small observable scales. The large scale is necessary for the factorisation of the hard scattering from the non-perturbative contributions to the cross section ( $\gg M_p \simeq 1$  GeV), whereas the small scale provides sensitivity to the non-perturbative partonic structure and should therefore be of the order of the intrinsic transverse momentum in the nucleon ( $\lesssim 1$  GeV). Di-hadron correlations are a somewhat special case, since they can be used within a collinear framework. The TMD approach for one scale  $pp \rightarrow h X$  processes, assumes the validity of a Generalised Parton Model.

Richer final states, depending on several variables, that would allow a more direct access to partonic dynamics, as in SIDIS processes, were not possible at early  $NN$  experiments due to limitations in energy, luminosity as well as detector capabilities. However, at RHIC, where longitudinal and transversely polarised protons can be collided with other protons or heavier nuclei, effects related to parton distribution functions can be accessed in two-scale processes at leading order and leading twist.

Before exploring these cases in more detail, we give a short overview of the advantages of studying the nucleon structure in  $NN$  collisions in addition to SIDIS. It should be noted that in the majority of cases discussed here both nuclei in the reactions are protons. This is natural, since this review is mainly concerned with the partonic structure of protons and for heavier nuclei additional nuclear effects would enter, which are not always well known. Furthermore, data on polarised nuclei beyond protons is quite rare as is data on heavier nuclei at center-of-mass energies beyond those within reach of fixed target experiments.

In hadronic collisions, there is no point-like probe; instead, at hard enough scales, the constituents of two composite particles scatter off each other. This inherently convolutes the structures of both particles into the physical observables as will be further detailed in Sec. 3.3. In particular, it is challenging to determine the kinematics of the partonic scattering. If the transverse energy in the event is sufficient, jets can be used as an approximation of the outgoing parton [40], allowing the calculation of the kinematics of the underlying  $2 \rightarrow 2$  partonic scattering in the Born approximation, leading to the expression in

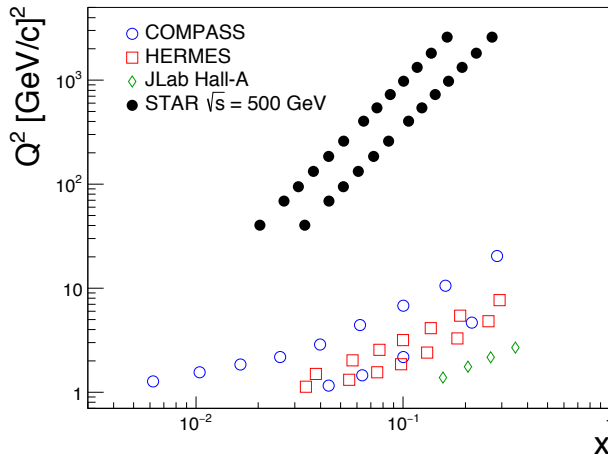


Figure 4:  $x - Q^2$  coverage of the STAR Collaboration measuring the Collins asymmetry for the production of hadrons in jets, compared with the Collins asymmetry measurement in SIDIS experiments. Figure reprinted from Ref. [43] and available under a Creative Commons Attribution 4.0 International.

Eq. (14) further below. Thus,  $NN$  data is complementary to SIDIS data and is crucial to complete our understanding of the proton structure.

Differently from SIDIS processes, in hadronic collisions such as  $pp$ , gluons can be accessed at leading-order, since the probe is most often a color charged object as well. The presence of a color-charged probe and the associated difference in color flow allows to check the process dependence of interactions. An important examples for this is the predicted sign-change of transverse single spin asymmetries in SIDIS compared to D-Y measurements [41] (see Section 4.2). This is an example of modified universality, where the modification is rather straightforward. Adding even more color-charges in the final state allows the existence of “entangled” gluon lines which is predicted to further complicate the process dependence [42]. However, it can be argued that a theoretical and experimental investigation of these effects is important for our full understanding of QCD.

While in SIDIS the coupling strength of the leptonic probe is given by  $e_q^2$ , where  $e_q$  is the charge of the struck quark (in units of the proton charge), in contrast, in hadronic collisions the coupling strength is the same for all partons. Therefore complementary information on the flavour structure of the proton can be extracted. This is possible in SIDIS as well using effective neutron targets, but it requires additional running, *e.g.* with a deuterium or  $^3\text{He}$  target. Nuclear effect in these targets can add complexity to the analysis.

The last point we want to consider here is the extended kinematic coverage of hadronic collisions. Till the arrival of the EIC, polarised SIDIS experiments will be confined to a rather limited range in  $Q^2$  due to their fixed target kinematics. In comparison, measurements at RHIC can reach values of  $Q^2$  that are more than two orders of magnitude higher, as shown in Fig. 4.

RHIC is the first and only polarised  $pp$  collider and naturally plays a prominent role in the study of transverse spin effects in hard  $NN$  collisions. Even though we focus here on the RHIC results, it should be mentioned that measurements of interest for the TMD partonic structure of the nucleon are also conducted at other  $NN$  machines, like the LHC. In these experiments there is obviously no access to observables that depend on polarisation in the initial state; however, measurements can be done that are sensitive *e.g.* to the intrinsic transverse momentum of partons in the nucleon by studying the  $p_T$  spectrum of  $W/Z$  bosons. For an overview, see Ref. [44].

Analogously to the SIDIS case, transverse spin and momentum dependent observables express them-

selves, given an appropriate reference system, in the dependence of the cross section on certain azimuthal angles which can be constructed from polarisation and momentum vectors. In the following we will summarise these observables for various processes in  $NN$  collisions. The focus will be on observables that have been measured experimentally. Due to the added complexity in  $NN$  collisions, the complete cross sections are rather lengthy, if they exist in the literature at all. Therefore they will not be reproduced here in their full length. The reader is referred to the appropriate given references. The phenomenology of hadronic collisions in terms of TMDs is discussed in detail in Sec. 3.

### 2.2.1 Transverse single spin asymmetries in $pN \rightarrow hX$ processes

As described above, the transverse single spin asymmetry  $A_N$  has a long history. For a forward moving transversely polarised beam, it is defined as:

$$A_N \equiv \frac{d\sigma^\uparrow - d\sigma^\downarrow}{d\sigma^\uparrow + d\sigma^\downarrow}, \quad (6)$$

where  $d\sigma$  is the differential cross section for the process  $pN \rightarrow h(\mathbf{p}_h) + X$ , and  $\uparrow, \downarrow$  indicate opposite spin polarisation vectors perpendicular to the scattering plane. It is easy to see that, by rotational invariance, one has

$$A_N \equiv \frac{d\sigma^\uparrow(\mathbf{p}_T) - d\sigma^\uparrow(-\mathbf{p}_T)}{d\sigma^\uparrow(\mathbf{p}_T) + d\sigma^\uparrow(-\mathbf{p}_T)}, \quad (7)$$

where  $\mathbf{p}_T$  is the component of the final hadron momentum  $\mathbf{p}_h$  transverse to the polarised beam direction. That is,  $A_N$  can also be simply seen as a left-right asymmetry in the inclusive production of a single hadron, while the beam polarisation remains fixed.

Significant asymmetries have been observed in  $pp$  collisions up to  $\sqrt{s} = 500$  GeV [33] for  $\pi^0$ . Data also exists for charged pions and kaons [45] as well as  $\eta$  mesons [46, 47] and  $J/\Psi$  [48]. Here we concentrate on the pseudo-scalar mesons. A common feature of the asymmetries is a rise with  $x_F$ , where the so-called Feynman- $x$  variable for a detected particle  $A$  is defined as  $x_F = p_L^A / (p_{L \max}^A)$ . Here  $p_L^A$  is its longitudinal momentum measured in a specific frame and  $p_{L \max}^A$  the maximum longitudinal momentum that the particle can have in this frame. For  $pp$  collisions with equal beam energies (in the c.m. system),  $x_F$  reduces to  $x_F = (2p_L^A) / \sqrt{s}$  and  $x_F = 0$  corresponds to particles detected at an angle  $\pi/2$  with respect to the beam axis in the lab frame.

Fig. 5 shows the world data on  $A_N$  for c.m. energies  $\sqrt{s}$  which go from 4.9 GeV at the ZGS up to 500 GeV at RHIC. As well as the rise in  $x_F$ , one can observe rising values of the asymmetries with the transverse momentum  $p_T$  of the detected meson. Even at the highest c.m. energies available, no fall with  $p_T$  was observed [33]. An interesting development has been the recent measurement of the nuclear dependence of  $A_N$  [49]. The Phenix experiment observed a dependence of the asymmetries on the atomic number of the unpolarised beam, which has not been confirmed by the STAR experiment. These measurements might be sensitive to gluon saturation effects, which are not a focus of this review. We refer to Ref. [50] for more details.

### 2.2.2 Transverse single spin asymmetries in $\gamma^*, W/Z, \gamma$ production

Closely related to the t-channel SIDIS process discussed earlier, are the corresponding s-channel processes in which the annihilation of a  $q\bar{q}$  pair creates a virtual  $\gamma^*$  or a real W/Z boson. For  $q + \bar{q} \rightarrow \gamma^* \rightarrow \ell^+\ell^-$ , where  $\ell^+\ell^-$  is a final state lepton pair, this is the Drell-Yan process [52]. Similarly to SIDIS, two non-perturbative objects enter the cross section of these processes, in this case two parton distribution functions, but no FF, due to the non-hadronic final state. This makes them relatively clean tools that allow a complementary access to TMD-PDFs. In particular, the Drell-Yan process with the possibility to measure transversity “squared” in transverse double spin asymmetries without FF

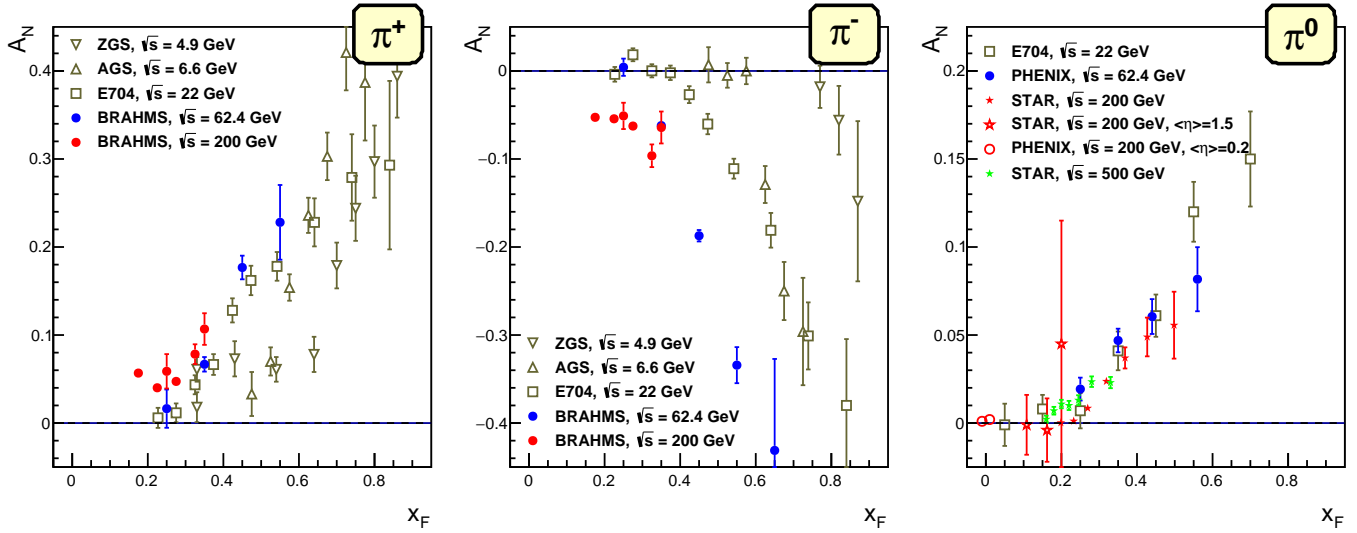


Figure 5: Selection of world data on  $A_N$  in  $pp$  interactions for neutral and charged pions. In particular in the  $\pi^0$  case, the so-called  $x_F$  scaling is evident, which means that the asymmetry is almost independent of  $\sqrt{s}$ . In general, the dependence of  $A_N$  on  $x_F$  is almost linear. Data compiled by Oleg Eyser [51].

contribution [53] as well as accessing the process dependence of the Sivers function [41], has attracted considerable attention in recent times.

When allowing for parton intrinsic motion, the TMDs express themselves in the dependence of the Drell-Yan cross-section on the azimuthal angles shown in Fig. 6. The first ones,  $\phi_V$  and  $\phi_S$ , are determined in the target rest frame and they are respectively the azimuthal angles of the momentum direction  $\mathbf{q}$  of the vector boson – the  $\gamma^*$  in D-Y or the  $W/Z$  in the case of weak boson production discussed further below – and the transverse spin orientation of the beam. It is convenient to define them in the target rest frame as this is the natural frame for the experimental setup and it has a closer connection to the partonic picture [54]. The remaining azimuthal angle  $\phi_{CS}$  is customarily defined in a lepton pair center-of-mass frame. In this frame one also defines the polar angle  $\theta_{CS}$ . Here the subscript CS in  $\theta_{CS}$  and  $\phi_{CS}$  designates the Collins-Soper (CS) frame [55]. Another common frame, related to the CS system by a rotation, is the Gottfried-Jackson frame [56].

The hard scale of the process is given by the virtuality  $q^2$  of the  $\gamma^*$  which can be determined from the invariant mass  $M_{\ell^+\ell^-}$  of the  $\ell^+\ell^-$  system. The TMD picture is valid for small transverse momenta  $q_T$  of  $\gamma^*$ . The cross section of the Drell-Yan process with one transversely polarised proton can be expressed in terms of azimuthal dependent structure functions analogous to the SIDIS process [54, 57].

The full expression for two polarized hadrons is quite lengthy (see *e.g.* Eq. (57) in Ref. [54]), as it contains various combinations of the TMDs of both hadrons. Therefore we will concentrate on two relevant cases here. First, considering the polarization of the hadrons (either longitudinal,  $S_L$ , or transverse,  $S_T$ ), but integrating out the angles  $\phi_{CS}$ ,  $\theta_{CS}$  of the leptonic system [54, 39]:

$$\begin{aligned}
\frac{d\sigma^{\text{DY}}}{d^4q} &= \frac{8\pi\alpha^2}{9s q^2} \left\{ F_{UU} + S_{AL} S_{BL} F_{LL} \right. \\
&+ |\mathbf{S}_{AT}| \left[ \sin(\phi_V - \phi_{S_A}) F_{TU}^{\sin(\phi_V - \phi_{S_A})} \right] + |\mathbf{S}_{BT}| \left[ \sin(\phi_V - \phi_{S_B}) F_{UT}^{\sin(\phi_V - \phi_{S_B})} \right] \\
&+ |\mathbf{S}_{AT}| S_{BL} \left[ \cos(\phi_V - \phi_{S_A}) F_{TL}^{\cos(\phi_V - \phi_{S_A})} \right] + S_{AL} |\mathbf{S}_{BT}| \left[ \cos(\phi_V - \phi_{S_B}) F_{LT}^{\cos(\phi_V - \phi_{S_B})} \right] \\
&+ |\mathbf{S}_{AT}| |\mathbf{S}_{BT}| \left[ \cos(2\phi_V - \phi_{S_A} - \phi_{S_B}) F_{TT}^{\cos(2\phi_V - \phi_{S_A} - \phi_{S_B})} + \cos(\phi_{S_A} - \phi_{S_B}) F_{TT}^1 \right] \left. \right\}. \quad (8)
\end{aligned}$$

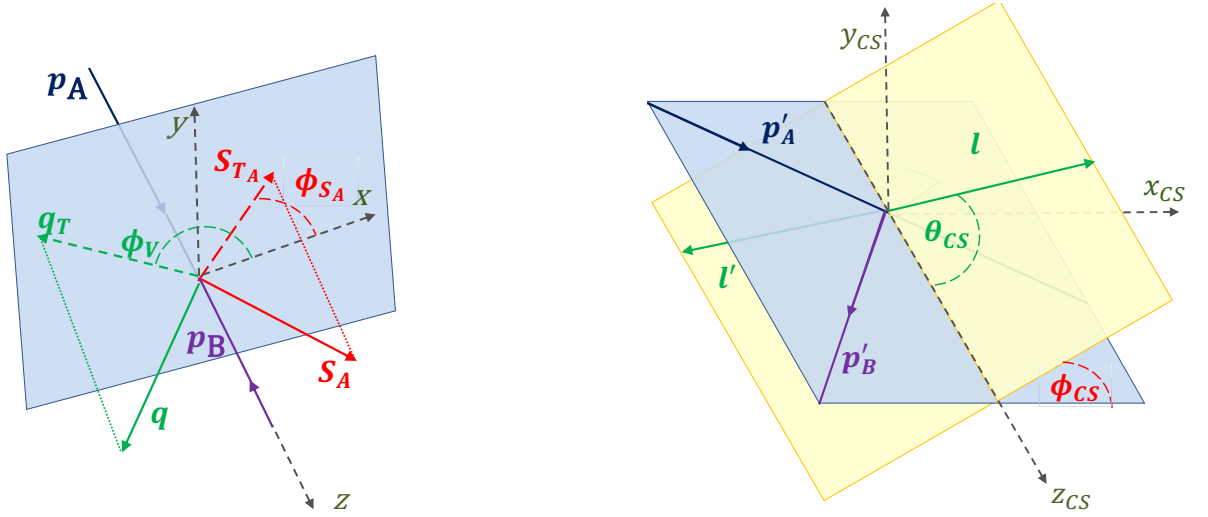


Figure 6: Two frames are commonly used in the analysis of the Drell-Yan process. The target rest frame and the Collins-Soper frame. Since it is also used in the  $W/Z$  case, here the center-of-mass frame of the colliding hadrons is shown on the left side which is related to the target rest frame by a boost along the  $z$ -axis. Therefore the azimuthal angles entering the cross-section are the same. The Collins-Soper frame is the lepton center-of-mass frame where the  $z$ -axis bisects the incoming hadron momenta as shown in the figure on the right. The angle  $\phi_{CS}$  is then the azimuthal angle of the lepton plane with respect to the hadron plane and the angle  $\theta_{CS}$  is the angle between the lepton direction and the  $z$ -axis.

As we will see in Sec 3.3.2, the  $F_{TU}$  and  $F_{UT}$  structure functions are sensitive to the Sivers functions of hadron  $A$  and  $B$ , respectively, convoluted with the unpolarized PDF of the other hadron. Section 3 will explore the interpretation of the structure functions in terms of TMDs.

Secondly, we consider the unpolarised cross-section in a di-lepton center of mass frame, *e.g.* the Collins-Soper frame. With  $\Omega$  denoting the solid angle of the leptons, one can arrive for the angular distribution of the leptons at [54]:

$$\frac{d\sigma^{\text{DY}}}{d^4q d\Omega} = \frac{\alpha_{\text{em}}}{2s q^2} \left[ (1 + \cos^2 \theta_{CS}) F_{UU}^1 + (1 - \cos^2 \theta_{CS}) F_{UU}^2 + \sin 2\theta_{CS} \cos \phi_{CS} F_{UU}^{\cos \phi_{CS}} + \sin^2 \theta_{CS} \cos 2\phi_{CS} F_{UU}^{\cos 2\phi_{CS}} \right], \quad (9)$$

where all angles are in the CS frame. Defining

$$\lambda = \frac{F_{UU}^1 - F_{UU}^2}{F_{UU}^1 + F_{UU}^2} \quad \mu = \frac{F_{UU}^{\cos \phi_{CS}}}{F_{UU}^1 + F_{UU}^2} \quad \nu = \frac{2F_{UU}^{\cos 2\phi_{CS}}}{F_{UU}^1 + F_{UU}^2} \quad (10)$$

the cross section takes the form [54]

$$\frac{dN}{d\Omega} \equiv \frac{d\sigma^{\text{DY}}}{d^4q d\Omega} \bigg/ \frac{d\sigma^{\text{DY}}}{d^4q} = \frac{3}{4\pi} \frac{1}{\lambda + 3} \left( 1 + \lambda \cos^2 \theta_{CS} + \mu \sin 2\theta_{CS} \cos \phi_{CS} + \frac{\nu}{2} \sin^2 \theta_{CS} \cos 2\phi_{CS} \right), \quad (11)$$

and the Lam-Tung relation [58] can be written as  $1 - \lambda = 2\nu$ . It is the analogue to the Callan-Gross relation in SIDIS, since it is also a consequence of the interaction with point-like, spin- $\frac{1}{2}$  quarks. Unlike the Callan-Gross relation, the Lam-Tung relation holds at  $\mathcal{O}(\alpha_s)$ . Therefore, violations of the Lam-Tung relation can be seen as an indication of non-perturbative effects. Most notably, the Boer-Mulders function  $h_1^\perp$ , which will be introduced as one of the TMDs, leads to such a violation [59].

Albeit attractive, measuring spin-dependent asymmetries in the Drell-Yan process is challenging, since a large part of the cross-section is in a  $M_{\ell\ell'}$  region that receives significant contributions from resonances that decay into lepton pairs, like the  $J/\Psi$ . Recently, the COMPASS collaboration showed a first result on a Drell-Yan measurement using a polarised target to measure asymmetries related to the Sivers effect [60]. That measurement is unusual compared to other D-Y experiments, since it uses a pion beam, thus the pion PDFs enter in the relevant cross-sections. A Drell-Yan measurement in  $pp$  interactions with a polarised target is also planned at the Fermilab experiment SpinQuest [61]

The  $\gamma^*$  in the D-Y process can be replaced by real W/Z bosons, which can then be detected via their hadronic or leptonic decay modes. Here the hard scale of the process is given by the mass of the weak boson. Similar to the D-Y process, TMDs can be accessed in W/Z production through the dependence of the cross section on several azimuthal angles [39]. In this case it is convenient to consider the azimuthal angles of the polarisation vectors of the colliding beams in their center-of-mass system,  $\varphi_{S_A}$  and  $\varphi_{S_B}$  defined again relative to the azimuthal direction of the W/Z boson momentum in this system. Given that the azimuthal angles are invariant with respect to boosts along the  $z$ -axis, these are the same as the angles defined above for D-Y in the target rest frame. The cross-section can then be written in terms of structure functions as [39]:

$$\begin{aligned}
\frac{d\sigma^W}{dy d^2\mathbf{q}_T} &= \frac{\pi G_F M_W^2}{3\sqrt{2}s} \left\{ F_{UU} + S_{AL} F_{LU} + S_{BL} F_{UL} + S_{AL} S_{BL} F_{LL} \right. \\
&+ |\mathbf{S}_{AT}| \left[ \sin(\phi_V - \phi_{S_A}) F_{TU}^{\sin(\phi_V - \phi_{S_A})} + \cos(\phi_V - \phi_{S_A}) F_{TU}^{\cos(\phi_V - \phi_{S_A})} \right] \\
&+ |\mathbf{S}_{BT}| \left[ \sin(\phi_V - \phi_{S_B}) F_{UT}^{\sin(\phi_V - \phi_{S_B})} + \cos(\phi_V - \phi_{S_B}) F_{UT}^{\cos(\phi_V - \phi_{S_B})} \right] \\
&+ |\mathbf{S}_{AT}| S_{BL} \left[ \sin(\phi_V - \phi_{S_A}) F_{TL}^{\sin(\phi_V - \phi_{S_A})} + \cos(\phi_V - \phi_{S_A}) F_{TL}^{\cos(\phi_V - \phi_{S_A})} \right] \\
&+ S_{AL} |\mathbf{S}_{BT}| \left[ \sin(\phi_V - \phi_{S_B}) F_{LT}^{\sin(\phi_V - \phi_{S_B})} + \cos(\phi_V - \phi_{S_B}) F_{LT}^{\cos(\phi_V - \phi_{S_B})} \right] \\
&+ |\mathbf{S}_{AT}| |\mathbf{S}_{BT}| \left[ \cos(2\phi_V - \phi_{S_A} - \phi_{S_B}) F_{TT}^{\cos(2\phi_V - \phi_{S_A} - \phi_{S_B})} + \cos(\phi_{S_A} - \phi_{S_B}) F_{TT}^1 \right. \\
&\quad \left. + \sin(2\phi_V - \phi_{S_A} - \phi_{S_B}) F_{TT}^{\sin(2\phi_V - \phi_{S_A} - \phi_{S_B})} + \sin(\phi_{S_A} - \phi_{S_B}) F_{TT}^2 \right] \left. \right\}, \tag{12}
\end{aligned}$$

where  $y$  is the rapidity, which in terms of the four-momentum  $q = (q_0, \mathbf{q}_T, q_L)$  is given by  $y = \frac{1}{2} \ln \frac{q_0 + q_L}{q_0 - q_L}$ .

As explained in more detail in Ref. [39], the transverse spin asymmetries in W/Z production differ from spin asymmetries in D-Y in two important ways. (1): Because the analogue of the decay-leptons is not accessible, the CS angles  $\phi$  and  $\theta$  are effectively integrated out. This means that certain TMDs that are accessible in D-Y are out of reach, *e.g.* the product of Boer-Mulders and transversity. And (2): The parity violating nature of the weak interaction allows access to “wormgear” type TMDs in single spin asymmetries, which are not accessible in D-Y. This will be discussed further in Sec. 3.

A pioneering measurement of transverse single spin asymmetries in  $W$  and  $Z^0$  production has been performed by the STAR experiment at RHIC [62] with the main objective to extract Sivers type asymmetries.

A process that at first sight is similar to the D-Y and W/Z production processes described above, is the direct photon production,  $p + p \rightarrow \gamma + X$ . However, since here a real photon is produced ( $p_\gamma^2 = 0$ ), this is a single scale process that, analogous to the  $A_N$  asymmetries discussed above, has better to be treated in the twist-3 framework. Due to the relation of twist-3 functions to TMDs, this process can nevertheless be used to restrict TMDs like the Sivers function and has been suggested as another avenue to test the process dependence of the Sivers effect [63] and to test the validity of the GPM approach which assumes TMD factorisation [64].

### 2.2.3 Transverse single spin asymmetries in di-hadron production

Recent data from RHIC made the exploration of richer hadronic final states possible. We discuss two examples, di-hadrons in this Section and hadrons inside jets in the next Section. In both cases, to our knowledge, a complete set of structure functions does not exist in the literature; therefore, we will not reproduce the full cross-section, but will concentrate on the structure functions that have been explored experimentally, which in both cases are modulations sensitive to the transversity distribution and, in the case of jets, the Sivers distribution, as will be discussed in Sections 3.3.3 and 3.3.4. Much more details on di-hadron fragmentation can be found in Ref. [65].

Considering only the practical relevant case of final states consisting of pseudo-scalar mesons, the hadronic tensor in di-hadron production can depend on an additional vector, the difference between the momenta of the outgoing hadrons  $\mathbf{R} = \mathbf{p}_{h,1} - \mathbf{p}_{h,2}$ . This additional vector allows sensitivity to the the transverse spin structure of the proton as noted by Collins, Heppelmann and Ladinsky [66]. Using a coordinate system where the  $z$ -axis is given by the momentum vector of the hadron pair, the polarization sensitive part of the cross-section is usually parameterised with an azimuthal angle  $\phi_R$ , a polar angle  $\theta$  and the invariant mass of the hadronic final state  $M_h$ . The angle  $\phi_R$  is connected to the relative angular momentum of the final state with a quantisation axis transverse to  $\mathbf{p}_h = \mathbf{p}_{h,1} + \mathbf{p}_{h,2}$ , which can be seen as a proxy for the outgoing quark. Therefore, modulations of the di-hadron cross-section in  $\phi_R$  are sensitive to the transverse spin structure of the proton. Well-known model calculations [67] for transverse polarisation dependent di-hadron fragmentation functions are based on the interference of hadron pairs in different partial waves <sup>1</sup>.

For the parent quark polarisation dependent fragmentation into charged pions, the most relevant effect would come from the interference of an  $s$ -wave from non-resonant production and a  $p$ -wave from resonant production and subsequent decay of  $\rho$  mesons. Expanded in partial waves, each interference term would then have a characteristic  $\theta$  dependence with the most relevant  $s$ - $p$  interference term having a  $\sin \theta$  dependence. Since the experimental acceptance usually peaks at  $\sin \theta = 1$  due to momentum cuts on the particles, current results in  $pp$  integrate over the  $\theta$  dependence, and only consider the dependence on the azimuthal angle  $\phi_R$ . The relevant quantities for this measurement are shown in Fig. 7.

Experimental results from  $pp$  interactions at RHIC have been published by the STAR Collaboration [70, 71] on the transverse single spin asymmetry  $A_{UT}^{\sin \phi_{RS}}$  defined analogously to the SIDIS asymmetries in (3) as

$$A_{UT}^{\sin \phi_{RS}} = 2 \frac{\int d\phi_{RS} [d\sigma^\uparrow - d\sigma^\downarrow] \sin \phi_{RS}}{\int d\phi_{RS} [d\sigma^\uparrow + d\sigma^\downarrow]}, \quad (13)$$

where  $\phi_{RS} = \phi_R - \phi_S$ .

As further discussed in Sec. 3.3.3, this asymmetry is sensitive to the contribution of the transversity PDF even after integrating over the transverse momentum degrees of freedom in the PDFs and FFs [37]. The STAR measurement has been used for the first global extraction of transversity from SIDIS,  $pp$  and  $e^+e^-$  data [72].

### 2.2.4 Transverse single spin asymmetries of jets and hadrons in jets

At high energies, hadronic final states in nuclear collisions are collimated into jets. Therefore, jets provide a connection to the initial state partonic kinematics. At leading order one can simply identify the parton direction with the jet [73], but the connection can also be done at higher orders [74].

Jets are usually described by their transverse momentum  $\mathbf{p}_T$ , with respect to the beam direction, as well as their position in  $\eta - \phi$  space, where  $\eta$  is the pseudo-rapidity and  $\phi$  the azimuthal angle. Since differences in rapidity are boost invariant, a rule of thumb is that jets will cover about one unit

---

<sup>1</sup>It should be mentioned that there are alternative models based on string fragmentation [68, 69]

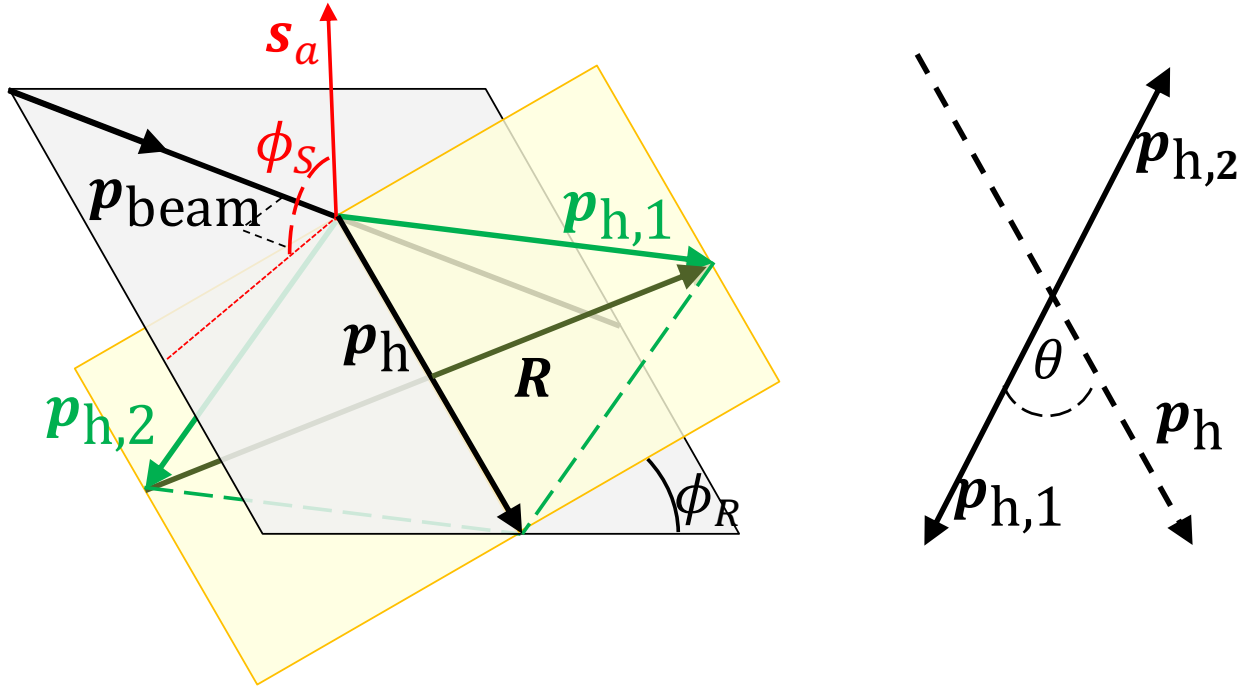


Figure 7: Left: Diagram of the azimuthal angles relevant for di-hadron measurements in  $pp$  interactions. Here  $\mathbf{p}_{h,1(2)}$  is the momentum of the positive (negative) pion,  $\mathbf{s}_a$  is the beam polarization, and  $\phi_R$  is the angle between the scattering plane (gray) and the di-hadron plane (yellow). The diagram on the right shows the polar angle  $\theta$  defined between the hadron direction in the center-of-mass system of the hadron pair and the direction of the sum of the hadron momenta  $\mathbf{p}_h$  in the target rest frame.

in  $\eta$  and  $\phi$  regardless of their  $x_F$ . In practice, experimental requirements, such as detector uniformity, contributions from underlying events or the beam remnants, will often require the use of a smaller jet radius in reconstruction. With the availability of high statistics datasets from the STAR experiment at RHIC, as well as the LHC experiments, interest in using jets to access proton structure has grown substantially.

The challenge for jet physics is that the c.m. energy has to be high enough for jets to be created, and the jets must have high enough  $p_T$  to provide a hard scale. At the same time, experiments have to have large enough acceptances to detect a jet. Given the rough size estimate of  $1 \times 1$  in  $\eta - \phi$  space, this means usually full azimuthal coverage as well as a significant coverage in the polar angle. Forward detector, like early  $NN$  experiments or current Fermilab experiments, are problematic for jet physics, since the geometry means that jets in the acceptance have low  $p_T$  and will often be contaminated by beam background. Therefore, most experimental input comes from the STAR experiment at RHIC as well as the LHC experiments.

Even though jets are among the most challenging observables in nuclear collisions, they are quite attractive, since they can be seen as proxies for the outgoing parton in the scattering. This makes an estimation of the underlying partonic kinematics in jet production possible; at LO we have  $2 \rightarrow 2$  underlying processes. For example, the partonic  $x$  can be calculated from the pseudo-rapidities  $\eta$  and transverse momenta  $p_T$  of the two jets as

$$x_1 = (p_{T,1} e^{\eta_1} + p_{T,2} e^{\eta_2})/\sqrt{s} \quad x_2 = (p_{T,1} e^{-\eta_1} + p_{T,2} e^{-\eta_2})/\sqrt{s}. \quad (14)$$

As it can be seen from the expression above, high  $p_T$  jets preferentially select high  $x$  partons. The fractional energy  $z$  can be determined as the ratio of the energy of the detected hadron to the jet energy. This measurement of  $z$  is obviously also available in inclusive jet measurements. If only a single jet is

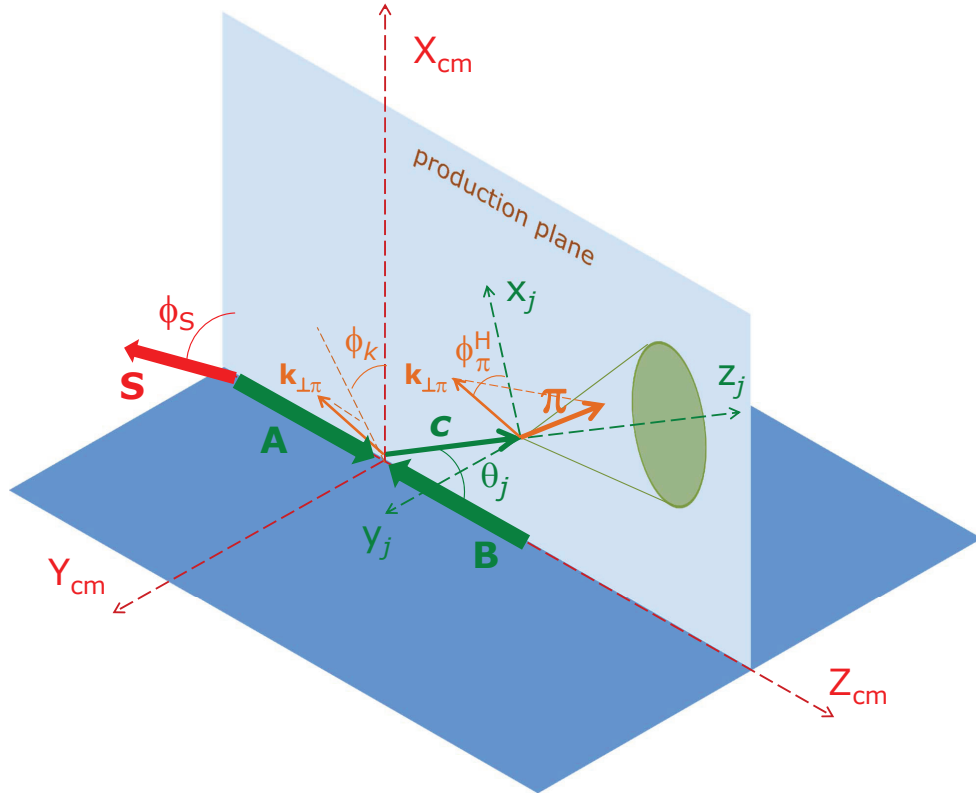


Figure 8: Diagram of the azimuthal angles relevant for hadron in jet measurements in  $pp$  interactions. The initial momenta of the colliding hadrons are denoted  $\mathbf{A}$  and  $\mathbf{B}$ , with  $\mathbf{A}$  being associated with the polarization vector  $\mathbf{S}$ . The outgoing parton momentum is denoted  $\mathbf{c}$  and has an azimuthal angle  $\phi_k$ . The azimuthal angle of  $\mathbf{S}$  is  $\phi_S$  and the pion within the jet has a transverse momentum of  $k_{\perp,\pi}$  with respect to the jet axis. The azimuthal angle of the pion around the jet axis is denoted  $\phi_\pi^H$ . Figure from [73]. Reprinted by permission from Springer Nature Customer Service Centre GmbH, Springer Phys. Part. Nucl., 45(4):676-691, 2014, "Collins and Sivers effects in  $p^\uparrow p \rightarrow \text{jet } \pi X$ : Universality and process dependence.", Umberto D'Alesio, Francesco Murgia, and Cristian Pisano, Copyright 2014.

detected, the formulae above to calculate  $x_i$  at LO are not applicable; however, there is still a strong correlation between the  $p_T$  and  $\eta$  of the detected jet with the underlying partonic kinematics since the underlying  $2 \rightarrow 2$  scattering in a high  $p_T$  jet measurement is usually quite asymmetric in  $x$ .

Compared to SIDIS processes, measurements of transverse spin phenomena in jets in  $pp$  scattering has the advantage that, at least in the LO interpretation, the initial and final state  $k_T$  dependences are separated, since presumably the jet is an approximation to the outgoing parton. However, if intrinsic transverse momenta are included, there are questions about the factorisation of this process [42]. For the Collins effect, *i.e.* the dependence of the transverse momentum of a hadron in a jet on the parent parton transverse polarisation, universality seems to hold [75, 76].

Figure 8 shows the relevant quantities for the process with one polarised proton. Polarisation dependent PDFs and FFs can be accessed by the dependence of the cross section on the azimuthal angles of the parent proton polarisation ( $\phi_S$ ), the azimuthal angle of the jet axis ( $\phi_k$ ) and the hadron (in this case a pion) within the jet ( $\phi_\pi^H$ ). As will be discussed in Section 3, in a LO treatment, the cross section has similarities with the SIDIS cross section when the lepton beam in the SIDIS case is replaced

with a quark from the unpolarised proton. In particular, the transversity distribution can be accessed by measuring modulations in the azimuthal angle of hadrons around the jet axis ( $\phi_\pi^H$ ) and the Sivers effect can be accessed by measuring the dependence of the cross section on the azimuthal angle of the jet axis ( $\phi_k$ ). Both of these measurements have been performed by the STAR Collaboration [77, 43] and a significant evidence for the Collins signal, consistent with expectations from global fits [76], has been observed.

Transverse Single Spin Asymmetries (TSSAs) for jets measured at STAR do not show a significant signal, as expected for jets detected at mid-rapidity. The AnDY experiment performed a measurement for forward jets [78] which shows an indication of a non-vanishing asymmetry. While for the observation of a hadron inside a jet the TMD picture is appropriate, due to the small transverse momentum of the hadron inside a jet, this is not so clear in single-jet measurements to access the Sivers effect. Here only a single hard scale, the  $p_T$  of the jet, is observed, which makes the twist-3 picture more appropriate. However, the twist-3 measurement can be related to the Sivers function in the intermediate  $p_T$  region, as discussed in Sec. 3.3.4. A measurement of the Sivers function that can be interpreted in the TMD picture are nearly back-to-back di-jets, where a spin dependence of the (small) relative transverse momentum of the two jets is observed. Such a measurement has been performed by the STAR Collaboration [79], but the measurement was limited by statistics. In addition, factorization and universality are problematic in this case as will be further discussed in Sec. 3.3.4. It should be noted that the aforementioned factorization issues in back-to-back jet production can be avoided in SIDIS jet production, such as a future EIC. Here one of the jets is replaced conceptually by the outgoing lepton. Such a measurement would therefore combine some of the advantages of jet measurements, in particular the decoupling of the fragmentation functions for the TMD-PDF measurements and vice-versa with the advantage of the clean theoretical understanding of SIDIS.

### 2.3 Spin effects in $e^+e^- \rightarrow h_1 h_2 X$ and $e^+e^- \rightarrow \Lambda^\uparrow X$ processes

Let us consider the process in which unpolarised leptons and anti-leptons annihilate into two jets of particles, and we look at two hadrons belonging to opposite jets. At first sight it might appear impossible to obtain spin effects in such a process: however, this is not the case [80]. As usual, in  $e^+e^-$  annihilation processes, the production of hadrons goes via the subprocess  $e^+e^- \rightarrow q\bar{q}$ . The final  $q$  and  $\bar{q}$  are also not polarised, that is they can have spin “up” or “down”, with respect to the scattering plane, with the same probability (1/2); however there is a correlation between the spin of the quark and that of the anti-quark. Not necessarily if the first is up, the second is down, or viceversa. To be precise, with reference to the kinematical configuration of Fig. 9, one has:

$$\frac{d\sigma^{e^+e^- \rightarrow q^\uparrow\bar{q}^\uparrow}}{d\cos\theta} = \frac{d\sigma^{e^+e^- \rightarrow q^\downarrow\bar{q}^\downarrow}}{d\cos\theta} = \frac{3\pi\alpha^2}{4s} e_q^2 \cos^2\theta \quad \frac{d\sigma^{e^+e^- \rightarrow q^\uparrow\bar{q}^\downarrow}}{d\cos\theta} = \frac{d\sigma^{e^+e^- \rightarrow q^\downarrow\bar{q}^\uparrow}}{d\cos\theta} = \frac{3\pi\alpha^2}{4s} e_q^2. \quad (15)$$

The hadronisation process  $q^{\uparrow,\downarrow} \rightarrow h X$ , might have (and indeed has) a transverse spin dependence which affects the angular distribution of the produced hadron; then, if one looks in each same event  $e^+e^- \rightarrow h_1 h_2 X$ , at the correlation between the angular distributions of the two hadrons in the opposite jets, one can learn about such a transverse spin dependence. Again, by rotational invariance, no spin dependence would be possible in a collinear quark fragmentation process, which leads to the necessity of introducing transverse motions also in the phenomenological description of a quark fragmentation.

The general form of the cross section for the process  $e^+e^- \rightarrow h_1 h_2 X$ , via  $e^+e^-$  annihilation into  $q\bar{q}$ , can be written in different ways, according to the reference frame used and the observables one looks at. For example, using the reference frame and the kinematical variables of Fig. 10 one has [80, 81]:

$$\frac{d\sigma^{e^+e^- \rightarrow h_1 h_2 X}}{dz_1 dz_2 d^2\mathbf{P}_{1T} d\cos\theta_2} = \frac{3\pi\alpha_{\text{em}}^2}{2s} \{D_{h_1 h_2} + N_{h_1 h_2} \cos(2\phi_1)\}, \quad (16)$$

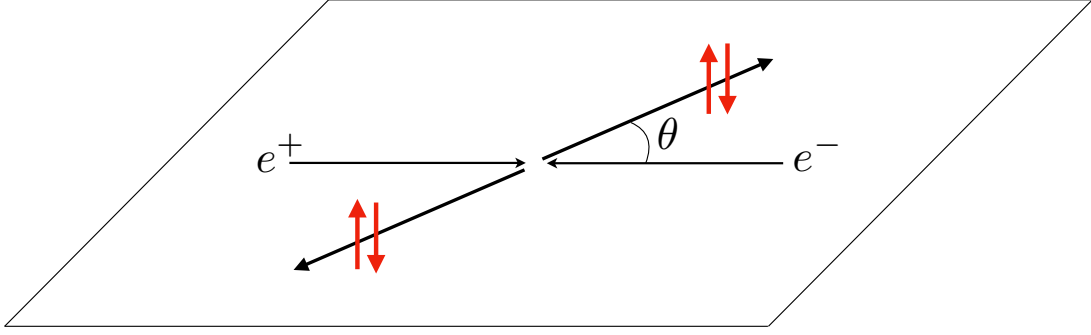


Figure 9: Center of mass scattering plane for the  $e^+e^- \rightarrow q\bar{q}$  process; the spin polarisation vectors are perpendicular to the plane.

where  $z_{1,2}$  are the light-cone momentum fractions of the hadrons  $h_{1,2}$  resulting from the fragmentation of the quark and antiquark. They are essentially the quark and antiquark energy fractions taken away by the hadrons.

The cross-section (16) has been measured by several experiments. The first measurement for  $\pi^+\pi^-$  pairs was done by the Belle Collaboration [82, 83] and confirmed by BaBar [84]. BaBar also extended the measurement to the transverse momentum dependence and included charged kaons [85]. While Belle and BaBar measurements were done at a center-of-mass energy close to the mass of the  $\Upsilon(4S)$ , BES-III did a similar measurement at lower cms energies [86]. Most recently, Belle published asymmetries of back-to-back hadrons including  $\pi^0$  and  $\eta$ 's [47].

In the next Section the form factors  $D_{h_1 h_2}$  and  $N_{h_1 h_2}$  will be interpreted in terms of Fragmentation Functions, either collinear FFs or TMD-FFs. Eq. (16) will be used to relate experimental data to spin dependent TMD-FFs.

The  $e^+e^-$  annihilation processes, with the observation of one or two final particles, are interesting in many respects. In addition to the case discussed above, the process  $e^+e^- \rightarrow (h_{a1} h_{a2})(h_{b1} h_{b2}) X$ , with back-to-back pairs of hadrons inside the same jet, can be used to get information on the polarized di-hadron fragmentation function [87], as discussed in Section 3.4.

The measured transverse polarisation of  $\Lambda$ s and other hyperons, as mentioned in Section 2.2, was among the seminal data which prompted the study of transverse spin effects. These data was obtained from unpolarised  $pp$  or  $pN$  inclusive processes, and a first attempted explanation was related to spin effects in the fragmentation of an unpolarised quark, a TMD-FF, in the framework of the GPM [88], with subsequent studies in SIDIS [89]. However, the usual reservations in using the GPM for a single scale  $pp$  process, together with the scarcity or absence of data in other interactions, could not allow definite conclusions and alternative explanations were presented [90].

Data on  $\Lambda$  polarisation in  $e^+e^- \rightarrow \Lambda^\uparrow X$ , due to the simplicity of such a process, would offer an ideal occasion to understand whether the hadronisation process of an unpolarised quark might build up a transverse polarisation; first data, although still limited, are becoming available [91].

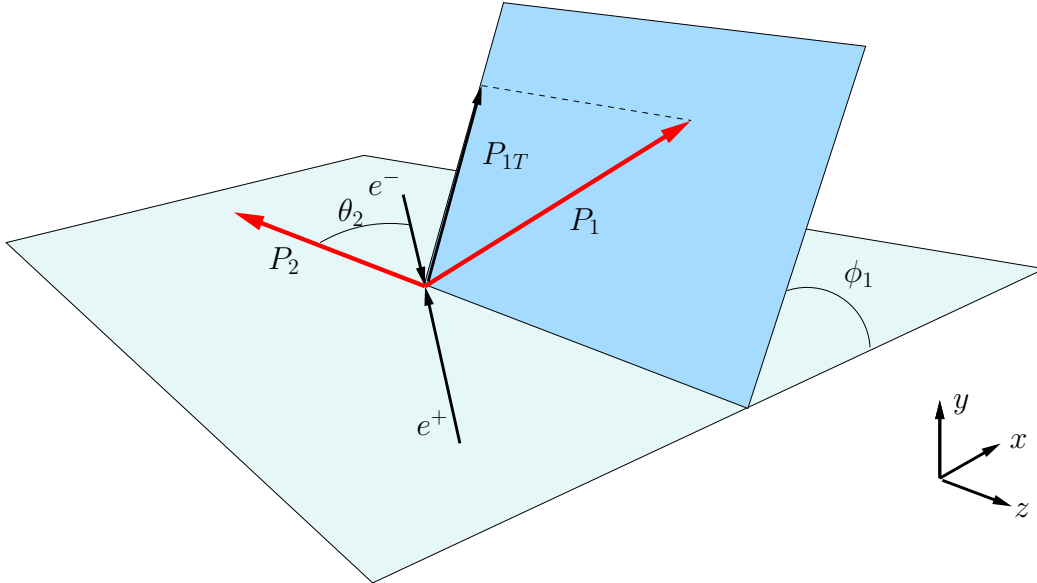


Figure 10: Kinematical configuration and definition of variables for the process  $e^+e^- \rightarrow h_1 h_2 X$ .  $e^+$  and  $e^-$  have opposite three-momenta,  $\mathbf{P}_2$  is the momentum of a jet or of a fast hadron in a jet, and  $\mathbf{P}_1$  is the momentum of a hadron belonging to the other jet.

### 3 Phenomenology of spin phenomena

We have discussed in the previous Section several examples of processes in which the simple – yet in many cases successful – 1D description of a fast moving nucleon as an almost free set of co-linearly moving quarks and gluons cannot explain the experimental data. We have argued that the reason for this is just the excessive simplicity of the 1D model; the neglected transverse degrees of freedom might play important roles, in particular, but not only, when such degrees of freedom are forced into existence by considering transversely polarised nucleons. Transverse always refers to the direction of motion of the nucleons.

Much progress has been achieved in the last one or two decades by extending the collinear factorisation theorem, which allows to describe hadronic cross sections as convolutions of elementary quark and gluon interactions with collinear PDFs or FFs. The PDFs give the number densities of partons inside a proton, while the FFs give the number densities of hadrons resulting in a parton hadronisation. The PDFs depend on the longitudinal momentum fraction  $x$  of the proton carried by the parton and the FFs on the fraction  $z$  of the parton momentum carried by the hadron; they both depend on the scale  $Q^2$  of the process, and such a dependence can be computed in QCD (QCD evolution of PDFs and FFs).

The extension of the collinear factorisation theorem allows to describe cross sections again as convolutions: of elementary interactions with Transverse Momentum Dependent Parton Distribution Functions (TMD-PDFs) and Fragmentation Functions (TMD-FFs). This TMD factorisation has been studied in a series of papers [57, 92, 93, 94, 95, 96, 97, 98, 54, 99] and proven to be valid for SIDIS, D-Y and  $e^+e^- \rightarrow h_1 h_2 X$  processes; the situation is less clear for single and double inclusive hadronic processes,  $pN \rightarrow hX$  and  $pN \rightarrow h_1 h_2 X$  [42, 100].

Throughout the paper we mainly adopt the TMD factorisation scheme and consider the TMDs, both TMD-PDFs and TMD-FFs, and their role in physical quantities at leading order. These TMDs have a partonic interpretation and we focus on their phenomenological extraction from data, which helps in trying to build a 3D imaging of the nucleon. In Section 4.3 we look at the possibility of a real knowledge of the full 3D partonic structure of the nucleon, both in momentum and configuration space,

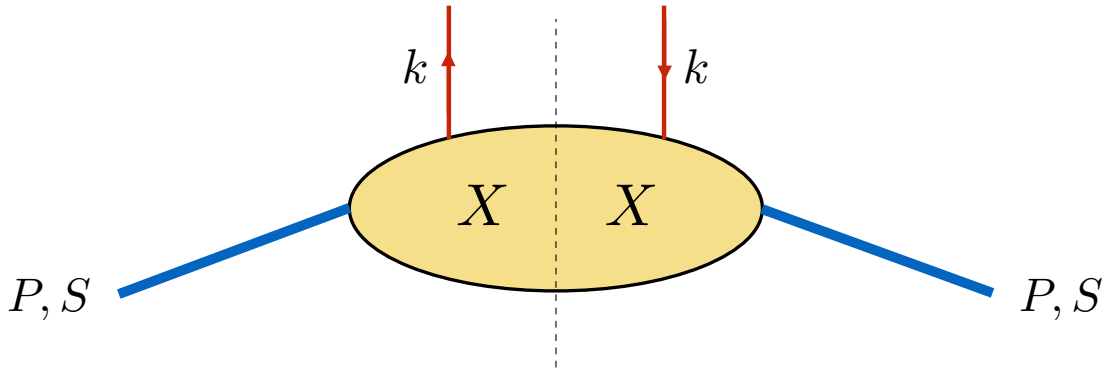


Figure 11: Quark-quark correlator contributing to inclusive processes; the off-diagonal version, in which the initial and final nucleon momenta are different, would contribute to amplitudes of exclusive processes.

with the Wigner function. We do not discuss the details of the QCD evolution of the TMDs (TMD evolution), which is studied at length in several papers [9, 101, 102, 103, 104]. The first phenomenological applications [105, 106, 107, 108, 109] show that the TMD evolution will play an important role in future experiments, but does not significantly affect the TMD phenomenology of the actual available data.

### 3.1 Transverse Momentum Dependent Parton Distributions (TMD-PDFs) and Fragmentation Functions (TMD-FFs)

#### 3.1.1 Quark TMD-PDFs

The quark TMD-PDFs contribute to cross sections of inclusive processes in which one quark interacts with an external probe, like a point-like lepton or another parton; one can think of the quark as “extracted” from the parent nucleon, which breaks up into unobserved particles. This is typically represented by the quark-quark correlator (handbag diagram) of Fig. 11, which in Dirac space is given by [1]:

$$\begin{aligned}
 \Phi_{ij}(k; P, S) &= \frac{1}{(2\pi)^4} \sum_X \int \frac{d^3 \mathbf{P}_X}{(2\pi)^3 2E_X} (2\pi^4) \delta^4(P - k - P_X) \langle PS | \bar{\Psi}_j(0) | X \rangle \langle X | \Psi_i(0) | PS \rangle \\
 &= \frac{1}{(2\pi)^4} \int d^4 \xi e^{ik \cdot \xi} \langle PS | \bar{\Psi}_j(0) \Psi_i(\xi) | PS \rangle .
 \end{aligned} \tag{17}$$

In the collinear case, in which, apart from mass corrections, the quark momentum is just a fraction  $x$  of the nucleon momentum, the most general dependence of the correlator on  $x$  can be written as:

$$\Phi(x, S) = \frac{1}{2} [f_1(x) \not{n}_+ + S_L g_{1L}(x) \gamma^5 \not{n}_+ + h_{1T}(x) i\sigma_{\mu\nu} \gamma^5 n_+^\mu S_T^\nu] . \tag{18}$$

In the above equations  $P$  and  $S$  are respectively the four-momentum and the covariant spin vector of the nucleon, which can be longitudinally ( $S_L$ ) or transversely ( $S_T$ ) polarised.  $n_+$  is a convenient light-like four-vector which, up to mass terms, is along the nucleon momentum. For completeness one should insert into the definition of the correlator, Eq. (17), a Wilson line, or gauge link, which guarantees the color gauge invariance of the correlator (see, for example, Refs. [12, 110]).

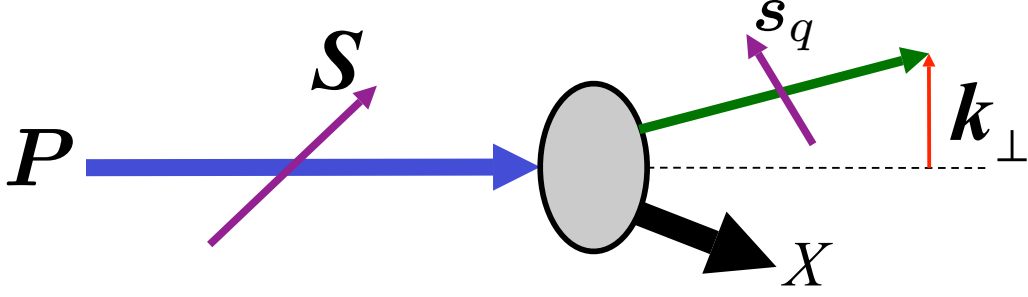


Figure 12: Usual graphical representation of the TMD-PDFs of quarks with spin vector  $\mathbf{s}_q$  and transverse intrinsic momentum  $\mathbf{k}_\perp$  inside a proton with momentum  $\mathbf{P}$  and spin vector  $\mathbf{S}$ .

In Eq. (18), for each quark flavour,  $f_1(x)$  is the unpolarised PDF,  $g_{1L}(x)$  is the helicity distribution and  $h_{1T}(x)$  the transversity distribution. These definitions conventionally refer to protons. These quantities sometimes appear in the literature with different names:

$$f_1(x) \equiv q(x) \quad g_{1L}(x) \equiv \Delta q(x) \quad h_{1T}(x) \equiv h_1(x) \equiv \Delta_T q(x) \equiv \delta q(x). \quad (19)$$

When letting the quark have an intrinsic motion  $\mathbf{k}_\perp$  inside the proton Eq. (18) gets more terms which vanish in the limit  $k_\perp \rightarrow 0$  [111, 112, 12, 59]:

$$\begin{aligned} \Phi(x, \mathbf{k}_\perp, S) = & \frac{1}{2} \left[ f_1 \not{n}_+ + f_{1T}^\perp \frac{\epsilon_{\mu\nu\rho\sigma} \gamma^\mu n_+^\nu k_\perp^\rho S_T^\sigma}{M} + \left( S_L g_{1L} + \frac{\mathbf{k}_\perp \cdot \mathbf{S}_T}{M} g_{1T}^\perp \right) \gamma^5 \not{n}_+ \right. \\ & \left. + h_{1T} i\sigma_{\mu\nu} \gamma^5 n_+^\mu S_T^\nu + \left( S_L h_{1L}^\perp + \frac{\mathbf{k}_\perp \cdot \mathbf{S}_T}{M} h_{1T}^\perp \right) \frac{i\sigma_{\mu\nu} \gamma^5 n_+^\mu k_\perp^\nu}{M} + h_1^\perp \frac{\sigma_{\mu\nu} k_\perp^\mu n_+^\nu}{M} \right]. \quad (20) \end{aligned}$$

Eq. (20) gives the most general expression of the quark-quark correlator at leading twist (twist-2); it contains 8 independent functions, which are usually referred to as the 8 leading twist quark TMD-PDFs. The notations in which they are written require some comments:  $f$ ,  $g$  and  $h$  indicate respectively unpolarised, longitudinally polarised and transversely polarised quarks; the subscript 1 refers to the fact that they are leading twist TMDs; the subscripts  $L$  and  $T$  show the polarisation, longitudinal or transverse, of the proton (no subscript stays for unpolarised nucleons); the superscript  $\perp$  appears for TMDs which do not contribute to the correlator in the collinear limit<sup>2</sup>. One could also add at each TMD a superscript  $q$  to identify the quark flavour.  $M$  is a mass parameter taken as the proton mass.

Eq. (20) is the usual formal definition of the quark-quark correlator. However, it is interesting to look at the TMDs in a simple and intuitive way, which clarifies their physical meaning and emphasises their partonic interpretation. It is customary to represent the PDFs and the TMDs as splitting processes in which a proton breaks up into a quark + remnants ( $X$ ), like in Fig. 12.

We can ask how many independent combinations of the vectors ( $\mathbf{p}$ ,  $\mathbf{k}_\perp$ ) and pseudo-vectors ( $\mathbf{S}$ ,  $\mathbf{s}_q$ ) can make up, as required by QCD parity invariance, a scalar quantity, which can then appear as an

<sup>2</sup>Notice, however, that in the original literature [112] the function  $g_{1T}^\perp$  does not have the superscript  $\perp$ , as the function itself might not vanish in the limit  $k_\perp \rightarrow 0$ .

independent term in the correlator. The answer can be written, in momentum space, as [113]:

$$\begin{aligned}
\tilde{\Phi}(x, \hat{\mathbf{P}}, \hat{\mathbf{k}}_{\perp}, \mathbf{S}, \mathbf{s}_q) &= \frac{1}{2} \left\{ f_{q/p}(x, k_{\perp}) \right. \\
&+ \Delta^N f_{q^{\uparrow}/p}(x, k_{\perp}) (\hat{\mathbf{P}} \times \hat{\mathbf{k}}_{\perp}) \cdot \mathbf{s}_q + \frac{1}{2} \Delta^N f_{q/p^{\uparrow}}(x, k_{\perp}) (\hat{\mathbf{P}} \times \hat{\mathbf{k}}_{\perp}) \cdot \mathbf{S} \\
&+ \Delta^- f_{s_y/S_T}^q(x, k_{\perp}) \left[ \mathbf{S} \cdot \mathbf{s}_q - (\hat{\mathbf{P}} \cdot \mathbf{S})(\hat{\mathbf{P}} \cdot \mathbf{s}_q) - (\hat{\mathbf{k}}_{\perp} \cdot \mathbf{S})(\hat{\mathbf{k}}_{\perp} \cdot \mathbf{s}_q) \right] \\
&+ \Delta f_{s_z/S_L}^q(x, k_{\perp}) (\hat{\mathbf{P}} \cdot \mathbf{S})(\hat{\mathbf{P}} \cdot \mathbf{s}_q) + \Delta f_{s_x/S_L}^q(x, k_{\perp}) (\mathbf{P} \cdot \mathbf{S})(\hat{\mathbf{k}}_{\perp} \cdot \mathbf{s}_q) \\
&+ \left. \Delta f_{s_z/S_T}^q(x, k_{\perp}) (\hat{\mathbf{k}}_{\perp} \cdot \mathbf{S})(\hat{\mathbf{P}} \cdot \mathbf{s}_q) + \Delta f_{s_x/S_T}^q(x, k_{\perp}) (\hat{\mathbf{k}}_{\perp} \cdot \mathbf{S})(\hat{\mathbf{k}}_{\perp} \cdot \mathbf{s}_q) \right\} \quad (21)
\end{aligned}$$

and indeed contains 8 independent terms. These are written adopting the notation of Ref. [16]; it has the advantage that the different functions are indeed polarised quark TMD-PDFs or differences between two of them with some opposite spin direction. The exact relation between the notations of Eqs. (20) and (21) is given in Eqs. (22)-(25) and (36), (37) of Ref. [16].

As we said, Eq. (21) can be read directly in terms of TMD-PDFs. If one averages over the proton spin  $\mathbf{S}$  and sums over the emitted quark spin  $\mathbf{s}_q$  one obtains:

$$\frac{1}{2} \sum_{\mathbf{S}, \mathbf{s}_q} \tilde{\Phi}(x, \hat{\mathbf{P}}, \hat{\mathbf{k}}_{\perp}, \mathbf{S}, \mathbf{s}_q) = f_{q/p}(x, k_{\perp}) \quad (22)$$

which is the unpolarised TMD-PDF of quark  $q$ . Similarly, summing over  $\mathbf{s}_q$  only, one has the Siverts distribution [34, 114] of unpolarised quarks inside a polarised proton:

$$\sum_{\mathbf{s}_q} \tilde{\Phi}(x, \hat{\mathbf{P}}, \hat{\mathbf{k}}_{\perp}, \mathbf{S}, \mathbf{s}_q) = f_{q/p}(x, k_{\perp}) + \frac{1}{2} \Delta^N f_{q^{\uparrow}/p}(x, k_{\perp}) (\hat{\mathbf{P}} \times \hat{\mathbf{k}}_{\perp}) \cdot \mathbf{S} \equiv f_{q^{\uparrow}/p}(x, \mathbf{k}_{\perp}). \quad (23)$$

Notice that, due to the scalar mixed product  $(\hat{\mathbf{P}} \times \hat{\mathbf{k}}_{\perp}) \cdot \mathbf{S}$ , only directions of  $\mathbf{S}$  transverse to the proton momentum  $\mathbf{P}$  contribute.

Averaging over the proton spin  $\mathbf{S}$  one has the Boer-Mulders distribution [59] of polarised quarks inside an unpolarised proton,

$$\frac{1}{2} \sum_{\mathbf{S}} \tilde{\Phi}(x, \hat{\mathbf{P}}, \hat{\mathbf{k}}_{\perp}, \mathbf{S}, \mathbf{s}_q) = \frac{1}{2} f_{q/p}(x, k_{\perp}) + \frac{1}{2} \Delta^N f_{q^{\uparrow}/p}(x, k_{\perp}) (\hat{\mathbf{P}} \times \hat{\mathbf{k}}_{\perp}) \cdot \mathbf{s}_q \equiv f_{q^{\uparrow}/p}(x, \mathbf{k}_{\perp}). \quad (24)$$

The other single terms in Eq. (21) can be seen as differences of polarised quark distributions inside polarised protons. Notice that the proton is taken to move along the longitudinal  $\hat{\mathbf{Z}}$ -direction,  $S_L = S_Z$ , while the quark  $\hat{\mathbf{x}}$ ,  $\hat{\mathbf{y}}$  and  $\hat{\mathbf{z}}$ -axes are defined in the quark helicity rest frame [16].

Let us summarise the meaning and different notations adopted for the 8 twist-2 TMDs; in each of them one can think of the quark as carrying a momentum  $\mathbf{p}_q = x\mathbf{P} + \mathbf{k}_{\perp}$ .

- The TMD-PDFs for unpolarised quarks of flavour  $q$  inside an unpolarised proton are usually written as

$$f_1^q(x, k_{\perp}) \equiv f_{q/p}(x, k_{\perp}) \equiv q(x, k_{\perp}) \quad (25)$$

- The Siverts distribution of unpolarised quarks inside a transversely polarised proton is given in Eq. (23). The function

$$\Delta^N f_{q^{\uparrow}/p}(x, k_{\perp}) \equiv -\frac{2k_{\perp}}{M} f_{1T}^{\perp q}(x, k_{\perp}) \quad (26)$$

is the Siverts function. Notice that, often,  $f_{1T}^{\perp}$  alone is referred to as the Siverts function.

- The Boer-Mulders distribution of polarised quarks inside an unpolarised proton is given in Eq. (24). The function

$$\Delta^N f_{q\uparrow/p}(x, k_\perp) \equiv -\frac{k_\perp}{M} h_1^{\perp q}(x, k_\perp) \quad (27)$$

is the Boer-Mulders function. Notice that, often,  $h_1^\perp$  alone is referred to as the Boer-Mulders function.

- The TMD helicity distribution, that is the difference between the distributions of quarks with positive and negative helicities, inside a positive helicity proton is given by:

$$\Delta f_{s_z/S_L}^q(x, k_\perp) \equiv \Delta q(x, k_\perp) \equiv g_{1L}^q(x, k_\perp) \quad (28)$$

- The TMD transversity distribution, that is the difference between the distributions of quarks with opposite transverse spin, inside a proton with transverse spin is given by [16]:

$$\frac{1}{2} \left( \Delta^- f_{s_y/S_T}^q(x, k_\perp) + \Delta f_{s_x/S_T}^q(x, k_\perp) \right) = h_{1T}^q(x, k_\perp) + \frac{k_\perp^2}{2M^2} h_{1T}^{\perp q}(x, k_\perp) \equiv h_1^q(x, k_\perp) \quad (29)$$

- The remaining three distributions in Eq. (21) refer to differences of polarised TMDs with opposite quark polarisations inside a polarised proton, as indicated by the indexes:

$$\Delta f_{s_x/S_L}^q(x, k_\perp) \equiv \frac{k_\perp}{M} h_{1L}^{\perp q}(x, k_\perp) \quad \Delta f_{s_z/S_T}^q(x, k_\perp) \equiv \frac{k_\perp}{M} g_{1T}^{\perp q}(x, k_\perp) \quad (30)$$

$$\Delta f_{s_x/S_T}^q(x, k_\perp) \equiv h_1^q(x, k_\perp) + \frac{k_\perp^2}{2M^2} h_{1T}^{\perp q}(x, k_\perp). \quad (31)$$

$h_{1T}^\perp$  is also denoted ‘‘pretzelosity’’, due to the typical shapes it produces in the proton rest frame [115, 116], while  $h_{1L}^\perp$  and  $g_{1T}^\perp$  are denoted ‘‘worm-gear’’ TMDs [117], as they relate quark and proton polarisations which are (almost) orthogonal.

In the collinear limit only the unpolarised, the helicity and the transversity TMDs do not vanish. Upon integration over  $d^2\mathbf{k}_\perp$  they give the usual collinear PDFs:

$$\int d^2\mathbf{k}_\perp f_{q/p}(x, k_\perp) = f_{q/p}(x) \equiv q(x) \equiv f_1^q(x) \quad (32)$$

$$\int d^2\mathbf{k}_\perp \Delta f_{s_z/S_L}^q(x, k_\perp) = \Delta q(x) \equiv g_{1L}(x) \quad (33)$$

$$\int d^2\mathbf{k}_\perp h_1^q(x, k_\perp) = \Delta_T q(x) \equiv h_1(x). \quad (34)$$

### 3.1.2 Gluon TMD-PDFs

We have so far only considered quarks TMDs, but similar quantities can be defined also for gluons [118, 119]. Again, there are 8 leading-twist TMDs, despite the fact that no transverse polarisation can exist for massless particles; its role is somewhat replaced by linear polarisation. We simply list here the gluon TMDs which have received more attention lately, pointing out several useful references, without any further discussion.

- The TMD-PDF for unpolarised gluons inside an unpolarised proton is usually written as

$$f_1^g(x, k_\perp) \equiv f_{g/p}(x, k_\perp) \equiv g(x, k_\perp). \quad (35)$$

- Analogously to the quark Sivers distribution one has the gluon Sivers distribution,

$$\Delta^N f_{g/p^\uparrow}(x, k_\perp) \equiv -\frac{2k_\perp}{M} f_{1T}^{\perp g}(x, k_\perp). \quad (36)$$

A review paper on the status and future prospects of the gluon Sivers function can be found in Ref. [120].

- The quantity denoted by  $h_1^{\perp g}(x, k_\perp)$  is somewhat the analogous of the Boer-Mulders distribution  $h_1^{\perp q}$ : it is related to the distribution of linearly polarised gluons inside an unpolarised proton and it can lead to several azimuthal asymmetries in heavy quark pair production in unpolarised  $e p$  and  $p p$  collisions [121, 122, 123, 124], and to typical transverse momentum distributions of Higgs bosons at LHC [125, 126, 127].
- The gluon TMD helicity distribution is similar to the quark TMD helicity distribution:

$$\Delta f_{s_z/S_L}^g(x, k_\perp) \equiv \Delta g(x, k_\perp). \quad (37)$$

Its integrated collinear version  $\Delta g(x)$ , plays an important role in several processes with longitudinal polarisation, which are not considered here.

### 3.1.3 TMD-FFs

Analogously to the distributions of quarks and gluons in a nucleon, also the fragmentation process of a parton into hadrons is not, in general, a collinear event; in many cases the transverse degrees of freedom can be safely integrated, leading to a 1-dimensional fragmentation function, usually denoted as  $D_1^q(z, Q^2)$  or  $D_{h/q}(z, Q^2)$ , which only depends, apart from the scale of the process, on the light-cone momentum fraction of the fragmenting quark taken away by the hadron.

Introducing the transverse momentum  $\mathbf{p}_\perp$  of the final hadron within the jet created in the quark hadronisation process, allows new transverse degrees of freedom. We consider the simple case of a final spinless or unpolarised hadron and refer to Fig. 13 as a guide for the TMD-FFs, like we did in Eq. (21). In this case we have less (pseudo)-vectors at our disposal and the most general, parity invariant expression for the TMD-FF can be written as:

$$D_{h/q, \mathbf{s}_q}(z, \mathbf{p}_\perp; \mathbf{s}_q) = D_{h/q}(z, p_\perp) + \frac{1}{2} \Delta^N D_{h/q^\uparrow}(z, p_\perp) \mathbf{s}_q \cdot (\hat{\mathbf{p}}_q \times \hat{\mathbf{p}}_\perp) \quad (38)$$

$$= D_{h/q}(z, p_\perp) + \frac{p_\perp}{zM_h} H_1^{\perp q} \mathbf{s}_q \cdot (\hat{\mathbf{p}}_q \times \hat{\mathbf{p}}_\perp). \quad (39)$$

Eqs. (38) and (39) show, in two different notations [16, 12], the Collins distribution [93], which correlates the transverse spin of the fragmenting quark with the final hadron transverse momentum in the jet. The quantities  $\Delta^N D_{h/q^\uparrow}$  or, often,  $H_1^{\perp q}$  are referred to as the Collins function (38) [16]. A recent and most comprehensive review paper on parton FFs can be found in Ref. [87].

In the case of the fragmentation of a quark into a spin 1/2 hadron, one has, similarly to the 8 TMD-PDFs, 8 independent TMD-FFs (see Ref. [87] and references therein). We only mention here the so-called ‘‘polarising fragmentation function’’, describing the fragmentation of an unpolarised quark into a polarised spin 1/2 hadron, with spin  $\mathbf{S}_h$ . Analogously to the Collins distribution and two different notations [88, 12], it is defined as

$$D_{h, \mathbf{S}_{h/q}}(z, \mathbf{p}_\perp; \mathbf{S}_h) = \frac{1}{2} D_{h/q}(z, p_\perp) + \frac{1}{2} \Delta^N D_{h^\uparrow/q}(z, p_\perp) \mathbf{S}_h \cdot (\hat{\mathbf{p}}_q \times \hat{\mathbf{p}}_\perp) \quad (40)$$

$$= \frac{1}{2} D_{h/q}(z, p_\perp) + \frac{p_\perp}{zM_h} D_{1T}^{\perp h/q} \mathbf{S}_h \cdot (\hat{\mathbf{p}}_q \times \hat{\mathbf{p}}_\perp). \quad (41)$$

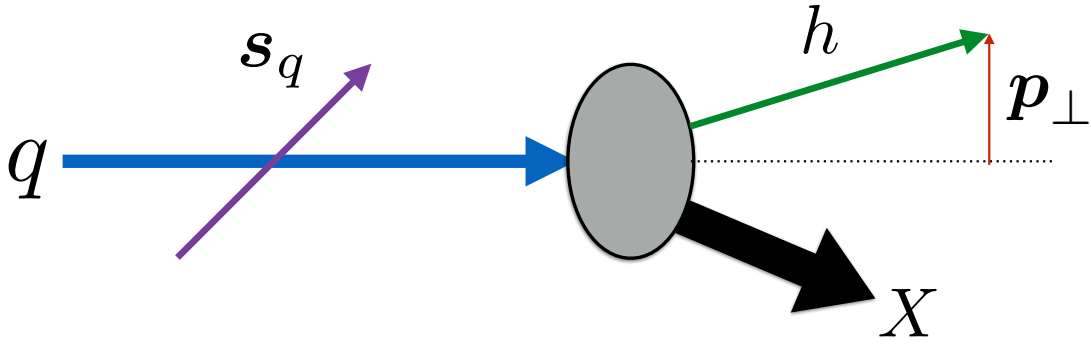


Figure 13: Usual graphical representation of the TMD-FF for a quark with spin vector  $\mathbf{s}_q$  which fragments into a hadron  $h$  with transverse momentum  $\mathbf{p}_\perp$  inside the jet,  $\mathbf{p}_h = z \mathbf{p}_q + \mathbf{p}_\perp$ .

The polarising fragmentation function  $\Delta^N D_{h^\dagger/q}$ , or  $D_{1T}^{\perp h/q}$ , might be responsible for the polarisation of the  $\Lambda$ s observed in the interactions of unpolarised nucleons [88]. As briefly discussed in Section 3.4, it could be accessed in  $e^+e^- \rightarrow \Lambda^\dagger X$  processes.

### 3.2 How to interpret spin data in SIDIS

In the previous Sections we have presented clear experimental evidence showing the necessity of considering, for the QCD partonic structure of nucleons in high energy inclusive processes, the full 3-dimensional motion of quarks and gluons. We do not address here the issue of the partonic distribution in coordinate space, which can be explored in exclusive processes [128]. We have introduced the TMD formalism appropriate to investigate and codify the 3D nucleon internal momentum structure. It is worth mentioning that the first parton model ideas date back exactly to 50 years ago [129], and, since then, despite many QCD successes and tests, not much progress has been achieved in understanding the proton and neutron inner composition.

SIDIS processes are the main source of information on the nucleon structure in momentum space. The SIDIS cross section has, at leading one photon exchange order, a well defined and rich expression, Eq. (1). Thanks to the TMD factorisation scheme, in the energy region in which  $P_T \simeq k_\perp \ll \sqrt{Q^2}$  [130], the form factors in Eq. (1) can be written as convolutions of TMD-PDFs and TMD-FFs. Then, by comparing Eq. (1), in which the TMDs have been inserted, with experimental data, one learns about the TMDs. Actually, it is very useful to consider the azimuthal moments of the spin asymmetries given in Eq. (3), which isolate a single form factor at a time, like in Eqs. (4) and (5). The full expressions of the form factors  $F_{UU}$  and  $F_{UT}$  as TMD convolutions can be found in Refs. [15, 16]. Notice, that three of the form factors of Eq. (1), that is  $F_{UU}^{\cos \phi_h}$ ,  $F_{UT}^{\sin \phi_S}$  and  $F_{UU}^{\sin(2\phi_h - \phi_S)}$ , are of  $\mathcal{O}(k_\perp/Q)$ . Also, as we are only considering nucleons transversely polarised ( $S_L = 0$ ,  $S_T = 1$ ) and unpolarised leptons, the TMDs  $g_{1L}$ ,  $g_{1T}^\perp$  and  $h_{1L}^\perp$  do not contribute to Eq. (1); they contribute to SIDIS cross sections with longitudinally polarised leptons and/or nucleons.

We concentrate here on the TMD interpretation of the form factors in Eq. (1) which have been clearly found not to be negligible and have large experimental support: they correspond to the unpolarised quark TMD, the Sivers function, the Collins function and the transversity distribution. Limited experimental information is also available for the Boer-Mulders function. Actually, some experimental data exist for all the other structure functions and TMDs [131, 132], but most of them are very small and compatible with zero.

At  $\mathcal{O}(k_\perp/Q)$ , the unpolarised cross section from Eq. (1) is given by [15, 16]:

$$\begin{aligned} \frac{d\sigma^{\ell+p \rightarrow \ell' h X}}{dx_B dQ^2 dz_h dP_T^2} &= \frac{2\pi^2 \alpha^2}{Q^4} [1 + (1-y)^2] F_{UU} \\ &= \frac{2\pi^2 \alpha^2}{Q^4} [1 + (1-y)^2] \\ &\times \sum_q e_q^2 \int d^2 \mathbf{k}_\perp d^2 \mathbf{p}_\perp \delta^{(2)}(\mathbf{P}_T - z_h \mathbf{k}_\perp - \mathbf{p}_\perp) f_{q/p}(x, k_\perp) D_{h/q}(z, p_\perp) \end{aligned} \quad (42)$$

where  $x_B = x$ ,  $z_h = z$  and  $\mathbf{p}_\perp = \mathbf{P}_T - z \mathbf{k}_\perp$ .

Notice that this expression can be derived from the TMD parton model expression [133]:

$$\frac{d\sigma^{\ell+p \rightarrow \ell' h X}}{dx_B dQ^2 dz_h d^2 \mathbf{P}_T} = \sum_q \int d^2 \mathbf{k}_\perp f_{q/p}(x, k_\perp) \frac{d\hat{\sigma}^{\ell q \rightarrow \ell q}}{dQ^2} D_{h/q}(z, p_\perp), \quad (43)$$

which shows the explicit convolution of the TMD-PDFs, the TMD-FFs and the cross section for the elementary process:

$$\frac{d\hat{\sigma}^{\ell q \rightarrow \ell q}}{dQ^2} = e_q^2 \frac{2\pi \alpha^2}{Q^4} [1 + (1-y)^2] + \mathcal{O}(k_\perp/Q). \quad (44)$$

The terms of  $\mathcal{O}(k_\perp/Q)$  give a dependence on  $\phi_h$  to Eq. (43) [133, 16], which vanishes in Eq. (42), which is integrated over  $\phi_h$ . Eq. (42) will be used to relate data on hadron multiplicities in unpolarised SIDIS with the unpolarised TMD-PDFs,  $f_{q/p}(x, k_\perp)$ , and TMD-FFs,  $D_{h/q}(z, p_\perp)$ .

The Sivers effect, that is the correlation between the proton spin and the parton transverse momentum, is hidden in the  $F_{UT}^{\sin(\phi_h - \phi_S)}$  term of Eq. (1). One could use the  $\sin(\phi_h - \phi_S)$  azimuthal moment of Eq. (4), together with the expression of  $F_{UT}^{\sin(\phi_h - \phi_S)}$  in [15, 16] to relate the Sivers function with data. Or, one can simply use the analogous of Eq. (43) in case of a transversely polarised proton [133]:

$$\frac{d\sigma^{\ell+p^\uparrow \rightarrow \ell' h X}}{dx_B dQ^2 dz_h d^2 \mathbf{P}_T d\phi_S} = \frac{1}{2\pi} \sum_q \int d^2 \mathbf{k}_\perp f_{q/p^\uparrow}(x, \mathbf{k}_\perp) \frac{d\hat{\sigma}^{\ell q \rightarrow \ell q}}{dQ^2} D_{h/q}(z, p_\perp), \quad (45)$$

inserting the Sivers distribution  $f_{q/p^\uparrow}(x, \mathbf{k}_\perp)$  given in Eq. (23). Then, from Eq. (3), one has:

$$A_{UT}^{\sin(\phi_h - \phi_S)} = \frac{\sum_q \int d\phi_S d\phi_h d^2 \mathbf{k}_\perp \Delta^N f_{q/p^\uparrow}(x, k_\perp) (\hat{\mathbf{P}} \times \hat{\mathbf{k}}_\perp) \cdot \mathbf{S} \frac{d\hat{\sigma}^{\ell q \rightarrow \ell q}}{dQ^2} D_q^h(z, p_\perp) \sin(\phi_h - \phi_S)}{\sum_q \int d\phi_S d\phi_h d^2 \mathbf{k}_\perp f_{q/p}(x, k_\perp) \frac{d\hat{\sigma}^{\ell q \rightarrow \ell q}}{dQ^2} D_q^h(z, p_\perp)}. \quad (46)$$

The momentum dependence  $(\hat{\mathbf{P}} \times \hat{\mathbf{k}}_\perp) \cdot \mathbf{S}$  of the Sivers distribution (23) gives a factor  $\sin(\varphi - \phi_S)$ , where  $\varphi$  is the azimuthal angle of  $\mathbf{k}_\perp$ . It is this factor which generates, when integrating  $(d\sigma^\uparrow - d\sigma^\downarrow)$  over  $d^2 \mathbf{k}_\perp$ , the typical  $\sin(\phi_h - \phi_S)$  dependence of the Sivers effect. Eq. (46), which could be further simplified, relates data on  $A_{UT}^{\sin(\phi_h - \phi_S)}$  to a convolution of the Sivers function  $\Delta^N f_{q/p^\uparrow}(x, k_\perp)$  with the unpolarised TMD-PDF. It will be used for extracting information on  $\Delta^N f_{q/p^\uparrow}(x, k_\perp)$ .

In a similar way, one can extract from Eq. (1) and the azimuthal moment (5) information on the structure function  $F_{UT}^{\sin(\phi_h + \phi_S)}$  which depends on the Collins function [15, 16]. Equivalently, one can follow the approach of Refs. [16, 134] which start by writing the SIDIS cross section in terms of helicity amplitudes, keeping into account all phase factors which appear in the different stages of the process.

From Eqs. (3) one obtains [16, 134]:

$$A_{UT}^{\sin(\phi_h+\phi_S)} = \frac{\sum_q e_q^2 \int d\phi_h d\phi_S d^2\mathbf{k}_\perp \Delta_{Tq}(x, k_\perp) \frac{d(\Delta\hat{\sigma})}{dQ^2} \Delta^N D_{h/q^\uparrow}(z, p_\perp) \sin(\phi_S + \varphi + \phi_q^h) \sin(\phi_h + \phi_S)}{\sum_q e_q^2 \int d\phi_h d\phi_S d^2\mathbf{k}_\perp f_{q/p}(x, k_\perp) \frac{d\hat{\sigma}}{dQ^2} D_{h/q}(z, p_\perp)}, \quad (47)$$

where

$$\frac{d(\Delta\hat{\sigma})}{dQ^2} \equiv \frac{d\hat{\sigma}^{\ell q^\uparrow \rightarrow \ell q^\uparrow}}{dQ^2} - \frac{d\hat{\sigma}^{\ell q^\uparrow \rightarrow \ell q^\downarrow}}{dQ^2} = \frac{4\pi\alpha^2}{Q^4} (1 - y) \quad (48)$$

is the transverse spin transfer in the elementary interaction.

Eq. (47) describes the asymmetry in a process in which a transversely polarised quark inside a transversely polarised proton scatters off an unpolarised lepton and then, with the remaining transverse polarisation, fragments into the final observed hadron  $h$ . In the TMD factorisation scheme it is a convolution of the TMD transversity with the spin transfer in the elementary interaction and the Collins TMD-FF. The azimuthal dependence  $\sin(\phi_S + \varphi + \phi_q^h)$  is a subtle effect which arises from the combination of phase factors in the transversity distribution function, the elementary interaction and the Collins distribution (38);  $\phi_q^h$  can be written in terms of  $\phi_h$  and  $\varphi$  [16].

Eq. (47) relates the measured asymmetry  $A_{UT}^{\sin(\phi_h+\phi_S)}$  to a convolution of the transversity distribution and the Collins fragmentation; it has allowed the first ever extraction of the transversity distribution  $\Delta_{Tq}(x) = h_1^q(x)$  [134], which is not accessible in DIS, due to its chiral odd nature. Independent information on the Collins function can be obtained in  $e^+e^- \rightarrow h_1 h_2 X$  processes.

Eqs. (42), (46) and (47) allow to get information on the unpolarised, the Sivers and the transversity TMDs. They are coupled to unpolarised TMD-FFs or to the Collins TMD-FF. Independent information on these quantities can be obtained from  $e^+e^-$  annihilation processes.

Similar relations to SIDIS observables can be found for the other TMDs [15, 16]; in particular the Boer-Mulders function, which contributes to  $F_{UU}^{\cos 2\phi_h}$ , has been studied [135, 136] and some data are available [137, 138, 139, 140, 141]. We do not discuss here these TMDs; in Sections 3.5, 4.1, 4.2 and 4.3 we look in more details at our actual knowledge of the Collins, the unpolarised, the Sivers and the transversity TMDs, emphasising what we learn from them about the nucleon structure.

### 3.3 How to interpret spin data in hard $NN$ collisions

As anticipated in Sec 2.2, hadronic collisions are more challenging to interpret in the TMD framework than the SIDIS process. Single scale processes, like the TSSA  $A_N$  or the inclusive production of polarised  $\Lambda$ 's in unpolarised  $pp$  scattering, can be described in a collinear framework. The mechanisms generating TSSA's in a collinear framework only enter at sub-leading twist, *i.e.* twist-3. To get further insights into this statements, it is valuable to consider the necessary ingredients for the existence of transverse spin effects.

In particular TSSAs require one helicity-flip amplitude and a phase shift between two amplitudes in order not to vanish. This is because TSSAs are related to matrix elements that are off-diagonal in the helicity basis due to decompositions of the kind:

$$|\uparrow\rangle / |\downarrow\rangle = (|+\rangle \pm |-\rangle) / \sqrt{2} \Rightarrow |\uparrow\rangle \langle\uparrow| - |\downarrow\rangle \langle\downarrow| = |+\rangle \langle-| + |-\rangle \langle+|. \quad (49)$$

Therefore, non-zero TSSAs require a non-vanishing helicity-flip amplitude. It was realised early on that such helicity-flip amplitudes are suppressed, in QCD or QED high energy scatterings, by factors  $m_q/\sqrt{Q^2}$ . This leads to the well-known suggestion of the measurement of TSSAs as a test of QCD by Kane, Pumplin and Repko [32]. Furthermore, TSSAs are so-called naive T-odd observables, since they

are T-odd if one does not consider the full final state, which is the case in semi-inclusive measurements. Only the imaginary part of the matrix element can contribute to T-odd effects. Since this needs the interference of amplitudes with a relative phase shift, another crucial ingredient to TSSAs are initial or final state interactions introducing such a shift. These interactions introduce a factor of  $\alpha_s$ , which is another reason to look for interactions in the non-perturbative regime for the sources of these asymmetries. It also shows that the TSSAs probe QCD at the amplitude level. At twist-3, the interference term can be generated by handbag diagrams, where an additional parton is exchanged on one side. For the initial state, an example of this is shown in Fig. 14 which is discussed in the next Section along with the respective twist-3 correlator. In the case of the TMD picture, model calculations show that at a microscopic level, initial and final state interactions, in Drell-Yan and SIDIS processes respectively, indeed provide the necessary phase shift [142, 143, 144, 145].

Intuitively, one can also expect the twist-3 framework and the TMD framework to be related since an integration over the intrinsic transverse momenta in the TMD framework should contribute to the asymmetries described in the twist-3 framework. And indeed, those exist in general via the Wandzura-Wilczek relations [35] as well as more specific relations in the case of the Sivers function and the Collins asymmetries, as will be discussed later in this section. The di-hadron TSSAs described here, are an exception, in that they can be described in a leading twist collinear framework. They are not sensitive to TMDs but to the collinear transversity  $h_1(x)$  coupling to a collinear FF. In this case, the additional degrees of freedom in the di-hadron final state plays a similar role as the polarisation degrees of freedom in semi-inclusive polarised hadron production, where the polarisation is measured with respect to the production plane and the necessary interference term comes from the amplitudes in which hadron pairs are produced with different relative angular momentum.

In  $NN$  processes with a large and a small scale, the TMD factorisation picture can be appropriate. However, an important difference to the SIDIS process is that hard hadronic collisions have two color charges in the initial state. If the final state also contains a color charge, *i.e.* in the production of hadrons, TMD factorisation becomes more problematic, leading to modified universality [42, 100] due to a phenomenon sometimes called “color entanglement”. However, for the “hadron-in-jet” measurements discussed here, recent theoretical progress indicates that the TMD framework is applicable [146]. On the other side of the spectrum, Drell-Yan and  $W/Z$  production can be seen as the crossed-channel analogue of the SIDIS process and can thus naturally be interpreted in the TMD framework. The difference in color flow is still present; however, the universality modification can be calculated and reduces to a sign flip of the observable.

Another complication in the interpretation of hadronic scattering observables should be mentioned. The initial partonic kinematics are not directly accessible, which means that observables are inherently convolutions over the initial kinematics. In the case of final state fragmentation, three non-perturbative functions are entering the cross-section. Since gluons enter the cross-section at leading order in hadronic collisions, the cross-sections can also contain convolutions over gluon PDFs and FFs which are less well known than their quark counterparts, injecting additional uncertainties. Keeping these points in mind, below the interpretation of the observables introduced in Sec 2.2 will be discussed.

### 3.3.1 Asymmetries in $p^\uparrow N \rightarrow h X$ processes

The first attempts of explaining the large observed TSSAs in  $p^\uparrow N \rightarrow h X$  were based on twist-3 matrix elements of the quark and gluon fields of the initial state by Efremov and Teryaev [147] and Qiu and Sterman [148, 149]. These twist-3 matrix elements encode three-parton correlations, *e.g.* quark-gluon-quark correlations represented by the handbag diagram shown in Fig. 14. In these handbag diagrams, an additional leg connects the outgoing quark to the blob representing the unobserved hadronic final state,  $X$ . Relevant here is the case when this leg is a gluon. The half of the handbag diagram with the extra leg therefore represents an amplitude with a final state interaction of the outgoing quark with  $X$ ,

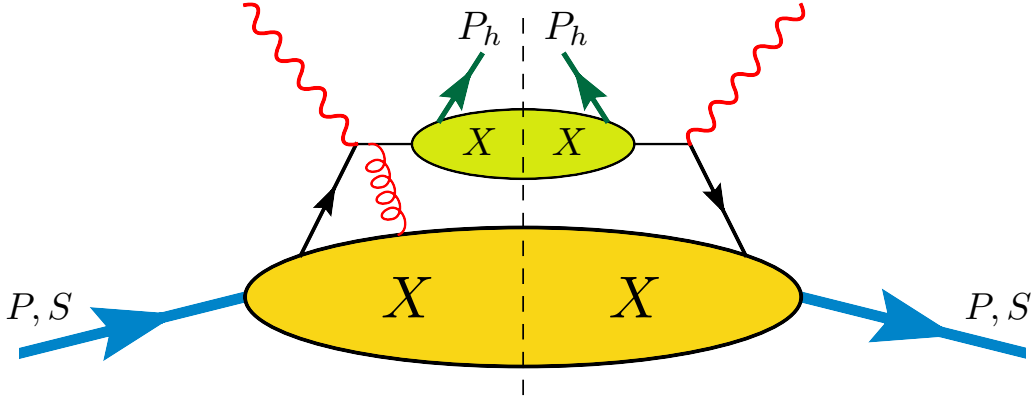


Figure 14: Quark-gluon-quark correlator contributing to inclusive processes at twist-3. The upper blob symbolizes the fragmentation process.

which is related to model calculations of TMDs [142]. Such an object would be expected to depend on the momentum fractions carried both by the gluon and by the quark; however, it turns out that the TSSAs receive their dominant contribution from the region in which the gluon is very soft. Therefore the gluon does not transmit momentum, but merely leads to the needed phase shift. These matrix elements are therefore known as the soft-gluon pole (SGP), or Efremov-Teryaev-Qiu-Sterman (ETQS) matrix elements  $T_F(x, x)$ . In general, twist-3 correlations are dependent on two partonic momentum fractions, but due to the softness of the exchanged gluon momentum, they can be taken as equal. The phase shift imparted by the gluon bears resemblance to the model calculations for the Sivers effect of Ref. [142] and therefore it might not be surprising that  $T_F$  can be related to the Sivers function [144, 97, 96, 150] in the kinematic region where both formalism are valid, *i.e.* at intermediate  $p_T$ ,  $\Lambda_{\text{QCD}} < p_T < Q$ , according to the relation:

$$g T_F(x, x) = - \int d^2 \mathbf{k}_\perp \frac{k_\perp}{M} f_{1T}^\perp(x, k_\perp). \quad (50)$$

Once the Sivers function was extracted with sufficient precision from SIDIS data, it also became clear that the ETQS matrix elements were not the dominant mechanism behind the large TSSAs of hadrons [151]. There was even a “sign mismatch” between the values of  $T_F(x, x)$  requested by the  $A_N$  data and the values obtained by inserting the Sivers function into Eq. (50) [152]. It should be mentioned, that SGPs can also come from  $ggg$  correlations [153] and that another pole contribution in the initial state, the soft-fermionic pole (SFP), was considered as well [154], but both, the  $ggg$  and the SFP contributions, also proved to be insufficient to explain the magnitude of  $A_N$  [153, 155, 156]. Other sizeable contributions might be expected from TMD effects in the fragmentation process. However, when fragmentation contributions do not play a role, such as in the production of prompt photons discussed in Sec. 3.3.2, the ETQS mechanism should be dominating and can shed light on the Sivers function in hadronic interactions.

An early attempt to include both initial state contributions as well as fragmentation contributions was performed in the framework of the so-called Generalized Parton Model (GPM) [119, 157] which is essentially an extension of the SIDIS TMD framework to various observables in  $pp$ . A review on the interpretation of hadronic interactions in the GPM can be found in Refs. [157, 158] and a study of the contribution of Collins and Sivers TMDs to  $A_N$  in such a scheme can be found in Refs. [159, 160].

A modified version of the GPM, which takes into account colour factors due to initial and final state interaction, is the so-called colour gauge invariant (CGI) GPM [161, 162], which leads to non universality of the TMDs. This modified universality, *e.g.* of the Sivers function, was implemented via the respective color factors in Ref. [162]. However, by construction this model misses other twist-3

contributions to  $A_N$  which do not have a leading twist TMD counterpart. Additionally, factorisation is only assumed.

The first calculation of the fragmentation contribution at twist-3 was performed in Ref [163]. As other twist-3 functions, they can generally be decomposed into so-called intrinsic, kinematical and dynamical parts. However, these parts are not independent from each other, so that the transverse spin dependent cross-section can be written in terms of  $H_1^{\perp(1)}$  and  $\tilde{H}$ . Here  $H_1^{\perp(1)}$  is the kinematical contribution, which can be written in terms of the  $\mathbf{k}_T$  integrated Collins FF. The dynamical contribution  $\tilde{H}$  describes quark-gluon-quark correlations. In terms of these functions, as well as the ETQS function  $T_F$  describing the initial state spin-dependent dynamics at twist-3, the transverse polarisation dependent cross section can be expressed as [36]:

$$d\Delta\sigma^{pp\rightarrow\pi X}(\mathbf{S}_T) = \frac{2|\mathbf{P}_{hT}|\alpha_s}{S} \sum_{i,a,b,c} \int_{z_{\min}}^1 \frac{dz}{z^3} \int_{x_{\min}} \frac{dx}{x} \frac{1}{x'} \frac{1}{xS + U/z} f_1^b(x') \left[ M_h h_1^a(x) \mathcal{H}^{\pi/c,i}(x, x'z) + \frac{M}{\hat{u}} \mathcal{F}^{a,i}(x, x', z) D_1^{\pi,c}(z) \right]. \quad (51)$$

Here  $\Delta\sigma(\mathbf{S}_T) = \sigma(\mathbf{S}_T) - \sigma(-\mathbf{S}_T)$  and  $\mathbf{P}_{hT}$  is chosen along the  $x$ -axis whereas  $\mathbf{S}_T$  is chosen along the  $y$ -axis so that  $\Delta\sigma$  is related to the observable  $A_N = \Delta\sigma/(\sigma(\mathbf{S}_T) + \sigma(-\mathbf{S}_T))$ . The indices  $a, b, c$  run over the partons participating in the hard scattering. Parton  $a$  is taken from the polarised proton and parton  $b$  from the unpolarised one, with parton  $c$  fragmenting into the observed pion. The index  $i$  runs over the different hard scattering processes. The elementary parton cross sections, which are dependent on the partonic Mandelstam variables  $\hat{s} = x x' S$ ,  $\hat{t} = x T/z$ ,  $\hat{u} = x' U/z$  with  $S = (P + P')^2$ ,  $T = (P - P_h)^2$ ,  $U = (P' - P_h)^2$ , are encapsulated in the ‘‘hard factors’’  $F = \{H, H_1^\perp, T_F\}$ ,  $S_F^i$  and  $\tilde{S}_F^i$ . They are explicitly given in Ref. [36]. Here  $P, P'$  are the initial four-momenta of the protons involved in the scattering and  $P_h$  the four-momentum of the outgoing hadron. The lower integration limits are  $x_{\min} = -(U/Z)(T/Z + S)$  and  $z_{\min} = -(T + U)/S$ . The momentum fraction  $x'$  of the unpolarized parton  $b$  is related to a given momentum fraction  $x$  of parton  $a$  by  $x' = -(xT/z)/(xS + U/z)$ . The functions  $\mathcal{F}$  and  $\mathcal{H}$  describe the spin-dependent, non-perturbative dynamics of the initial and final state, respectively

$$\mathcal{F}^a(x, x', z) = \pi \left[ T_F^a(x, x) - x \frac{dT_F^a(x, x)}{dx} \right] S_{T_F}^i \quad (52)$$

and

$$\mathcal{H}(x, x', z) = \left[ H_1^{\perp(1)}(z) - z \frac{dH_1^{\perp(1)}(z)}{dz} \right] \tilde{S}_{H_1^\perp}^i + \left[ -2H_1^{\perp(1)}(z) + \frac{1}{z} \tilde{H}(z) \right] \tilde{S}_H^i. \quad (53)$$

The functions have been calculated using a Wandzura-Wilczek approximation [36] and, with input for  $H^{\perp(1)}$  and  $h_1$  using a recent global fit [107], numerical estimates for  $A_N$  have been obtained. Figure 15 shows these estimates compared with some  $A_N$  data from RHIC. Note that these curves are not fits, but estimates based on previous extractions of transversity and the Collins FF. As is shown in the figure, the leading uncertainty originates from the uncertainty on  $h_1$  which is probed in a kinematic regime at high  $x$  that is not well constrained yet from existing data. Conversely, this illustrates the opportunity to constrain transversity from existing  $A_N$  data from RHIC.

### 3.3.2 Asymmetries in $\gamma^*$ , $W/Z$ , $\gamma$ production

Similar to the expansion of the structure functions in the SIDIS case, *e.g.* for  $F_{UU}$  given in Eqs. (42), the structure functions for Drell-Yan and  $W$  production given in Eqs. (8), (9) and (12) can be expanded at  $\mathcal{O}(k_\perp/Q^2)$  in terms of TMDs. The main difference to the SIDIS case is that the terms entering this expansion are now convolutions of the TMDs describing the parton distributions in the two interacting

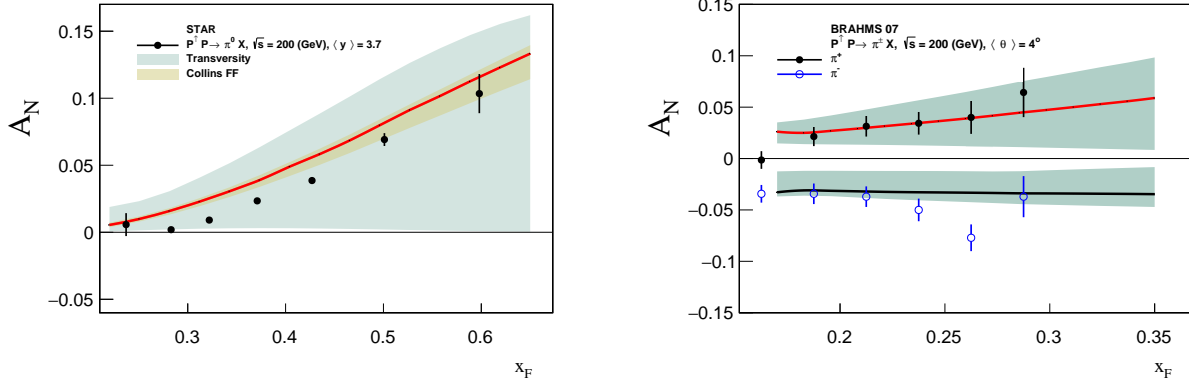


Figure 15: Calculations of  $A_N$  for  $\pi^0$  at  $\sqrt{s} = 200$  GeV compared with STAR data (left) and for charged pions compared with Brahm's data (right) [36]. The calculations show quite a good agreement with the data. The main source of uncertainty comes from the poor knowledge of  $h_1$  and  $H_1^\perp$  in the kinematic regime probed. Figure from Ref. [36].

protons, while in the SIDIS case those are convolutions of PDFs and FFs. This reflects the fact that D-Y and  $W$ -production are  $s$ -channel processes, while SIDIS is a  $t$ -channel process. The difference in color flow between them, coloured states in the initial vs. final state, leads to the predicted modified universality of TMD functions measured in D-Y or  $W$ -production compared to SIDIS, most notably the sign change of the Sivers function [41, 142, 143], Eq. (82).

The notation used here will not distinguish between the TMDs measured in D-Y/ $W$  and SIDIS. Focusing first on the experimentally relevant transverse single spin asymmetry in the case where the angular distribution of the final state leptons is integrated out, the structure function  $F_{UT}^{\sin(\phi_V - \phi_S)}$  can be written, in the aforementioned approximation, as:

$$F_{UT}^{\sin(\phi_V - \phi_S)} = C [f_1 f_{1T}^\perp] \text{ (DY)} \quad (54)$$

and

$$F_{UT}^{\sin(\phi_V - \phi_S)} = C^W 2 [f_1 f_{1T}^\perp] \text{ (W-production)}. \quad (55)$$

Here the Sivers function of the polarized hadron  $A$  in the reaction is probed and the azimuthal angles are defined in Sec. 2.2.2. The convolution over transverse momenta, again analogous to the SIDIS expression in (42), is given by

$$\begin{aligned} & \mathcal{C}[w(\mathbf{k}_{a,\perp}, \mathbf{k}_{b,\perp}) f_1 \bar{f}_2] = \\ & \frac{1}{3} \sum_q e_q^2 \int d^2 \mathbf{k}_{a,\perp} d^2 \mathbf{k}_{b,\perp} \delta^{(2)}(\mathbf{q}_\perp - \mathbf{k}_{a,\perp} - \mathbf{k}_{b,\perp}) w(\mathbf{k}_{a,\perp}, \mathbf{k}_{b,\perp}) [f_1^q(x_a, \mathbf{k}_{a,\perp}) \bar{f}_2^{\bar{q}}(x_b, \mathbf{k}_{b,\perp}) + q \leftrightarrow \bar{q}] , \end{aligned} \quad (56)$$

where  $\mathbf{q}$  is the momentum of the virtual photon. The weight function  $w$  is introduced for completeness and later use; in the case of the SSA that is sensitive to the Sivers function it is unity. For  $W$  production the convolution integral has to be modified to respect the coupling of the weak force. It reads:

$$\begin{aligned} & \mathcal{C}^W[w(\mathbf{k}_{a,\perp}, \mathbf{k}_{b,\perp}) f_1 \bar{f}_2] = \\ & \frac{1}{3} |V_{qq'}| \sum_{q,q'} \int d^2 \mathbf{k}_{a,\perp} d^2 \mathbf{k}_{b,\perp} \delta^{(2)}(\mathbf{q}_\perp - \mathbf{k}_{a,\perp} - \mathbf{k}_{b,\perp}) w(\mathbf{k}_{a,\perp}, \mathbf{k}_{b,\perp}) [f_1^q(x_a, \mathbf{k}_{a,\perp}) \bar{f}_2^{\bar{q}'}(x_b, \mathbf{k}_{b,\perp}) + q \leftrightarrow \bar{q}'] , \end{aligned} \quad (57)$$

where  $V_{qq'}$  is the relevant entry in the CKM matrix. Also note that the sum now runs over all flavour combinations.  $Z$  production is not considered here, but the corresponding expression can be found in Ref. [39]. Eq. (55) acquires a factor of two compared to (54) due to the different coupling constants of the weak force.

As discussed in Sec. 2.2.2, further information about TMDs can be gained from the dependence of the unpolarised structure function on the decay angles of the leptons in the D-Y process. Here we use the angles in the Collins-Soper frame. In this frame, the  $\cos 2\phi_{CS}$  modulation of the cross-section is sensitive to the Boer-Mulders functions of the colliding hadrons as

$$F_{UU}^{\cos 2\phi_{CS}} = C \left[ \frac{(\mathbf{h} \cdot \mathbf{k}_{a,\perp})(\mathbf{h} \cdot \mathbf{k}_{b,\perp}) - \mathbf{k}_{a,\perp} \cdot \mathbf{k}_{b,\perp}}{M_a M_b} h_1^\perp \bar{h}_1^\perp \right]. \quad (58)$$

The quantity  $\mathbf{h}$  is a shorthand notation for the unit vector  $\mathbf{q}_\perp/q_\perp$ .

In the D-Y limit  $Q^2 = 0$ , *i.e.* for real photon production, the TMD picture cannot be used anymore; instead, the ETQS matrix elements discussed in Sec. 3.3.1 can be accessed in transverse single spin asymmetries [164, 152, 63, 165]. The spin dependent part of the cross section for direct photon production, with  $\mathbf{P}_\gamma$  and  $E_\gamma$  denoting the photon momentum and energy, can be written as [63]:

$$\begin{aligned} \frac{d\Delta\sigma^{pp\rightarrow\gamma X}}{d^3\mathbf{P}_\gamma} &= \epsilon_{\alpha\beta} \mathbf{S}_T^\alpha \mathbf{P}_{\gamma\perp}^\beta \frac{\alpha_{\text{em}} \alpha_s}{E_\gamma s} \sum_{a,b} \int \frac{dx'}{x'} f_{b/B}(x') \int \frac{dx}{x} \left[ T_F^a(x, x) - x \frac{d}{dx} T_F^a(x, x) \right] \\ &\times \frac{1}{\hat{u}} S^{ab\rightarrow\gamma}(\hat{s}, \hat{t}, \hat{u}) \delta(\hat{s} + \hat{t} + \hat{u}), \end{aligned} \quad (59)$$

where  $\Delta\sigma = [\sigma(\mathbf{S}_T) - \sigma(-\mathbf{S}_T)]/2$  and  $S^{ab\rightarrow\gamma}$  is the hard factor of the process, which depends on the partonic Mandelstam variables and is explicitly given in Ref. [63]. Fragmentation photons can also contribute to the asymmetries, *e.g.* via the Collins effect, but the contribution by direct photons sensitive to the Sivers effect dominates [63]. In this process, similar to D-Y production, only initial state interactions are responsible for the phase shift in the QCD amplitude, leading to the transverse single spin asymmetry. Due to the connection between the ETQS functions and the Sivers function shown in Eq. (50), the production of direct photons in hadronic collisions can therefore also be used to test the sign-change of the Sivers function from SIDIS.

### 3.3.3 Asymmetries in di-hadron production

A detailed overview of Di-hadron FFs (DiFFs) can be found in Refs [65] and [87]. DiFFs can be introduced similarly to the TMD-FFs described in Sec. 3.1.3. If the production of two unpolarised hadrons  $h_{1,2}$  is considered, where each of the hadrons carry the light-cone momentum fraction  $z_i$  and the transverse momentum dependence is integrated over, the DiFFs depend on the quantities  $z = z_1 + z_2$ ,  $\zeta = (z_1 - z_2)/z$ ,  $\mathbf{R}_T^2$  and  $\phi_R$ . For the  $pp$  case discussed here,  $\mathbf{R}$  and  $\phi_R$  are defined in Sec. 2.2.3. The vector  $\mathbf{R}_T$  is the transverse projection of  $\mathbf{R}$ . At large invariant masses  $M_h$  of the two hadron system, the DiFFs can be calculated perturbatively and are connected to similar twist-3 matrix elements as the Collins FF at large transverse momentum [166]. The relevant case to explore the partonic structure of the nucleon is the regime in which  $M_h$  is small and the DiFFs are non-perturbative objects. Here, analogously to the TMD-FF regime where  $p_\perp$  is small, polarisation quantum numbers of the parent quark are imprinted in the correlations of the two hadrons. In this regime  $\zeta$  can be shown to be a linear polynomial in  $\cos\theta$ , with  $\theta$  the polar angle defined in Sec. 2.2.3, and the DiFFs can be expanded in partial waves [67]. Different partial waves carry different angular momentum quantum numbers; therefore, di-hadron fragmentation can be treated analogously to single hadron fragmentation with the corresponding angular momentum [167].

Similar to the expression for TMD-FFs in Eq. (38), the di-hadron FF of a transversely polarised quark with polarisation vector  $\mathbf{s}_q$  into unpolarised hadrons can then be written as

$$D_{h_1, h_2/q, \mathbf{s}_q}(z, \zeta, \mathbf{R}_T, \phi_R) = D_{h_1, h_2/q} + H_1^{\langle q} \frac{\mathbf{s}_q \cdot (\hat{\mathbf{p}}_q \times \mathbf{R}_T)}{M_h}. \quad (60)$$

It is important to note, that, unlike the single-hadron case, the transverse polarisation dependence does not vanish upon integration over transverse momenta. The shift in the strong phase, which is needed to generate the TSSA (see Sec. 3.3) can be understood in terms of the partial wave expansion as being generated by the interference of different partial waves. There have been several suggestions as to the channels which interfere in  $\pi^+\pi^-$  production [168, 169, 170], leading to different predicted  $M_h$  dependences. Data seems to prefer models similar to those of Refs. [169, 170], where the dominant contribution at the energy of current experiments originates from the interference of pions produced in a relative  $p$ -wave from  $\rho$  decay, with the non-resonant production in a relative  $s$ -wave. It should be mentioned that a similar  $M_h$  dependence can be generated from NJL models [69].

Since for DiFFs the transverse polarisation dependence survives upon integration over intrinsic transverse momenta and thus a collinear framework can be recovered, they are a natural way to extract the transversity distribution in  $pp$  collisions, where the partonic kinematics are not known a priori and can only be approximated from reconstructed jets. In  $pp$  processes at leading order the transverse polarisation dependent di-hadron production for small  $M_h$  can then be written as [37]:

$$d\sigma_{UT} \propto \sum_{a,b,c,d} |\mathcal{S}| \sin(\phi_{RS}) \int \frac{dx_a dx_b}{z_c} f_1^a(x_a) h_1^b \frac{d\Delta\hat{\sigma}_{ab^\dagger \rightarrow c^\dagger d}}{d\hat{t}} \sin\theta H_1^{\langle}(z, \cos\theta, M_h). \quad (61)$$

Here,  $a, b, c, d$  are the partons participating in the  $2 \rightarrow 2$  scattering and  $\phi_{RS}$  is the angle between  $\mathbf{R}_T$  and the polarisation of the proton, introduced in Sec. 2.2.3. Since the di-hadron asymmetries in  $pp$  can be interpreted in a collinear framework, where factorisation and evolution is presumably understood, they can be incorporated in a global analysis of transversity, which has been performed in Ref. [72], leading to the first global extraction of transversity from SIDIS,  $pp$  and  $e^+e^-$  annihilation data.

Because in  $pp$  collisions the partons dominantly interact via flavour blind gluon exchange,  $u$ -quark dominance, important in the case of SIDIS data with a proton target, is much less of a concern. Therefore,  $pp$  data can in principle give significant information on the  $d$ -quark transversity, which in current global extractions of transversity from SIDIS and  $e^+e^-$  data is mainly constrained from data taken on deuterium targets, which is very limited. However, while the overall uncertainty on  $h_1$  is reduced by the inclusion of  $pp$  data, the essentially unknown unpolarised gluon DiFFs, which appears in the denominator of the spin asymmetries in  $pp$ , leads still to quite large systematic uncertainties on the extracted values.

### 3.3.4 Asymmetries of jets and hadrons in jets

Intuitively, azimuthal asymmetries of hadrons within jets, as described in Sec. 2.2.4, should be sensitive to the Collins effect as it has been suggested in Refs. [75, 171]. If the jet axis can be identified with the outgoing quark direction, these measurements actually have an advantage compared to the corresponding SIDIS measurements, because the intrinsic quark momenta in the initial and the final state decouple. However, there are also challenges in the interpretation. On the one hand, as is typical in  $pp$  processes, a considerable range in  $x$  of the PDFs of the polarised and unpolarised proton is contributing. Jet reconstruction mitigates this issue somewhat, since the rapidity and the  $p_T$  of the reconstructed jet impose some constraints on this distribution. Additionally, there were questions about the validity of TMD factorisation in the context of more than 2 color charges participating in a  $2 \rightarrow 2$  process, due to an effect dubbed “color-entanglement” [42, 100], as already discussed in the

introduction. However, a recent re-evaluation of the hadron in jet observables [146] indeed showed that the TMD fragmentation functions entering the hadron in jet cross sections are universal. This supports the conclusion of Refs. [75, 171], which also argued that the Collins function would be the same as measured in SIDIS and  $e^+e^-$ . This finding is specific to TMD-FFs, where the separation of the color charges in the final state is large enough, so that there are no gluons reconnecting to the initial state TMDs.

A first study for the Collins and other asymmetries in jets has been presented in the context of the GPM [38], according to which the single polarised cross section for the  $p^\uparrow p \rightarrow (h, \text{jet})X$  process can be schematically written as:

$$\begin{aligned} \frac{d^6 \sigma^{p^\uparrow p \rightarrow (h, \text{jet})X}}{d^3 \mathbf{P}_{\text{jet}} dz d^2 \mathbf{P}_{hT}} &\propto \sum_{a,b,c,d} \int \frac{dx_a}{x_a} d^2 \mathbf{k}_{\perp a} \int \frac{dx_b}{x_b} d^2 \mathbf{k}_{\perp b} \delta(\hat{s} + \hat{t} + \hat{u}) \\ &\times \left( \hat{\sigma}_{\text{unp}}^{ab \rightarrow cd} f_{a/p^\uparrow}(x_a, \mathbf{k}_{\perp a}) f_1^b(x_b, k_{\perp b}) D_{h/c}(z, k_{\perp h}) \right. \\ &\quad \left. + \sin(\phi_S - \phi_h) \hat{\sigma}_{\text{pol}}^{ij \rightarrow kl} h_1^a(x_a, k_{\perp a}) f_1^b(x_b, k_{\perp b}) H_1^{\perp c}(z, k_{\perp h}) + \dots \right), \end{aligned} \quad (62)$$

where one recognises the TMD-PDFs and FFs defined in Eqs. (23), (25), (29) and (39).  $\phi_S$  and  $\phi_h$  are the azimuthal angles respectively of the transverse spin vector of the polarised hadron and the transverse momentum of the hadron relative to the jet, as described in Sec. 2.2.4. Later work [76] including TMD evolution agrees well with STAR data.

If in Eq. 62 the hadron  $\mathbf{P}_{hT}$  is integrated over and only the dependence on  $\phi_S$  is considered, sensitivity to the Sivers functions is obtained in the GPM [160]. However, the applicability of this framework for  $pp$  processes is limited. As we already commented, this is for instance due to questions about the validity of factorisation and universality. Additionally, in the case of the Sivers measurement in jets, only a single hard scale, the jet  $P_T$ , is measured. Then, it might be considered more natural to use the collinear twist-3 approach; calculations within this framework [172] seem to agree with the AnDY results [78]. Since the color factors in the twist-3 framework have a correspondence to the Wilson lines entering in the TMD framework, which lead to the modified universality (the sign change), the jet  $A_N$  has been claimed to be the first evidence of this effect. The structure of the jet  $A_N$  cross section is quite similar to the one in Eq. (59) for prompt photons. They only differ in the color factors corresponding to the final state interactions, which, in the case of jet production, suppress the asymmetries. It should be mentioned, that, within the cited uncertainties, the AnDY results also agree with the GPM calculations from Ref. [160].

### 3.4 *How to interpret azimuthal correlations of back-to-back hadrons and the $\Lambda$ polarisation in semi-inclusive $e^+e^-$ annihilations*

This sub-section focuses on the sensitivity of the structure functions defined in Eq. (16) in Sec. 2.3 to the Collins FF, which is most relevant for this review. Additionally, a short interpretation of the back-to-back production of hadron pairs, sensitive to the di-hadron FF  $H_1^\triangleleft$  as well as the production of  $\Lambda^\uparrow$  hyperons will be given, as these channels are relevant for the extraction of (TMD)-FFs entering in processes discussed in other sections in this review.

A detailed review of TMD FFs and their interpretation, including  $H_1^\perp$ ,  $H_1^\triangleleft$  and the polarising FF  $D_{1T}^{\perp \Lambda}$  can be found in Ref. [87]. Coming back to Eq. (16), that is the production of two back-to-back hadrons in  $e^+e^- \rightarrow h_1 h_2 X$  processes, the cross section was worked out in Ref. [80] for one photon annihilation. A complete discussion including electroweak and polarisation effects can be found in Ref [173] and papers quoted therein.

At leading order in perturbation theory and in  $1/Q$  the cross section reads [80]

$$\begin{aligned} \frac{d^5\sigma^{e^+e^- \rightarrow h_1 h_2 X}}{d\cos\theta_2 dz_1 dz_2 d^2\mathbf{P}_{1T}} &= \frac{6\pi\alpha_{\text{em}}^2}{Q^2} z_1^2 z_2^2 \left( A(y) \mathcal{C}_{e^+e^-} [D_1 \bar{D}_1] \right. \\ &+ \left. B(y) \cos(2\phi_1) \mathcal{C}_{e^+e^-} \left[ \frac{2\hat{\mathbf{h}} \cdot \mathbf{k}_{1T} \hat{\mathbf{h}} \cdot \mathbf{k}_{2T} - \mathbf{k}_{1T} \cdot \mathbf{k}_{2T}}{M_1 M_2} H_1^\perp \bar{H}_1^\perp \right] \right), \end{aligned} \quad (63)$$

where  $\hat{\mathbf{h}}$  is the unit vector along  $\mathbf{P}_{1\perp}$  and the angles  $\theta_2$  and  $\phi_1$  are defined in Fig. 10. The convolution  $\mathcal{C}$  is defined as

$$\begin{aligned} \mathcal{C}_{e^+e^-} [w D \bar{D}] &= \sum_q e_q^2 \int d^2\mathbf{k}_{1T} d^2\mathbf{k}_{2T} \delta^{(2)}(\mathbf{k}_{1T} + \mathbf{k}_{2T} + \mathbf{P}_{1T}/z_1) \\ &\times w(\mathbf{k}_{1T}, \mathbf{k}_{2T}) D^q(z_1, z_1^2 \mathbf{k}_{1T}^2) \bar{D}^q(z_2, z_2^2 \mathbf{k}_{2T}^2) + \{q \leftrightarrow \bar{q}\}. \end{aligned} \quad (64)$$

$A(y)$  and  $B(y)$  are kinematic factors:

$$A(y) = \frac{1}{2} - y + y^2, \quad B(y) = y(1 - y), \quad (65)$$

with  $y = (1 + \cos\theta_2)/2$ . They are the analogue of the spin transfer coefficients in Eq. (48) in the SIDIS case and can be interpreted as the projection of the transverse polarisation of the produced quarks. In the  $e^+e^-$  CMS system, the maximal sensitivity to the transverse polarisation of the quarks is therefore reached at a direction normal to the beam axis, see Eqs. (15). Information on the Collins functions can be obtained by looking at the azimuthal modulation of the cross section, second line of Eq. (63).

Comparing Eq. (63) to Eq. (16), the structure function  $N_{h_1 h_2}$  can then be identified with the term including the Collins functions,

$$4 z_1^2 z_2^2 B(y) \mathcal{C}_{e^+e^-} \left[ \frac{2\hat{\mathbf{h}} \cdot \mathbf{k}_{1T} \hat{\mathbf{h}} \cdot \mathbf{k}_{2T} - \mathbf{k}_{1T} \cdot \mathbf{k}_{2T}}{M_1 M_2} H_1^\perp \bar{H}_1^\perp \right], \quad (66)$$

and  $D_{h_1 h_2}$  with the term containing the unpolarised FFs,

$$4 z_1^2 z_2^2 A(y) \mathcal{C}_{e^+e^-} [D_1 \bar{D}_1]. \quad (67)$$

Notice that the definitions of  $\mathbf{k}_T$  and  $D_1$  differ by factors  $z$  from the definition of  $\mathbf{p}_\perp$  and  $D_{h/q}$ .

For completeness, it should be mentioned that the Collins FF can also be accessed in a symmetric coordinate system, where the axis around which the azimuthal angles are measured is given by the thrust axis in the event. In this case, instead of the convolution of the Collins FFs of quark and anti-quark, the product of the  $\mathbf{k}_T$  moments of the respective Collins FFs are measured [174, 134].

The term in the cross-section of back-to-back hadron production  $e^+e^- \rightarrow h_1 h_2 X$  that is sensitive to the Collins FF  $H_1^\perp$  can be symbolically expressed as

$$\sum_q e_q^2 H_1^{\perp h_a/q}(z_a, k_{aT}) \otimes H_1^{\perp h_b/\bar{q}}(z_b, k_{bT}) + \{q \leftrightarrow \bar{q}\}, \quad (68)$$

where the convolution over the transverse momenta is expressed as  $\otimes$ . In a similar way, one can consider the process, in which two hadron pairs are created back-to-back:

$$e^+e^- \rightarrow (h_{a1}, h_{a2}) (h_{b1}, h_{b2}) X. \quad (69)$$

Here, the di-hadron FF  $H_1^\perp$  is accessed, which can *e.g.* be used in the extraction of the transversity distribution from the di-hadron asymmetries measured in  $pp$  and described in Sec 2.2.3. This is further

discussed in Sec. 3.3.3. Instead of the angle  $\phi_1$ , which enters the asymmetries sensitive to the Collins effect, the di-hadron cross section depends on  $\phi_R$ , which is defined analogously to the  $pp$  case (see Sec 2.2.3). Since  $H_1^\triangleleft$  does not vanish upon the integration over intrinsic transverse momenta, the amplitude of the  $\sin(2\phi_R)$  modulation is then sensitive to the product of the di-hadron FFs:

$$\sum_q e_q^2 H_1^{\triangleleft h_a h_a 2/q}(z_a, M_{ha}) H_1^{\triangleleft h_b h_b 2/\bar{q}}(z_b, M_{hb}). \quad (70)$$

Finally, the transverse polarization of  $\Lambda$  hyperons in  $e^+e^-$  annihilation

$$e^+e^- \rightarrow \Lambda^\uparrow X \quad (71)$$

is sensitive to the term  $\sum_q e_q^2 D_{1T}^{\perp\Lambda/q}(z, \mathbf{p}_\perp)$ , with the polarising fragmentation function  $D_{1T}^{\perp\Lambda/q}$ . In the case where another hadron is detected opposite to the  $\Lambda$ , some flavour sensitivity can be gained by the entrance of the unpolarised FF of the associated hadron in the expression of the cross section. The relevant term can then be expressed symbolically as

$$\sum_q e_q^2 D_{1T}^{\perp\Lambda/q}(z, \mathbf{p}_\perp) D_{\Lambda/\bar{q}}(z). \quad (72)$$

Notice that the polarised  $\Lambda$  production enjoyed increased relevance recently, due to the recent Belle measurements [91], discussed earlier, and their possible interpretation in terms of Polarising Fragmentation Functions [175]. The Belle experiment measured a two-scale process in which the hyperon polarisation was determined with respect to the plane spanned by the hyperon momentum as well as a proxy for the outgoing quark momentum. This was either the thrust axis or a hadron in the opposite hemisphere. Therefore the TMD picture is appropriate and has very recently been used for first extractions of the polarizing FF  $D_{1T}^{\perp\Lambda/q}(z, \mathbf{p}_\perp)$  [176, 177]. However, similar to the scalar hadron production processes discussed earlier, there is a related single-scale process, which can be treated in a twist-3 picture. Here the hyperon polarisation is measured with respect to the plane spanned by hyperon momentum and beam-axis. See Refs. [178, 179] for recent work using this framework.

### 3.5 The Collins fragmentation function

Before discussing, in the next Section, our actual knowledge of the TMD-PDFs and the nucleon 3-dimensional structure, let us comment on the information we have gathered so far on the Collins FF. This function is not directly related to the nucleon structure, but it is an essential piece of information which we need, as it often combines with TMF-PDFs into physical observables.

The TMD fragmentation function, Eqs. (38) and (39), first introduced by Collins [93], embeds fundamental properties of the mysterious hadronisation process of quarks; it correlates the transverse spin of the fragmenting quark to the azimuthal distribution, around the quark direction, of the final hadrons. It is believed to be universal, the same in  $e^+e^-$ , SIDIS and Drell-Yan processes [94], for which TMD factorisation holds.

As discussed in previous Sections, the Collins function, being chiral-odd, must couple, in physical observables, to another chiral-odd function; this can be the transversity distribution, in SIDIS, or another Collins function in  $e^+e^-$  processes. The combined fit of azimuthal asymmetries in these two processes has indeed allowed an extraction of the Collins function [134, 180, 181, 81, 107].

An example of the extracted Collins functions is shown in Fig. 16, from Ref. [81]. The usual assumption, for pion production, is that of defining two kinds of functions: the favourite Collins functions, which is generated by a valence quark of the pion, like  $\Delta^N D_{\pi^+/u^\uparrow}$ , and the disfavoured Collins function, which is generated by a sea quark of the pion, like  $\Delta^N D_{\pi^-/u^\uparrow}$ . The plots show the values of

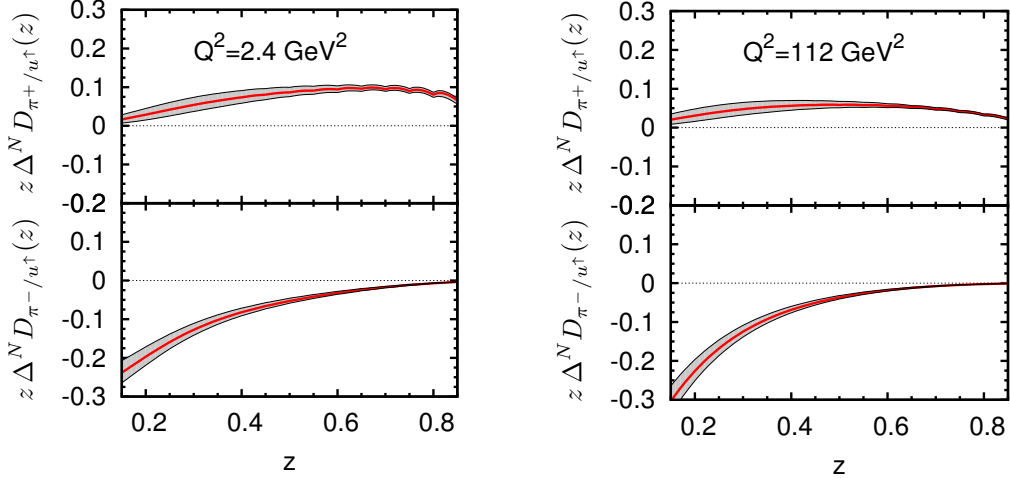


Figure 16: The values of  $z$  times the lowest  $p_\perp$  moment of the favoured (upper plots) and disfavoured (lower plots) Collins functions at  $Q^2 = 2.4 \text{ GeV}^2$  (left panel) and at  $Q^2 = 112 \text{ GeV}^2$  (right panel). The figure is adapted with permission from Ref. [81]. Copyrighted by the American Physical Society.

$z \Delta^N D_{h/q^\uparrow}(z, Q^2)$ , where

$$\Delta^N D_{h/q^\uparrow}(z, Q^2) = \int d^2 \mathbf{p}_\perp \Delta^N D_{h/q^\uparrow}(x, p_\perp, Q^2), \quad (73)$$

at two different values of  $Q^2$ , which are the mean  $Q^2$  of the SIDIS data and the  $Q^2$  of the Belle  $e^+e^-$  data; all details can be found in Ref. [81].

Let us stress once more that the data on the azimuthal distribution of two hadrons in  $e^+e^- \rightarrow q\bar{q} \rightarrow h_1 h_2 X$  processes, discussed in Section 3.3.4, are a clear indication of the Collins effect at work. Such effects have been observed by the Belle [82, 83], the BaBar [84] and the BESIII [86] Collaborations.

## 4 From data to the 3-dimensional imaging of the nucleon

### 4.1 The unpolarised TMD-PDFs

The first information one can try to obtain on the transverse motion of quarks and gluons inside the proton is given by the unpolarised parton distribution  $f_{a/p}(x, k_\perp)$ . For quarks, this could be easily accessed in unpolarised SIDIS processes, from data on the cross section, Eqs. (42) or (43). The unpolarised TMD-PDFs couple to the unpolarised TMD-FFs,  $D_{h/q}(z, p_\perp)$ .

However, data on unpolarised SIDIS cross section are not so abundant. The first attempts to obtain information on the unpolarised TMDs were performed in Refs. [133, 182, 183]. A most simple factorised Gaussian parameterisation was assumed for the unknown TMDs:

$$f_{q/p}(x, k_\perp) = f_{q/p}(x) \frac{e^{-k_\perp^2 / \langle k_\perp^2 \rangle}}{\pi \langle k_\perp^2 \rangle} \quad (74)$$

$$D_{h/q}(z, p_\perp) = D_{h/q}(z) \frac{e^{-p_\perp^2 / \langle p_\perp^2 \rangle}}{\pi \langle p_\perp^2 \rangle}, \quad (75)$$

where  $f_{q/p}(x)$  and  $D_{h/q}(z)$  are the usual collinear PDFs and FFs and where the Gaussian widths were assumed to be flavour independent and constant.

Ref. [133] exploited Fermilab [184] and EMC data [185] on  $\langle \cos \phi_h \rangle$ , a kinematical effect originated by the terms of  $\mathcal{O}(k_\perp/Q)$  in the elementary interaction [see Eq. (44)], the so-called Cahn effect, contributing to  $F_{UU}^{\cos \phi_h}$ . Ref. [182] best fitted values of  $\langle P_T \rangle$  from Ref. [186], while Ref. [183] compared with JLab data on cross section [187, 188] and HERMES data on  $\langle P_T^2 \rangle$  [189]. The Gaussian model of the TMDs proved to be adequate to fit the data and the values of  $\langle k_\perp^2 \rangle$  and  $\langle p_\perp^2 \rangle$  resulting in these three cases are comparable, in the approximate range (in  $\text{GeV}^2$ ):  $0.25 \leq \langle k_\perp^2 \rangle \leq (0.38 \pm 0.06)$  and  $0.15 \leq \langle p_\perp^2 \rangle \leq 0.20$ .

More recently, plenty of new data became available by the COMPASS and HERMES Collaborations, which measured, rather than the cross section, the hadron multiplicity. According to COMPASS notation [190, 191] the differential hadron multiplicity is defined as:

$$\frac{d^2 n^h(x_B, Q^2, z_h, P_T^2)}{dz_h dP_T^2} \equiv \frac{1}{\frac{d^2 \sigma^{DIS}(x_B, Q^2)}{dx_B dQ^2}} \frac{d^4 \sigma(x_B, Q^2, z_h, P_T^2)}{dx_B dQ^2 dz_h dP_T^2}, \quad (76)$$

while HERMES definition [192] is:

$$M_n^h(x_B, Q^2, z_h, P_T) \equiv \frac{1}{\frac{d^2 \sigma^{DIS}(x_B, Q^2)}{dx_B dQ^2}} \frac{d^4 \sigma(x_B, Q^2, z_h, P_T)}{dx_B dQ^2 dz_h dP_T}, \quad (77)$$

where the index  $n$  denotes the kind of target and the Deep Inelastic Scattering (DIS) cross section has the usual leading order collinear expression,

$$\frac{d^2 \sigma^{DIS}(x_B, Q^2)}{dx_B dQ^2} = \frac{2 \pi \alpha^2}{Q^4} [1 + (1 - y)^2] \sum_q e_q^2 f_{q/p}(x_B). \quad (78)$$

From Eqs. (42) and (76)–(78) one simply has:

$$\frac{d^2 n^h(x_B, Q^2, z_h, P_T)}{dz_h dP_T^2} = \frac{1}{2P_T} M_n^h(x_B, Q^2, z_h, P_T) = \frac{\pi F_{UU}}{\sum_q e_q^2 f_{q/p}(x_B)}. \quad (79)$$

The first analyses of data based on Eq. (79) have been performed in Refs. [193, 194] assuming for the TMDs the factorised and gaussian behaviour of Eqs. (74) and (75). In this case the expression of  $F_{UU}$  (42) can be exactly calculated:

$$F_{UU} = \sum_q e_q^2 f_{q/p}(x_B) D_{h/q}(z_h) \frac{e^{-P_T^2/\langle P_T^2 \rangle}}{\pi \langle P_T^2 \rangle}, \quad (80)$$

where

$$\langle P_T^2 \rangle = \langle p_\perp^2 \rangle + z_h^2 \langle k_\perp^2 \rangle. \quad (81)$$

As we said, in the simplest version of the gaussian model for the TMDs, they are assumed to be flavour independent and their widths  $\langle k_\perp^2 \rangle$  and  $\langle p_\perp^2 \rangle$  to be constant [194]; this cannot be true for all values of  $x$  and  $z$ , but might be adequate for analysing the available experimental data which cover limited kinematical regions. The possible flavour,  $x$  and  $z$  dependence of the gaussian widths was studied in Refs. [193, 108].

From this first study of the unpolarised TMDs, based on hadron multiplicity and the HERMES [192] and COMPASS [190, 191] data, it turns out that the gaussian assumptions (74) and (75) – possibly with flavour,  $x$  and  $z$  dependences – are able to fit well most data.

However, the hadron multiplicity, as given by Eqs. (79)–(81), depends on the parameter  $\langle P_T^2 \rangle$ , which, in turns, is a combinations of the two parameters  $\langle k_\perp^2 \rangle$  and  $\langle p_\perp^2 \rangle$ . This correlations makes it difficult to

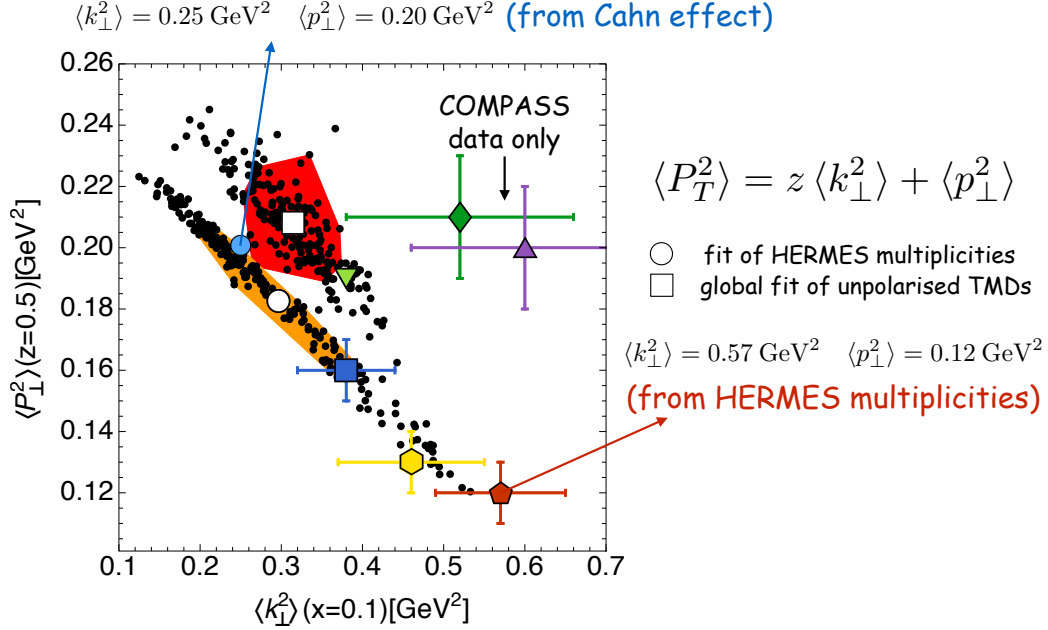


Figure 17: Values of  $\langle k_{\perp}^2 \rangle(x = 0.1)$  and  $\langle p_{\perp}^2 \rangle(z = 0.5)$  obtained from different fits of the hadron multiplicities, as shown in the figure. For further details we refer to the text and to Ref. [108] from which this figure has been taken and adjusted. Original figure available under a Creative Commons Attribution 4.0 International.

extract separately and independently the gaussian widths of  $f_{q/p}(x, k_{\perp})$  and  $D_{h/q}(z, p_{\perp})$ ; similarly good fits of the multiplicities, corresponding to different values of  $\langle k_{\perp}^2 \rangle$  and  $\langle p_{\perp}^2 \rangle$ , are possible. This is shown in Fig. 17, which is adjusted from Ref. [108]. The black dots around the central values are the outcome of different replicas of the fit and the coloured regions contains the 68% of the replicas that are closest to the average value. The red region shows the results of the first global fit to unpolarised TMDs [108], which takes into account SIDIS, Drell-Yan and Z boson production data, with TMD evolution. This study clearly shows the crucial role of TMDs in explaining the shape of the differential cross section for Z-boson production at Tevatron, Fig. 8 of Ref. [108].

The study of the unpolarised TMDs, mainly from SIDIS, but also from Drell-Yan and Z-boson production, clearly shows the need to introduce the transverse motions of partons inside the nucleon; this conclusion, based on experimental data, has solid theoretical grounds for processes in which one can identify two scales: a small one of the order of a few hundreds of MeV, and a large one, possibly of the order of few or more GeV [130]. Thus, one can separate a soft non perturbative region, which pertains to the nucleon structure, and a large energy region, described by perturbative Standard Model interactions. From data fitting, the resulting values of  $\langle k_{\perp} \rangle$ , are indeed of the order of few hundreds of MeV, giving us information on the quark intrinsic motion.

The knowledge of  $\langle k_{\perp}^2 \rangle$ , even neglecting its uncertainty due to the strong correlation with  $\langle p_{\perp}^2 \rangle$ , is important, but far from resolving the momentum distribution of partons inside the nucleon; crucial questions like the spin and the orbital momentum of quarks, and the correlation with the nucleon spin, remain open.

## 4.2 The Sivers function

The Sivers distribution of unpolarised partons inside a transversely polarised proton has a long and interesting history. It was introduced in 1990 [34, 114], to explain the large and unexpected values of the SSA  $A_N$  observed in  $pN \rightarrow \pi X$  processes, as explained in Section 2.2.1. It was then criticised [93] and dismissed as violating fundamental parity and time reversal properties of QCD. Then, a model calculation in Ref. [142] showed explicitly the possibility of having a non zero Sivers function in SIDIS processes, thanks to final state interactions of the scattered quark with the proton remnants. The criticism of Ref. [93] was reconsidered [41], taking into account the path-ordered exponential of the gluon field (gauge link) in the operator definition of parton densities, Eq. (11). This led, rather than to a vanishing of the Sivers function, to the prediction that such a function should have opposite signs in SIDIS and Drell-Yan processes [41]:

$$(f_{1T}^\perp)_{\text{SIDIS}} = -(f_{1T}^\perp)_{\text{DY}}. \quad (82)$$

This prediction is considered as an important test of our understanding of the origin and nature of SSAs in SIDIS and Drell-Yan processes, within a QCD TMD factorisation scheme. First experimental results [62] hint at a confirmation of the sign change [39], but no definite conclusion can still be drawn [195, 196].

The quark Sivers function has been extracted from SIDIS data on the weighted asymmetry  $A_{UT}^{\sin(\phi_h - \phi_S)}$  [17, 18, 19, 20, 21, 24], interpreted through Eq. (46), by several groups [197, 133, 198, 199, 182, 200, 201, 202, 81, 195]. This extraction requires some assumptions on the functional shape of the Sivers function and a choice of parameters. A most typical and simple assumption for  $\Delta^N f_{q/p^\uparrow}(x, k_\perp)$ , Eq. (26), is, again, a factorisation of the  $x$  and  $k_\perp$  dependences and a gaussian shape for the  $k_\perp$  dependence.

For example, a parameterisation of the Sivers function is given by [198, 201]

$$\Delta^N f_{q/p^\uparrow}(x, k_\perp) = 2\mathcal{N}_q(x) h(k_\perp) f_{q/p}(x, k_\perp), \quad (83)$$

with

$$\mathcal{N}_q(x) = N_q x^{\alpha_q} (1-x)^{\beta_q} \frac{(\alpha_q + \beta_q)^{(\alpha_q + \beta_q)}}{\alpha_q^{\alpha_q} \beta_q^{\beta_q}}, \quad (84)$$

$$h(k_\perp) = \sqrt{2e} \frac{k_\perp}{M_S} e^{-k_\perp^2/M_S^2}, \quad (85)$$

where  $N_q$ ,  $\alpha_q$ ,  $\beta_q$  and  $M_S$  (GeV/ $c$ ) are free parameters to be determined by fitting the experimental data. The functional shapes of  $\mathcal{N}_q(x)$  (with  $-1 \leq N_q \leq 1$ ) and  $h(k_\perp)$  are such that the positivity bound for the Sivers function,

$$\frac{|\Delta^N f_{q/p^\uparrow}(x, k_\perp)|}{2f_{q/p}(x, k_\perp)} \leq 1, \quad (86)$$

is automatically fulfilled for any value of  $x$  and  $k_\perp$ . The unpolarised TMD  $f_{q/p}(x, k_\perp)$  is given in Eq. (74), so that:

$$\Delta^N f_{q/p^\uparrow}(x, k_\perp) = 2\mathcal{N}_q(x) f_{q/p}(x) \sqrt{2e} \frac{k_\perp}{M_S} e^{-k_\perp^2/M_S^2} \frac{e^{-k_\perp^2/\langle k_\perp^2 \rangle}}{\pi \langle k_\perp^2 \rangle} \quad (87)$$

$$\equiv \Delta^N f_{q/p^\uparrow}(x) \sqrt{2e} \frac{k_\perp}{M_S} \frac{e^{-k_\perp^2/\langle k_\perp^2 \rangle_S}}{\pi \langle k_\perp^2 \rangle} \quad (88)$$

where

$$\langle k_\perp^2 \rangle_S = \frac{\langle k_\perp^2 \rangle M_S^2}{\langle k_\perp^2 \rangle + M_S^2}. \quad (89)$$

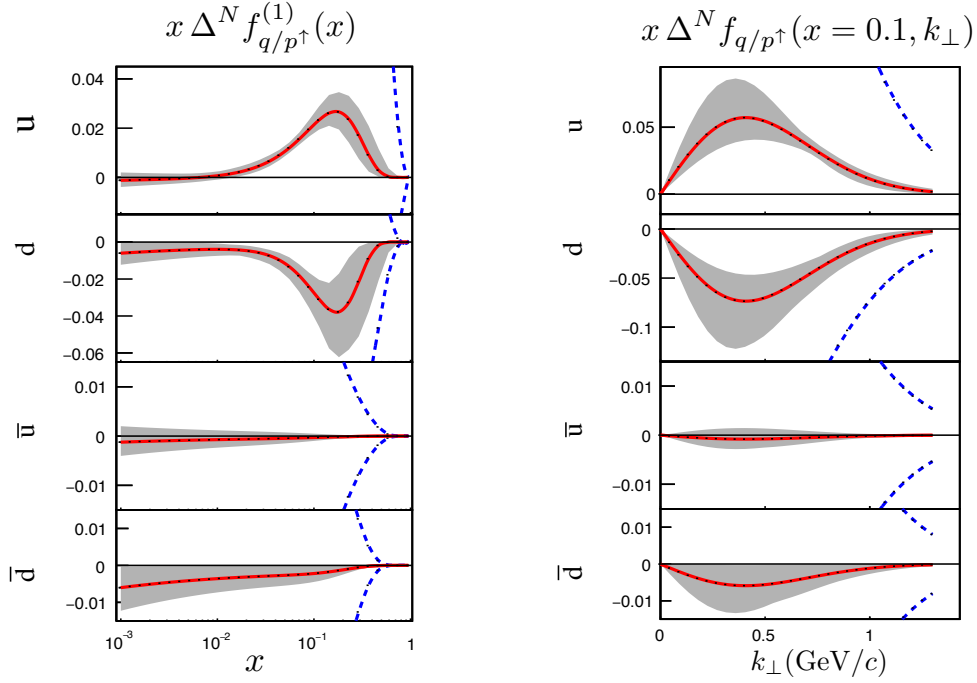


Figure 18: The Sivers distributions for  $u = u_v + \bar{u}$ ,  $d = d_v + \bar{d}$ ,  $\bar{u}$  and  $\bar{d}$  as extracted in Ref. [195]. Left panel: the  $x$  dependence of the first moment of the Sivers functions, Eq. (92), multiplied by  $x$ . Right panel: the  $k_\perp$  dependence of  $x$  times the Sivers functions, at  $x = 0.1$ . Details can be found in Ref. [195]. Figure from Ref. [195] available under a Creative Commons Attribution 4.0 International.

From Eqs. (46) and (88) one obtains [16, 203]:

$$A_{UT}^{\sin(\phi_h - \phi_S)} = \frac{\sum_q e_q^2 \Delta^N f_{q/p^\uparrow}(x) D_{h/q}(z) \times \sqrt{\frac{e}{2}} \frac{P_T}{M_S} \frac{z \langle k_\perp^2 \rangle_S^2}{\langle k_\perp^2 \rangle} \frac{e^{-P_T^2 / \langle P_T^2 \rangle_S}}{\pi \langle P_T^2 \rangle_S}}{\sum_q e_q^2 f_{q/p}(x) D_{h/q}(z) \frac{e^{-P_T^2 / \langle P_T^2 \rangle}}{\pi \langle P_T^2 \rangle}}, \quad (90)$$

where:

$$\langle P_T^2 \rangle = \langle p_\perp^2 \rangle + z^2 \langle k_\perp^2 \rangle \quad \langle P_T^2 \rangle_S = \langle p_\perp^2 \rangle + z^2 \langle k_\perp^2 \rangle_S. \quad (91)$$

The Sivers distribution, more than the unpolarised TMDs, offers a subtle and deeper way of probing the 3D structure of nucleons, as it couples the intrinsic motion of partons to a fundamental property of the the proton, its spin. The results so far reached deserve some comments.

- Fig. 18 shows a recent extraction of the quark Sivers functions from SIDIS data; they are taken from Ref. [195] but do not differ, qualitatively, from other extractions. The quantity shown on the left plot is the first moment of the Sivers function [197] (multiplied by  $x$ ):

$$\Delta^N f_{q/p^\uparrow}^{(1)}(x) = \int d^2 \mathbf{k}_\perp \frac{k_\perp}{4M} \Delta^N f_{q/p^\uparrow}(x, k_\perp) = -f_{1T}^{k_\perp(1)q}(x). \quad (92)$$

At this stage, despite the simple and approximate interpretation of the data, Eq. (90), one can definitely conclude that the Sivers effect, as origin of SSAs, at least in SIDIS processes, is well

established. The corresponding Sivers functions need not be too large, and are well below the positivity limit (86) (dashed blue lines in Fig. 18). The  $u$  and  $d$  quark Sivers functions are opposite in sign and peak at  $x$ -values in the valence region; in fact, the sea quark Sivers functions are compatible with zero.

- The Burkardt sum rule for the Sivers distribution [204]:

$$\sum_a \int dx d^2 \mathbf{k}_\perp \mathbf{k}_\perp f_{a/p^\uparrow}(x, \mathbf{k}_\perp) \equiv \sum_a \langle \mathbf{k}_\perp^a \rangle = 0, \quad (93)$$

is almost saturated by valence quarks alone ( $a = u, d$ ) [201], leaving little room to a contribution from a gluon Sivers function, as confirmed by other studies [205, 206, 207].

The gluon Sivers functions could be directly accessed in  $p^\uparrow N$  interactions, in particular via the large  $P_T$  inclusive production of charmed particles (like  $D$  or  $J/\psi$  mesons) [208, 209, 210] or prompt photons [211]. However, for these processes, the simple TMD factorisation scheme might not be fully justified.

- The Sivers distribution, Eq. (23), induces a correlation between the parton intrinsic motion  $\mathbf{k}_\perp$  and the parent nucleon polarisation  $\mathbf{S}$ , through the scalar expression  $(\hat{\mathbf{P}} \times \hat{\mathbf{k}}_\perp) \cdot \mathbf{S}$ . At fixed values of the proton momentum  $\mathbf{P}$  the density number of partons inside the transversely polarised proton is not isotropic in  $\mathbf{k}_\perp$ . The evidence of a non zero Sivers function has allowed the first 3-dimensional imaging of a proton. An example is shown in Fig. 19 which shows the density of  $u$  and  $d$  quarks in the transverse momentum plane, for a proton moving along the  $\hat{z}$ -axis and polarised along the  $\hat{y}$ -axis. The  $(\hat{\mathbf{P}} \times \hat{\mathbf{k}}_\perp) \cdot \mathbf{S}$  correlation induces a momentum deformation in  $k_x$ . Similar pictures can be drawn for different  $x$ -values, the so-called nucleon-tomography.
- Even if the Sivers function might contribute to SSAs with opposite signs in SIDIS and Drell-Yan processes [41], one can think that it is related to fundamental features of the proton structure. Then, as it does not depend on the spin of the partons, which are unpolarised, but depends on the proton spin, it must be related to another pseudo-vector, that is the parton orbital angular momentum, say  $\mathbf{L}_q$ . It would be interesting to find a dependence on  $\mathbf{S} \cdot \mathbf{L}_q$  embedded in the Sivers function; this was indeed proposed by Sivers [212, 213], as a possible normalisation of  $\Delta^N f_{q/p^\uparrow}(x, k_\perp)$ .

### 4.3 The transversity distribution

The transversity distribution is one of the three basic PDFs, which survive in the collinear limit; however, differently from the unpolarised PDF and the helicity distribution, it cannot be accessed in DIS processes, due to its chiral odd nature [1]. It can be accessed in SIDIS processes, coupled to the Collins TMD-FF, as detailed in Eq. (47). Independent information on the Collins function can be obtained from  $e^+e^- \rightarrow h_1 h_2 X$  processes, as discussed in Section 3.5.

The combined extraction of the transversity and the Collins functions was performed in Refs. [134, 180, 181, 81, 107]. As in the case of the Sivers function, a simple functional form was chosen for the unknown transversity and Collins TMDs:

$$\Delta_T q(x, k_\perp) = \frac{1}{2} \mathcal{N}_q^T(x) [f_{q/p}(x) + \Delta q(x)] \frac{e^{-k_\perp^2 / \langle k_\perp^2 \rangle}}{\pi \langle k_\perp^2 \rangle}, \quad (94)$$

$$\Delta^N D_{h/q^\uparrow}(z, p_\perp) = 2 \mathcal{N}_q^C(z) D_{h/q}(z) h(p_\perp) \frac{e^{-p_\perp^2 / \langle p_\perp^2 \rangle}}{\pi \langle p_\perp^2 \rangle}, \quad (95)$$

$x f_1(x, \mathbf{k}_T, S_T)$

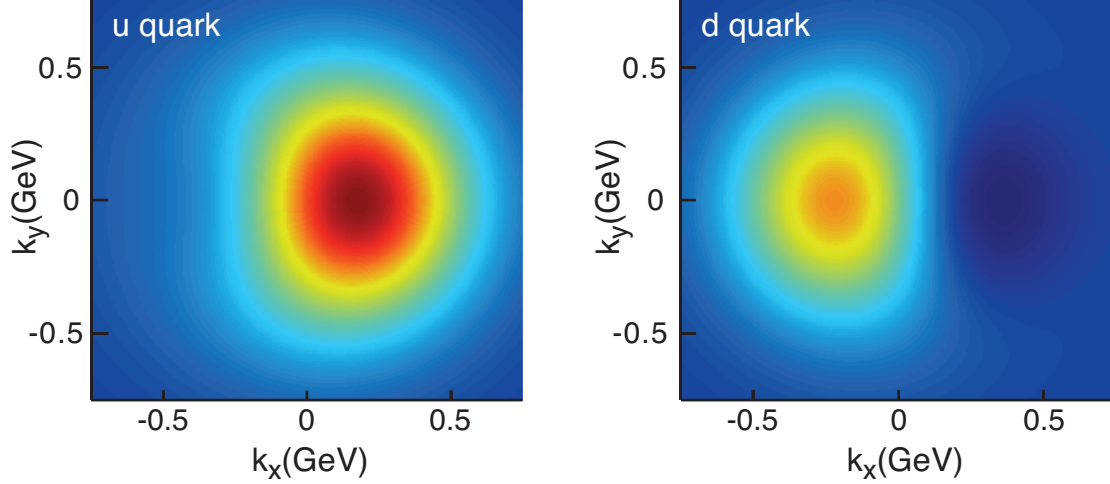


Figure 19: The transverse-momentum distribution of  $u$  (left) and  $d$  (right) quarks with longitudinal momentum fraction  $x = 0.1$  in a transversely polarised proton moving in the  $\hat{z}$ -direction, while polarised in the  $\hat{y}$ -direction. The corresponding Siverts distribution,  $f_1(x, k_\perp, S_T) = f_{q/p^\uparrow}(x, \mathbf{k}_\perp)$ , is evaluated using the Siverts function from Ref. [214]. The color code indicates the probability of finding the quarks. Figure from Ref. [8] and available under a Creative Commons Attribution 4.0 International.

with

$$h(p_\perp) = \sqrt{2}e \frac{p_\perp}{M} e^{-p_\perp^2/M^2}. \quad (96)$$

Simple parameterisations were adopted for  $\mathcal{N}_q^T(x)$  and  $\mathcal{N}_q^C(z)$  [181, 81] in such a way that the transversity distribution function automatically obeys the Soffer bound [215]

$$|\Delta_T q(x)| \leq \frac{1}{2} [f_{q/p}(x) + \Delta q(x)], \quad (97)$$

and the Collins function satisfies the positivity bound

$$|\Delta^N D_{h/q^\uparrow}(z, p_\perp)| \leq 2D_{h/q}(z, p_\perp). \quad (98)$$

By insertion of the above expressions into Eq. (47) one obtains [134, 11, 12]:

$$A_{UT}^{\sin(\phi_S + \phi_h)} = \frac{\sum_q e_q^2 \mathcal{N}_q^T(x) [f_{q/p}(x) + \Delta q(x)] \mathcal{N}_q^C(z) D_{h/q}(z) \times \frac{P_T}{M} \frac{1-y}{s x y^2} \sqrt{2}e \frac{\langle p_\perp^2 \rangle_C^2}{\langle p_\perp^2 \rangle} \frac{e^{-P_T^2/\langle P_T^2 \rangle_C}}{\langle P_T^2 \rangle_C}}{\sum_q e_q^2 f_{q/p}(x) D_{h/q}(z) \frac{e^{-P_T^2/\langle P_T^2 \rangle}}{\langle P_T^2 \rangle} \frac{[1 + (1-y)^2]}{s x y^2}}, \quad (99)$$

where

$$\langle p_\perp^2 \rangle_C = \frac{M^2 \langle p_\perp^2 \rangle}{M^2 + \langle p_\perp^2 \rangle} \quad \langle P_T^2 \rangle = \langle p_\perp^2 \rangle + z^2 \langle k_\perp^2 \rangle \quad \langle P_T^2 \rangle_C = \langle p_\perp^2 \rangle_C + z^2 \langle k_\perp^2 \rangle. \quad (100)$$

Some results on the transversity distributions are shown in Fig. 20, obtained by different groups, with different best fitting procedures. The red solid lines, both in the left and right plots, have been obtained in Ref. [107] by fitting SIDIS data from HERMES [17], COMPASS [21, 217] and Jlab [23],

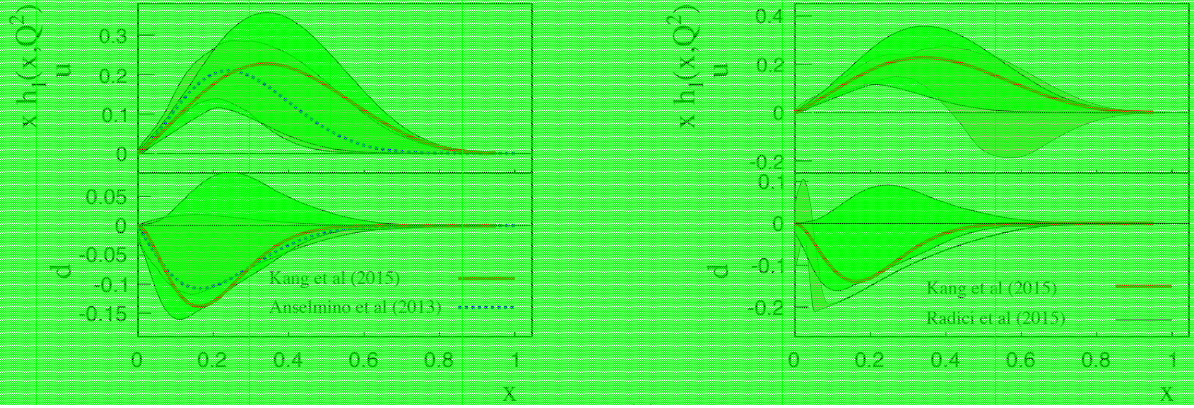


Figure 20: Plots of  $x$  times the transversity distribution,  $x h_1^q = x \Delta q$ , for  $u$  and  $d$  quarks, as obtained in Refs. [107] (Kang et al. (2015)), Ref. [181] (Anselmino et al. (2013)) and Ref. [216] (Radici et al. (2015)). See text for further details. Reprinted with permission from Zhong-Bo Kang, Alexei Prokudin, Peng Sun, and Feng Yuan, Phys. Rev., D93(1):014009, 2016. Copyright 2016 by the American Physical Society.

together with  $e^+e^-$  data from Belle [83] and BaBar [84]. The QCD evolution of the TMDs have been taken into account. The dotted blue line in the left plots is from Ref. [181], obtained by a combined fitting of SIDIS [18, 218] and  $e^+e^-$  data [83], without TMD evolution. The remaining line in the right plot is from Ref. [216], which couples the chiral-odd transversity distribution with the chiral-odd di-hadron fragmentation functions.

Let us summarise our knowledge on the transversity distribution.

- The combined fit of  $A_{UT}^{\sin(\phi_S + \phi_h)}$  from SIDIS data and azimuthal modulations in  $e^+e^- \rightarrow h_1 h_2 X$  processes, has allowed the first extraction of the transversity distributions of  $u$  and  $d$  quarks. The results obtained by different groups are in good agreement, and show reasonable values of  $\Delta_T u(x) = h_1^u(x)$  and  $\Delta_T d(x) = h_1^d(x)$ , not far from the corresponding helicity distributions, and peaked in the quark valence region. However, in SIDIS, the transversity distribution is coupled to the Collins function, and, in  $e^+e^-$ , one measures the product of two Collins functions: then, one cannot fix independently the signs of  $\Delta_T u(x)$  and  $\Delta_T d(x)$ , only their relative values, which turn out to be opposite. It is natural, following the helicity distributions or the  $SU(6)$  spin-flavour symmetry, to assume  $\Delta_T u(x)$  to be positive and  $\Delta_T d(x)$  to be negative, but this is not determined by the extraction procedure.
- An alternative way of accessing the transversity distribution, by coupling it to the di-hadron fragmentation function [219, 169], has been developed in Refs. [220, 221, 216]. Information on the di-hadron fragmentation function is obtained from  $e^+e^-$  data [222]. This analysis yields results similar to those obtained from the combined fits of transversity and Collins functions, but it has the advantage that it can be used also in  $pp$  interactions [37, 72], proving the universality of the transversity distribution [223]. Also in this case one can only fix the relative sign of  $u$  and  $d$  quark transversities.

- The transversity distribution has the important feature that it is related to the tensor charge [224],

$$\delta q \equiv \int_0^1 dx [h_1^q(x) - h_1^{\bar{q}}(x)] , \quad (101)$$

which can be computed on a lattice [225, 226, 227]. The available data on  $h_1^q(x)$  cover only a limited region in  $x$ , so that one needs some extrapolation in order to compute the full integral of Eq. (101); at the moment, there seems to be a discrepancies between the value of  $\delta u$ , as obtained from the extracted  $h_1^u(x)$ , and the lattice results [228, 229, 230, 231]. A very recent global analysis of data on Transverse Single Spin Asymmetries [232] includes, for the first time, results on the single spin asymmetry  $A_N$  in  $p^\uparrow p$  scattering and sees less tension with the lattice results. The inclusion of  $A_N$  in this extraction is based on the connection of  $A_N$ , with transversity in the twist-three framework discussed in Sec. 3.3.1.

- It is worth mentioning that the optimal access to the transversity distributions could, in principle, be obtained by measuring double transverse spin asymmetries in proton-antiproton Drell-Yan processes,  $p^\uparrow \bar{p}^\uparrow \rightarrow \ell^+ \ell^- X$ , which would mainly involve valence quark transversities. In order to enhance the amount of events, one could even think of measuring the di-lepton production at the  $J/\psi$  peak,  $p^\uparrow \bar{p}^\uparrow \rightarrow J/\psi X \rightarrow \ell^+ \ell^- X$  [53]. The availability of a polarised antiproton beams proves, however, to be a very difficult task [233].

## 5 The ultimate goal: the nucleon Wigner functions

The TMDs give a three-dimensional momentum space information about the quarks and gluons inside the nucleon. They do not give any information about their spatial distribution. Spatial information about the quarks and gluons can be obtained in terms of nucleon form factors; the Fourier transform of the form factor gives the charge distribution of the nucleon. Form factors are obtained by taking moments of the Generalised Parton Distributions (GPDs), which are defined as off-forward matrix elements of quarks and gluon operators, in a generalisation of Eq. (17) in which the initial and final proton momenta differ by an amount usually defined as  $\xi$  (for the longitudinal direction) and  $\Delta_\perp$  or  $\mathbf{q}_\perp$  (for the transverse direction). GPDs can be accessed in exclusive processes and are not discussed here; a seminal review paper can be found in [128]. In Ref. [234] it was shown that a Fourier transform of the GPDs with respect to the transverse momentum transfer,  $\Delta_\perp$ , taken at  $\xi = 0$ , gives Impact Parameter Dependent Parton Distribution Functions (IPDPDFs or, shortly, IPDs)). The IPDs give the density of partons with light-cone momentum fraction  $x$  and transverse impact parameter  $\mathbf{b}_\perp$ . However, the most general information about the quark and the gluon distribution in the nucleon could be obtained in terms of the phase space or Wigner distributions, and the Generalised Transverse Momentum Dependent parton distributions (GTMDs), which we shall discuss in the next Sections. The Wigner function is related, by some integration and by taking particular limits or Fourier transforms, to TMDs, GPDs, PDFs, form factors, IPDs and GTMDs. A comprehensive table of all these connections can be found in Ref. [235] and is shown for convenience in Fig. 21.

### 5.1 Introduction to Wigner distributions for quarks and gluons

In classical mechanics, the laws of dynamics are formulated in phase space, that describes the position  $\mathbf{r}$  as well as the momentum  $\mathbf{p}$  of each particle. In quantum mechanics, due to Heisenberg's uncertainty principle, the position and momentum of a particle cannot be determined simultaneously. In 1932, Wigner [236] introduced a quantum phase space distribution, which, in one space and one momentum

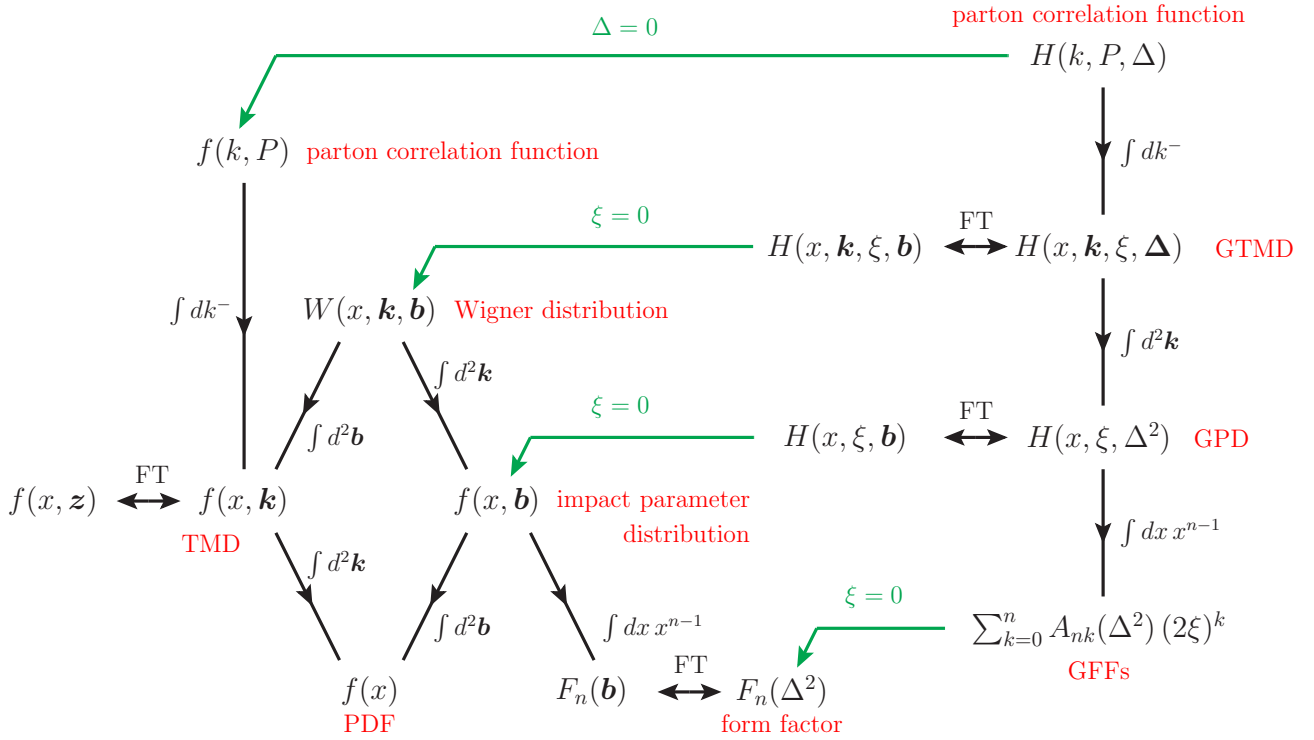


Figure 21: Summary of the relations between different distributions and correlators. The Table is reprinted from Ref. [235], where more details can be found. Notice that the vectors  $\mathbf{k}$ ,  $\mathbf{b}$  and  $\mathbf{\Delta}$  of the figure are defined respectively as  $\mathbf{k}_\perp$ ,  $\mathbf{b}_\perp$  and  $\mathbf{\Delta}_\perp$  in the text. Reprinted with kind permission of The European Physical Journal (EPJ), Markus Diehl, "Introduction to GPDs and TMDs", Eur. Phys. J., A52(6):149, 2016, ©Società Italiana di Fisica/ Springer-Verlag 2016.

dimensions, reads:

$$W(x, p) = \int d\eta e^{i p \eta} \psi^*(x - \eta/2) \psi(x + \eta/2). \quad (102)$$

$\psi(x)$  is the wave function of the system at the position  $x$  and  $p$  is the conjugate momentum. Wigner distributions are the analog of classical phase space distributions, to which they reduce in the classical limit. They have been used widely in different branches of physics, for example in quantum information, heavy ion physics, nonlinear dynamics, optics, image processing and so on [237, 238, 239]. The quantum mechanical Wigner distributions have also been measured in some particular cases [240, 241, 242]. Wigner distributions by themselves are not positive definite, and do not have a probabilistic interpretation; however, upon integration over  $p$  or  $x$  they give respectively the probability density of the quantum system in  $x$  or  $p$  space. A few modified Wigner type distributions have been used in the literature, notably the Husimi distributions [243], that are positive definite.

Wigner type phase space distributions for nucleons were introduced in Refs. [244, 245]. The impact parameter dependent parton distributions (IPDs) originally introduced by Burkardt had the skewness  $\xi = 0$ , in which limit they have a probability interpretation. A generalisation to non-zero  $\xi$  was discussed in [246]. Refs. [247, 248] discussed the Compton scattering amplitudes in longitudinal position space by taking their Fourier transform with respect to the skewness. The two dimensional position space picture of the IPDs was extended to three dimensions, in the rest frame of the nucleon, in Ref. [244].

The Wigner operator for quarks can be defined as

$$\hat{W}^\Gamma(\mathbf{r}, k) = \int d^4\eta e^{ik\cdot\eta} \bar{\psi}(\mathbf{r} - \eta/2) \Gamma \psi(\mathbf{r} + \eta/2), \quad (103)$$

where  $\Gamma$  is a Dirac matrix structure and  $k$  is the 4-momentum conjugate to the space-time separation  $\eta$ . A gauge link, not shown, has to be included for the color gauge invariance of QCD. The corresponding Wigner function for a non-relativistic system can be defined by taking an expectation value of the above operator for a state with the center-of-mass at  $\mathbf{R} = 0$ . As the proton is a relativistic object, recoil effects cannot be neglected, and the rest frame state cannot be uniquely defined. The Wigner distribution for the proton is defined in the Breit frame [244, 245]. The most general Wigner distribution is a function of seven variables, three positions, and four momenta. Integrating out the light cone energy  $k^-$  of the quarks, one gets the six dimensional reduced Wigner distribution. A five dimensional Wigner distribution was introduced in [249] in the infinite momentum frame or light-cone formalism by defining the Wigner operator for quarks at fixed light-cone time  $z^+ = 0$ :

$$\hat{W}^\Gamma(\mathbf{b}_\perp, \mathbf{k}_\perp, x) = \frac{1}{2} \int \frac{dz^- d^2\mathbf{z}_\perp}{(2\pi)^3} e^{i(xp^+z^- - \mathbf{k}_\perp \cdot \mathbf{z}_\perp)} \bar{\psi}(y - z/2) \Gamma \mathcal{W} \psi(y + z/2) |_{z^+=0}. \quad (104)$$

Here  $y^\mu = \{0, 0, \mathbf{b}_\perp\}$ ,  $x$  is the average light-cone longitudinal momentum fraction of the nucleon carried by the quark,  $x = k^+/p^+$ ,  $\Gamma = \gamma^+, \gamma^+\gamma_5, i\sigma^{j+}\gamma_5$  with  $j = 1, 2$  at twist two; different choices of  $\Gamma$  would give different phase space distribution.  $\mathcal{W}$  is the gauge link or Wilson line. It should be noted that in the above expression  $\mathbf{k}_\perp$  and  $\mathbf{b}_\perp$  are not Fourier conjugate variables.  $\mathbf{k}_\perp$  is the average transverse momentum of the active quark. The transverse impact parameter  $\mathbf{b}_\perp$  is the conjugate of the momentum transfer  $\Delta_\perp$  from the initial to the final state. Most studies of the Wigner functions in the literature consider the Drell-Yan-West frame, where  $\Delta^+ = 0$ . Including a non-zero  $\Delta^+$  would spoil the semi-classical probabilistic interpretation of the Wigner functions.

The Wigner distribution is defined, for a nucleon state with polarisation  $\mathbf{S}$ , as:

$$\rho^\Gamma(\mathbf{b}_\perp, \mathbf{k}_\perp, x, \mathbf{S}) = \int \frac{d^2\Delta_\perp}{(2\pi)^2} e^{-i\Delta_\perp \cdot \mathbf{b}_\perp} W^\Gamma(\Delta_\perp, \mathbf{k}_\perp, x, \mathbf{S}), \quad (105)$$

where,

$$W^\Gamma(\Delta_\perp, \mathbf{k}_\perp, x, \mathbf{S}) = \langle p^+, \Delta_\perp/2, \mathbf{S} | \hat{W}^\Gamma(\mathbf{0}_\perp, \mathbf{k}_\perp, x) | p^+, -\Delta_\perp/2, \mathbf{S} \rangle. \quad (106)$$

As transverse boosts are Galilean in light-front framework, one can construct a nucleon state localised in transverse coordinates, with its transverse center-of-momentum fixed. Thus, Eq. (105) is consistent with special relativity. Different choices of  $\Gamma$  matrix give different Wigner distributions, that probe various combinations of the quark and nucleon polarisation.

## 5.2 Wigner distributions and Generalized Transverse Momentum Dependent parton distribution functions (GTMDs)

There is a direct relation between the Wigner distributions and the most general parton correlation functions [250]. These are the completely unintegrated parton correlators of the nucleon, described in Fig. 22 and defined as [235]:

$$H^\Gamma(k, P, \Delta) = (2\pi)^{-4} \int d^4z e^{ikz} \langle p(P + \frac{1}{2}\Delta) | \bar{q}(-\frac{1}{2}z) \Gamma q(\frac{1}{2}z) | p(P + \frac{1}{2}\Delta) \rangle, \quad (107)$$

where the Dirac matrix  $\Gamma$  selects the parton spin degrees of freedom; the proton spin labels and the necessary gauge link, or Wilson operator, between the quark fields have been omitted.

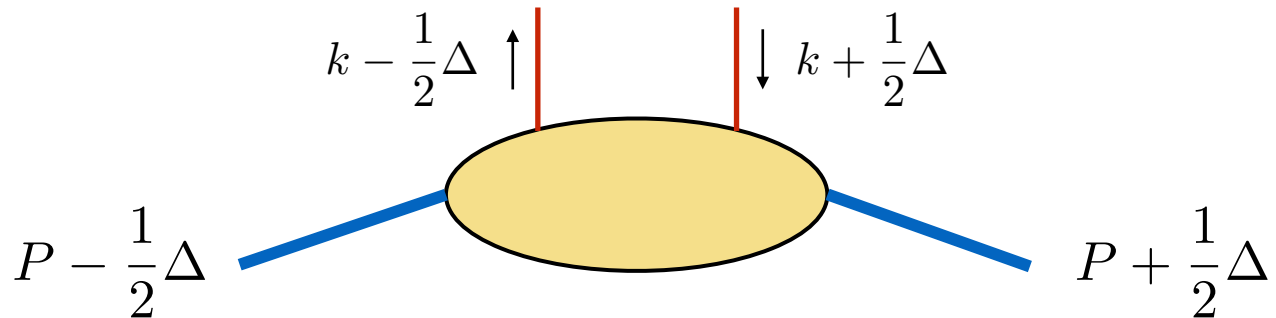


Figure 22: The most general off-forward quark-quark correlator;  $P$ ,  $\Delta$  and  $k$  are unintegrated 4-momenta. When  $\Delta = 0$  one recovers the correlator, for inclusive processes, of Fig. 11.

Integrating  $H^\Gamma$  over the light-cone energy of the quark,  $k^-$ , see Fig. 21, one gets the Generalized Transverse Momentum Dependent parton distributions (GTMDs). The Wigner distributions are Fourier transforms of the GTMDs. The most general parametrization of the GTMD correlator for a nucleon is given in Refs. [250, 251]. At leading twist, there are 16 GTMDs depending on the choice of  $\Gamma$ . The GTMDs are in general complex quantities. They are constrained by Hermiticity and time reversal [251] properties. The GTMDs can be written as

$$X(P, k, \Delta, \eta) = X^e(P, k, \Delta) + iX^o(P, k, \Delta, \eta), \quad (108)$$

where  $\eta$  denotes the direction of the gauge link (plus or minus).  $X^e$  is even under time reversal and  $X^o$  is odd. Due to the Hermiticity property of the GTMDs, the Wigner distributions, which are 2D Fourier transforms of the GTMDs, are real, although they can also be separated into a T-even and T-odd part. In the limit  $\Delta_\perp = 0$ , the GTMDs reduce to the TMDs. It can be shown that due to the Hermiticity constraint all GTMDs which are odd in  $\Delta_\perp$  vanish in the TMD limit. Upon integration over the parton momentum  $\mathbf{k}_\perp$ , they are related to the GPDs. In this case all effects of the T-odd part of the GTMDs vanish and there is no dependence on  $\eta$ . Thus, the GTMDs and the Wigner functions can be thought of as “mother distributions”, providing all information about the quark and gluon distributions of the nucleon, and beyond. A complete list of the relations between the various GTMDs and the corresponding TMDs and GPDs upto twist-four is given in [250]. Some nontrivial relations between GPDs and TMDs can be understood in terms of GTMDs. Three model independent relations exist at twist-two level between the GPDs and TMDs, these connect the GPD  $H(x, 0, 0)$  to the moment of  $f_1(x, k_T^2)$ ,  $\tilde{H}(x, 0, 0)$  to the moment of  $g_{1L}(x, k_T^2)$  and  $H_T(x, 0, 0)$  to a linear combination of moments of  $h_{1T}(x, k_T^2)$  and  $h_{1T}^\perp(x, k_T^2)$ . These are model independent relations as the corresponding GPDs and TMDs are related to the same GTMDs. On the other hand, in spectator type models relations have been derived connecting the Siverson function to the GPD  $E$  and Boer-Mulders function to a combination of GPDs  $E_T$  and  $\tilde{H}_T$ . These are called relations of the second kind and cannot be derived in a model independent way as these GPDs and TMDs are not related to the same GTMDs [250]. There are also relations of the third kind for example connecting the T-even pretzelosity distribution to the GPD  $\tilde{H}_T$ . This is also a model dependent relation as these are related to different GTMDs. At twist three and twist four there are no non-trivial model independent relations between GPDs and TMDs.

Unlike quark GTMDs, gluon GTMDs and unintegrated gluon distributions are known in the literature since a long time: for example, they were discussed in the small  $x$  regime in [252] in the context of diffractive vector meson production process and in [253] for Higgs production. Parametrizations of gluon GTMDs are given in Ref. [251].

### 5.3 Definitions

The Wigner distributions are not positive definite. Integrating out one or more variables they can be related to better known objects: integrating over  $\mathbf{b}_\perp$  effectively sets  $\mathbf{\Delta}_\perp$  to zero and one obtains the standard TMD correlator; on the other hand, by integration over  $\mathbf{k}_\perp$ , the Wigner distributions reduce to the impact parameter dependent PDFs (IPDs), which are the Fourier transforms of the GPD correlations. TMDs and IPDs can be interpreted as densities in momentum and transverse position space respectively. New distributions are obtained from  $\rho^\Gamma(\mathbf{b}_\perp, \mathbf{k}_\perp, x, \mathbf{S})$  by integrating over  $k_x$  and  $b_y$  or  $k_y$  and  $b_x$ ; these are not related to any known TMDs or GPDs, and therefore carry further information beyond what can be probed by the TMDs and GPDs. At leading twist one can define 16 independent Wigner distributions corresponding to different quark and proton polarisations ( $U$ ,  $L$  and  $T$ ) [249, 254]. In the list below the first subscript refers to the proton and the second to the quark;  $\hat{\mathbf{e}}_j$  ( $j = 1, 2, 3$  or  $x, y, z$ ) denote the unit vectors along the coordinate axes and the nucleon moves along  $\hat{\mathbf{e}}_z$ .

#### 5.3.1 Unpolarized target and different quark polarizations

The unpolarized Wigner distribution:

$$\rho_{UU}(\mathbf{b}_\perp, \mathbf{k}_\perp, x) = \frac{1}{2} \left[ \rho^{[\gamma^+]}(\mathbf{b}_\perp, \mathbf{k}_\perp, x, \hat{\mathbf{e}}_z) + \rho^{[\gamma^+]}(\mathbf{b}_\perp, \mathbf{k}_\perp, x, -\hat{\mathbf{e}}_z) \right]. \quad (109)$$

The unpolarized-longitudinally polarized Wigner distribution:

$$\rho_{UL}(\mathbf{b}_\perp, \mathbf{k}_\perp, x) = \frac{1}{2} \left[ \rho^{[\gamma^+\gamma^5]}(\mathbf{b}_\perp, \mathbf{k}_\perp, x, \hat{\mathbf{e}}_z) + \rho^{[\gamma^+\gamma^5]}(\mathbf{b}_\perp, \mathbf{k}_\perp, x, -\hat{\mathbf{e}}_z) \right]. \quad (110)$$

The unpolarized-transversely polarized Wigner distribution ( $j = 1, 2$ ):

$$\rho_{UT}^j(\mathbf{b}_\perp, \mathbf{k}_\perp, x) = \frac{1}{2} \left[ \rho^{[i\sigma^+j\gamma^5]}(\mathbf{b}_\perp, \mathbf{k}_\perp, x, \hat{\mathbf{e}}_z) + \rho^{[i\sigma^+j\gamma^5]}(\mathbf{b}_\perp, \mathbf{k}_\perp, x, -\hat{\mathbf{e}}_z) \right]. \quad (111)$$

#### 5.3.2 Longitudinally polarized target and different quark polarizations

The longitudinal-unpolarized Wigner distribution:

$$\rho_{LU}(\mathbf{b}_\perp, \mathbf{k}_\perp, x) = \frac{1}{2} \left[ \rho^{[\gamma^+]}(\mathbf{b}_\perp, \mathbf{k}_\perp, x, \hat{\mathbf{e}}_z) - \rho^{[\gamma^+]}(\mathbf{b}_\perp, \mathbf{k}_\perp, x, -\hat{\mathbf{e}}_z) \right]. \quad (112)$$

The longitudinal Wigner distribution:

$$\rho_{LL}(\mathbf{b}_\perp, \mathbf{k}_\perp, x) = \frac{1}{2} \left[ \rho^{[\gamma^+\gamma^5]}(\mathbf{b}_\perp, \mathbf{k}_\perp, x, \hat{\mathbf{e}}_z) - \rho^{[\gamma^+\gamma^5]}(\mathbf{b}_\perp, \mathbf{k}_\perp, x, -\hat{\mathbf{e}}_z) \right]. \quad (113)$$

The longitudinal-transversely polarized Wigner distribution ( $j = 1, 2$ ):

$$\rho_{LT}^j(\mathbf{b}_\perp, \mathbf{k}_\perp, x) = \frac{1}{2} \left[ \rho^{[i\sigma^+j\gamma^5]}(\mathbf{b}_\perp, \mathbf{k}_\perp, x, \hat{\mathbf{e}}_z) - \rho^{[i\sigma^+j\gamma^5]}(\mathbf{b}_\perp, \mathbf{k}_\perp, x, -\hat{\mathbf{e}}_z) \right]. \quad (114)$$

#### 5.3.3 Transversely polarized target and different quark polarizations

The transverse-unpolarized Wigner distribution ( $j = 1, 2$ ):

$$\rho_{TU}^j(\mathbf{b}_\perp, \mathbf{k}_\perp, x) = \frac{1}{2} \left[ \rho^{[\gamma^+]}(\mathbf{b}_\perp, \mathbf{k}_\perp, x, \hat{\mathbf{e}}_j) - \rho^{[\gamma^+]}(\mathbf{b}_\perp, \mathbf{k}_\perp, x, -\hat{\mathbf{e}}_j) \right]. \quad (115)$$

The transverse-longitudinally polarized Wigner distribution ( $j = 1, 2$ ):

$$\rho_{TL}^j(\mathbf{b}_\perp, \mathbf{k}_\perp, x) = \frac{1}{2} \left[ \rho^{[\gamma^+ \gamma^5]}(\mathbf{b}_\perp, \mathbf{k}_\perp, x, \hat{\mathbf{e}}_j) - \rho^{[\gamma^+ \gamma^5]}(\mathbf{b}_\perp, \mathbf{k}_\perp, x, -\hat{\mathbf{e}}_j) \right]. \quad (116)$$

The transversely polarised Wigner distribution ( $j, k = 1, 2$ ):

$$\rho_{TT}^{jk}(\mathbf{b}_\perp, \mathbf{k}_\perp, x) = \frac{1}{2} \delta_{jk} \left[ \rho^{[i\sigma^+ k \gamma^5]}(\mathbf{b}_\perp, \mathbf{k}_\perp, x, \hat{\mathbf{e}}_j) - \rho^{[i\sigma^+ k \gamma^5]}(\mathbf{b}_\perp, \mathbf{k}_\perp, x, -\hat{\mathbf{e}}_j) \right]. \quad (117)$$

The pretzelous Wigner distribution ( $j, k = 1, 2$ ):

$$\rho_{TT}^{\perp jk}(\mathbf{b}_\perp, \mathbf{k}_\perp, x) = \frac{1}{2} \epsilon_{jk} \left[ \rho^{[i\sigma^+ k \gamma^5]}(\mathbf{b}_\perp, \mathbf{k}_\perp, x, \hat{\mathbf{e}}_j) - \rho^{[i\sigma^+ k \gamma^5]}(\mathbf{b}_\perp, \mathbf{k}_\perp, x, -\hat{\mathbf{e}}_j) \right]. \quad (118)$$

### 5.3.4 Properties: connection to GPDs and TMDs and orbital angular momentum

The Wigner distributions could, in principle, offer a complete information on the nucleon structure and a few comments might help in understanding their importance and their relations with TMDs.

- In the above definitions  $\mathbf{S} = +\hat{\mathbf{e}}_z$  ( $-\hat{\mathbf{e}}_z$ ) corresponds to helicity  $+$  ( $-$ ) of the target state.  $\pm\hat{\mathbf{e}}_j$  ( $j = 1, 2$ ) correspond to transversity states and can be expressed in terms of helicity states. Notice that in the pretzelous Wigner function the transverse polarisations of the quark and of the proton are in orthogonal directions.
- By integration over  $x$  one gets the Wigner distributions in  $\mathbf{b}_\perp$  and  $\mathbf{k}_\perp$  space.  $\rho_{UU}(\mathbf{b}_\perp, \mathbf{k}_\perp)$  probes unpolarized quarks in unpolarized nucleon. Any distortion in the  $\mathbf{b}_\perp$  or  $\mathbf{k}_\perp$  space is a measure of the effect of the orbital motion of the quarks.

$\rho_{LU}$  gives the distortion in the  $\mathbf{b}_\perp$  and  $\mathbf{k}_\perp$  space in the distribution of the unpolarised quarks due to the longitudinal polarisation of the proton. In fact, this is related to the quark Orbital Angular Momentum (OAM) [249, 255, 256]:

$$l_z^q = \int dx \int d^2\mathbf{b}_\perp \int d^2\mathbf{k}_\perp (\mathbf{b}_\perp \times \mathbf{k}_\perp)_z \rho_{LU}^q(\mathbf{b}_\perp, \mathbf{k}_\perp, x). \quad (119)$$

At the density level, *i.e.* without integrating over  $x$ , the above expression gives the canonical OAM of the quark, when the gauge link in the Wigner distribution [see Eqs. (105), (106) and (104)] is staple-like, irrespective of its direction, future pointing or past pointing [257]. This reduces to the Jaffe-Manohar OAM [258] in the light-cone gauge. On the other hand, for a straight line gauge link, Eq. (119) gives the kinetic OAM, which is related to the GPD  $E$  through Ji's relation [259]. The kinetic and canonical OAM are related through a potential term (see Refs. [257] and [260] for a review). The kinetic OAM is related to the pretzelosity distribution in some models. The relation of quark and gluon OAM to unintegrated correlators was first discussed in Ref. [261].

$\rho_{UL}$  probes longitudinally polarised quarks in unpolarised proton, and this is related to the correlation between quark spin and OAM,

$$C_z^q = \int dx \int d^2\mathbf{b}_\perp \int d^2\mathbf{k}_\perp (\mathbf{b}_\perp \times \mathbf{k}_\perp)_z \rho_{UL}^q(\mathbf{b}_\perp, \mathbf{k}_\perp, x). \quad (120)$$

- By integration over  $d^2\mathbf{b}_\perp$ , as shown in Fig. 21, 8 of the 16 Wigner distributions, (109)–(118), reduce to the leading twist distributions of Eq. (21), while the other 8 vanish. Similarly, by integration over  $d^2\mathbf{k}_\perp$  one recovers the eight leading twist IPDs, which have not been discussed here.

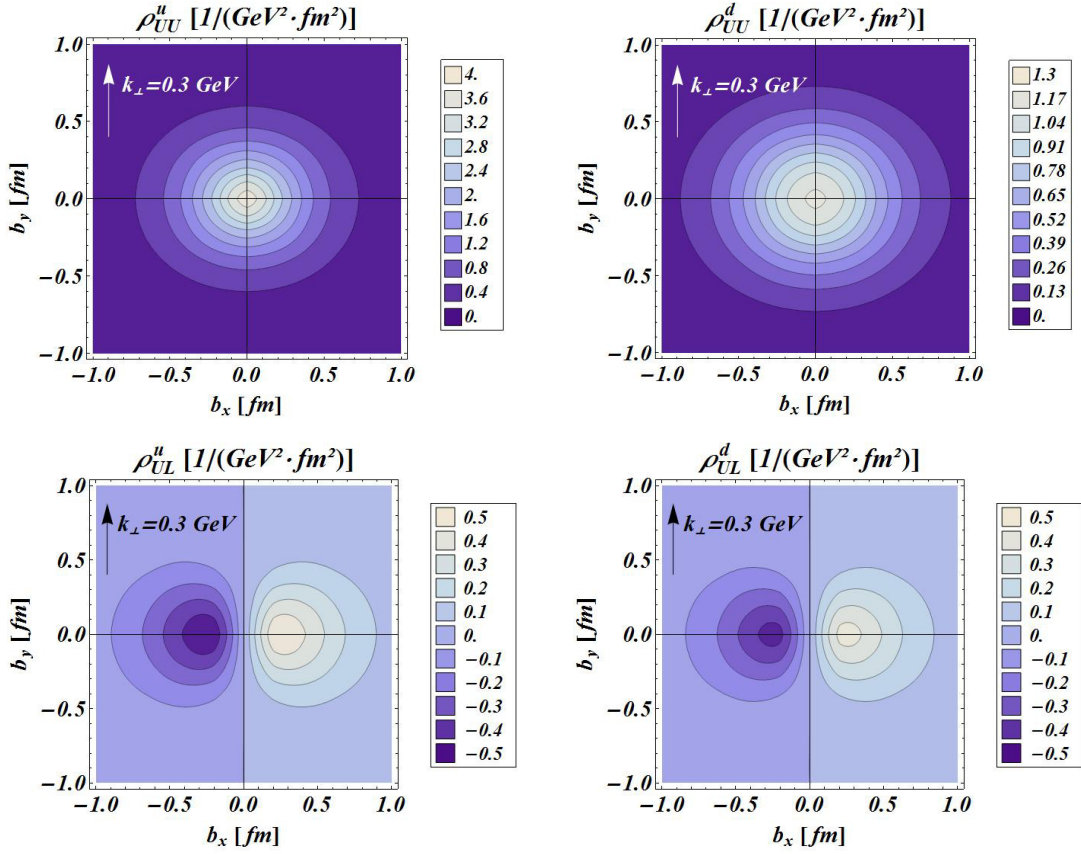


Figure 23: Wigner distributions for  $u$  and  $d$  quarks in  $\mathbf{b}_\perp$  space, at fixed  $\mathbf{k}_\perp = k_\perp \hat{e}_y$  with  $k_\perp = 0.3$  GeV, in a constituent quark model, from Ref. [249]. The upper panels refer to unpolarised protons and the lower ones to longitudinally polarised ones. Reprinted with permission from C. Lorcé and B. Pasquini, Phys. Rev., D84:014015, 2011. Copyright 2011 by the American Physical Society.

In particular,  $\rho_{UU}$  is related to the unpolarised quark TMD,  $f_1(x, k_\perp)$ .  $\rho_{LL}$  gives the correlation of the longitudinal spin of the quark in a longitudinally polarised proton and in the TMD limit it is related to the helicity distribution  $g_{1L}(x, k_\perp)$ . The TMD limit of  $\rho_{TU}$  and  $\rho_{UT}$  are respectively connected to the T-odd Sivers function,  $f_{1T}^\perp$ , and Boer-Mulders function,  $h_1^\perp$ .

$\rho_{LT}$  gives the correlations between a transversely polarized quark in a longitudinally polarised proton. In the TMD limit,  $\rho_{LT}$  it is related to the longitudinal-transversity worm-gear TMD  $h_{1L}^\perp$ . Similarly,  $\rho_{TL}$  describes the correlation between the longitudinally polarized quark in a transversely polarised proton and in the TMD limit is linked to the transverse-helicity worm-gear TMD  $g_{1T}^\perp$ .  $\rho_{TT}$  and  $\rho_{TT}^\perp$  are related, in the TMD limit, to the transversity and pretzelosity TMDs,  $h_{1T}$  and  $h_{1T}^\perp$ .

Notice that by integration over  $d^2\mathbf{k}_\perp$  or  $d^2\mathbf{b}_\perp$  both  $\rho_{LU}$  and  $\rho_{UL}$  vanish: they do not have a TMD or GPD limit. Thus, they carry completely new information about the nucleon structure, as shown in Eqs. (119) and (120).

Multipole decomposition of the Wigner distributions were investigated in Ref. [262].

## 5.4 Model Calculations

Model calculations of the Wigner distributions and the GTMDs are important as so far they have not been extracted from experimental data. In Ref. [249] the quark Wigner distributions for unpolarised as well as longitudinally polarised protons were investigated in a light-cone constituent quark model as well as in a light-cone chiral quark soliton model, using the valence light-front wave function (LFWF). The results for these two models are rather similar and some of them are shown as examples of 3D imaging of the proton.

The two upper plots in Fig. 23 show the transverse phase space distribution  $\rho_{UU}(\mathbf{b}_\perp, \mathbf{k}_\perp)$  obtained by integrating the Wigner distribution over  $x$ , for unpolarised  $u$  and  $d$  quarks inside an unpolarised proton. The results are given in the  $b_x$  and  $b_y$  plane, at fixed value of  $\mathbf{k}_\perp = k_\perp \hat{\mathbf{e}}_y$  with  $k_\perp = 0.3$  GeV. It is seen that the distribution is spread in the direction  $\mathbf{b}_\perp \perp \mathbf{k}_\perp$  more than  $\mathbf{b}_\perp \parallel \mathbf{k}_\perp$ . This is expected in a model with confinement, where the radial momentum of a quark decreases at the periphery of the  $\mathbf{b}_\perp$  space and the polar momentum dominates due to the OAM.

The two lower plots in Fig. 23 show the same  $\mathbf{b}_\perp$  distribution for a longitudinally (*i.e.* along  $\hat{\mathbf{e}}_z$ ) polarised proton. In this case  $\rho_{UL}(\mathbf{b}_\perp, \mathbf{k}_\perp)$  shows the effect of the net OAM, which for  $u$  quarks tend to align with the nucleon spin whereas for  $d$  quarks is anti-aligned. The Jaffe-Manohar OAM and Ji OAM have also been computed in this Ref. [249]. Both definitions of the OAM give the same result for the total quark ( $u + d$ ) OAM in the two models, although contributions from each flavour varies. This is expected as there is no gluon in these models.

All the 16 leading twist quark Wigner distributions for a nucleon have been calculated in Ref. [254] in a light cone spectator model, with the inclusion of both scalar and axial vector diquarks. Dipole and quadrupole structures are seen for the Wigner distributions that are related to the correlations between the spin and OAM of the quarks and the nucleon, as well as the transverse momentum. Results in this model show some difference compared to the models in [249] in impact parameter space. Both for  $u$  and  $d$  quarks, the spin-orbit correlation  $C_z^q$  is negative in this model which is opposite to what is observed in light cone constituent quark model [249]. This is a model dependent result. The 16 leading twist Wigner distributions were investigated in a diquark model in [263] including both scalar and axial vector diquarks, the analytic form of the light-front wave function (LFWF) was obtained using soft wall ADS/QCD prediction. Unlike the other models, there is no favored configuration between  $\mathbf{b}_\perp$  and  $\mathbf{k}_\perp$  here. In this model  $C_z^q$  is negative, meaning the quark OAM is anti-aligned to quark spin which agrees with the observation in scalar diquark model [254, 264].  $\rho_{UT}$  and  $\rho_{TV}$  show a dipolar behaviour which is similar to that of Ref. [254]. The above phenomenological models do not have gluonic degrees of freedom and the calculations describe the T-even part of the Wigner distributions.

The quark OAM through GTMDs was calculated in Ref. [265] in the MIT bag model. In Ref. [266] gluon Wigner, Husimi distributions and GTMDs were investigated in color glass condensate in the small  $x$  regime taking into account the gluon saturation effects. The Husimi distribution is obtained from the Wigner distribution by using a Gaussian smearing in  $\mathbf{b}_\perp$  and  $\mathbf{k}_\perp$ . As a result the Husimi distributions do not reduce to GPDs or TMDs after integration over  $\mathbf{k}_\perp$  or  $\mathbf{b}_\perp$ . However, the Husimi distributions are positive and unlike Wigner distributions can be interpreted as probability distributions in phase space.

The above phenomenological models for the nucleon do not include gluonic degrees of freedom. In Refs. [267, 268, 269, 270] the quark and gluon Wigner distributions and GTMDs were calculated for a spin-1/2 system of a quark dressed with a gluon, which may be thought of as a relativistic composite system of a quark and a gluon. The quark and gluon OAM and spin-orbit correlations were also calculated in this model. A similar model was also used in Ref. [271] for the GTMDs  $F_{14}$  and  $G_{11}$  and the results agree. The results for the quark and the gluon OAM and spin-orbit correlations were found to depend on the quark mass parameter, and the helicity sum rule is found to be satisfied. The Jaffe-Manohar OAM is different from Ji's OAM in this model. In Refs. [267, 268, 269, 270] the gauge

link was taken to be unity and as a result only the T-even part of the GTMDs were calculated. The T-odd part of the Wigner functions and the GTMDs were calculated in Ref. [272] by incorporating the final state interactions at the level of one gluon exchange in the LFWF. In a recent work [273] an ab initio world line approach was used to construct the phase space distributions of systems with internal symmetries.

## 5.5 Experiments to access the Wigner Distributions and GTMDs

Although several model calculations exist for both quark and gluon GTMDs and Wigner distributions, accessing them in experiments is still a challenge. Quite a few theoretical studies are available in the literature on how to probe the GTMDs in specific processes. In Ref. [274] it was shown that the quark GTMDs in the ERBL region ( $-\xi < x < \xi$ ) can be accessed in exclusive double Drell-Yan process in pion-nucleon scattering where one detects the two di-lepton pairs and the nucleon. As this process involve a staple-like Wilson line, the GTMDs here can probe the canonical or Jaffe-Manohar OAM. In Ref. [275] it was shown that the gluon GTMDs can be accessed in exclusive production of double pseudo-scalar quarkonium in nucleon-nucleon collision. Gluon Wigner distributions at small  $x$  can be accessed through the corresponding GTMDs in hard diffractive di-jet production at the future EIC [276]. This process probes the dipole gluon GTMDs. The longitudinal SSA in this process is a direct probe of the gluon OAM and helicity at small  $x$  [277] as well as moderate  $x$  [278]. Ref. [279] suggested to probe the gluon Wigner distributions in ultra-peripheral  $pA$  collisions.

## 6 Conclusions

We have discussed our present knowledge of the 3-dimensional nucleon structure, mainly in momentum space; that is, within the QCD parton model, we have summarised the attempts, both experimental and theoretical, to understand the intrinsic motion of quarks and gluons inside the proton.

First, we have presented plenty of experimental evidence, which requires the extension of the simple 1-dimensional picture of a fast moving proton as a set of almost free partons co-linearly moving, to a 3-dimensional picture including the transverse motion of partons. Such evidence is particularly striking when looking at experiments with transversely polarised protons; many transverse spin effects, for long time wrongly considered irrelevant or unnecessary, can only be understood in terms of the intrinsic 3D motion of quarks.

Then, we have described the phenomenological approach which allows to gather 3D information on the nucleon structure. The TMD-PDFs give the number densities of partons inside a proton, taking into account their longitudinal and transverse momenta, together with the spin degrees of freedom. They often couple with TMD-FFs, giving the number densities of hadrons resulting in the fragmentation of a quark or gluon: also in this case, the transverse momentum of the hadron with respect to the parton direction and the transverse spin degrees of freedom have to be taken into account. The TMD-PDFs and TMD-FFs appear in the theoretical expressions of several physical observables, which can be measured; thus, their extraction from data is possible.

Some of the TMD-PDFs and FFs have been found to play crucial roles in SIDIS and Drell-Yan processes, as well as in  $e^+e^-$  annihilations. In particular the effects resulting from the intrinsic motion of unpolarised quarks inside both unpolarised and transversely polarised protons have been well established and explored. Similarly for the fragmentation of a transversely polarised quark into spinless hadrons. A first attempt at a 3D imaging of the proton in momentum space is possible, as shown in Fig. 19. Notice that a 3D imaging in coordinate space is possible through the study of particular exclusive processes, which are not discussed in this paper.

Finally, a full 3D imaging of the nucleon would be possible only through a knowledge of the Wigner

distribution, the quantum analog of the classical phase-space distribution. This is a much more demanding task, although it should be the ultimate goal of a complete study of the nucleon structure. So far, models for the light-cone wave function of the proton have been used to construct model Wigner functions.

The introduction of the new concepts of TMD-PDFs and TMD-FFs has allowed a much better description of many, otherwise mysterious, transverse spin data; our way of exploring the nucleon structure has deeply changed, with a lot of encouraging and crucial results. Much more work remains to be done. The validity of the TMD factorisation scheme, crucial for the phenomenological extraction of the TMDs from data, seems to be limited to few processes and particular kinematical ranges. The huge amount of data on the hyperon polarisation in unpolarised inclusive  $pN$  interactions still lack a fundamental precise explanation, capable of reliable predictions. The origin of some TMDs, like the Sivers distribution, from basic QCD interactions, which leads to the prediction of the sign change of the Sivers function in SIDIS and D-Y processes, still has to be definitely tested.

New precise data from the “safe” processes – SIDIS, D-Y and  $e^+e^- \rightarrow h_1 h_2 X$  – will allow a much better determination of the TMDs and their parameterisation; in parallel, the theoretical study of the TMD evolution will improve and allow more precise predictions. New data are expected from the ongoing JLab experiments at 12 GeV and the next COMPASS run with a transversely polarised deuteron target, from RHIC and the  $e^+e^-$  facilities. All these efforts should be combined with models of the proton wave function and the Wigner distribution, from which TMDs and other observables can be computed and compared with data. In particular, the orbital angular momentum of quarks and gluons, which is a fundamental piece of information, is still unknown; its knowledge should finally allow the complete understanding of the proton spin.

Great expectations, among the international hadron and nuclear physics community, are linked to the planned Electron Ion Collider, a facility with good hopes of being built in the USA. Its scientific program [8] has a large part and strong motivations devoted to the study of the 3D nucleon structure, both in momentum and position space. Much larger kinematical ranges of  $x$  and  $Q^2$  could be explored, with high luminosity, providing a great amount of new data, and leading to a much improved understanding and imaging of the nucleon structure.

## Acknowledgements

M.A. would like to thank the Physics Department of the Indian Institute of Technology in Mumbai (IIT Bombay), where part of the paper was written, for hospitality and support. This material is based upon work supported by the U.S. Department of Energy, Office of Science, Office of Nuclear Physics under Award Numbers de-sc0019230 and DE-AC05-06OR23177.

## References

- [1] Vincenzo Barone, Alessandro Drago, and Philip G. Ratcliffe. Transverse polarisation of quarks in hadrons. *Phys. Rept.*, 359:1–168, 2002. [arXiv:hep-ph/0104283](#), [doi:10.1016/S0370-1573\(01\)00051-5](#).
- [2] U. D’Alesio and F. Murgia. Azimuthal and Single Spin Asymmetries in Hard Scattering Processes. *Prog. Part. Nucl. Phys.*, 61:394–454, 2008. [arXiv:0712.4328](#), [doi:10.1016/j.pnpnp.2008.01.001](#).
- [3] Vincenzo Barone, Franco Bradamante, and Anna Martin. Transverse-spin and transverse-momentum effects in high-energy processes. *Prog. Part. Nucl. Phys.*, 65:267–333, 2010. [arXiv:1011.0909](#), [doi:10.1016/j.pnpnp.2010.07.003](#).

- [4] Christine A. Aidala, Steven D. Bass, Delia Hasch, and Gerhard K. Mallot. The Spin Structure of the Nucleon. *Rev. Mod. Phys.*, 85:655–691, 2013. arXiv:1209.2803, doi:10.1103/RevModPhys.85.655.
- [5] Mariaelena Boglione and Alexei Prokudin. Phenomenology of transverse spin: past, present and future. *Eur. Phys. J.*, A52(6):154, 2016. arXiv:1511.06924, doi:10.1140/epja/i2016-16154-6.
- [6] H. Avakian, B. Parsamyan, and A. Prokudin. Spin orbit correlations and the structure of the nucleon. *Riv. Nuovo Cim.*, 42(1):1–48, 2019. doi:10.1393/ncr/i2019-10155-3.
- [7] Editors, M. Anselmino, M. Guidal, and P. Rossi. The 3-dimensional nucleon structure. *Eur. Phys. J.*, A52(6):149–164, 2016.
- [8] A. Accardi et al. Electron Ion Collider: The Next QCD Frontier. *Eur. Phys. J.*, A52(9):268, 2016. arXiv:1212.1701, doi:10.1140/epja/i2016-16268-9.
- [9] John Collins. Foundations of perturbative QCD. *Camb. Monogr. Part. Phys. Nucl. Phys. Cosmol.*, 32:1–624, 2011.
- [10] M. Gourdin. Semiinclusive reactions induced by leptons. *Nucl. Phys.*, B49:501–512, 1972. doi:10.1016/0550-3213(72)90615-3.
- [11] Aram Kotzinian. New quark distributions and semiinclusive electroproduction on the polarized nucleons. *Nucl. Phys.*, B441:234–248, 1995. arXiv:hep-ph/9412283.
- [12] P. J. Mulders and R. D. Tangerman. The Complete tree level result up to order  $1/Q$  for polarized deep inelastic lepton production. *Nucl. Phys.*, B461:197–237, 1996. [Erratum: *Nucl. Phys.*B484,538(1997)]. arXiv:hep-ph/9510301, doi:10.1016/S0550-3213(96)00648-7, 10.1016/0550-3213(95)00632-X.
- [13] Alessandro Bacchetta, Piet J. Mulders, and Fetze Pijlman. New observables in longitudinal single-spin asymmetries in semi-inclusive DIS. *Phys. Lett.*, B595:309–317, 2004. arXiv:hep-ph/0405154, doi:10.1016/j.physletb.2004.06.052.
- [14] M. Diehl and S. Sapeta. On the analysis of lepton scattering on longitudinally or transversely polarized protons. *Eur. Phys. J.*, C41:515–533, 2005. arXiv:hep-ph/0503023, doi:10.1140/epjc/s2005-02242-9.
- [15] Alessandro Bacchetta, Markus Diehl, Klaus Goeke, Andreas Metz, Piet J. Mulders, and Marc Schlegel. Semi-inclusive deep inelastic scattering at small transverse momentum. *JHEP*, 02:093, 2007. arXiv:hep-ph/0611265, doi:10.1088/1126-6708/2007/02/093.
- [16] M. Anselmino, M. Boglione, U. D’Alesio, S. Melis, F. Murgia, E. R. Nocera, and A. Prokudin. General Helicity Formalism for Polarized Semi-Inclusive Deep Inelastic Scattering. *Phys. Rev.*, D83:114019, 2011. arXiv:1101.1011, doi:10.1103/PhysRevD.83.114019.
- [17] A. Airapetian et al. Observation of the Naive-T-odd Sivers Effect in Deep-Inelastic Scattering. *Phys. Rev. Lett.*, 103:152002, 2009. arXiv:0906.3918, doi:10.1103/PhysRevLett.103.152002.
- [18] A. Airapetian et al. Effects of transversity in deep-inelastic scattering by polarized protons. *Phys. Lett.*, B693:11–16, 2010. arXiv:1006.4221, doi:10.1016/j.physletb.2010.08.012.

- [19] C. Adolph et al. Experimental investigation of transverse spin asymmetries in muon-p SIDIS processes: Collins asymmetries. *Phys. Lett.*, B717:376–382, 2012. arXiv:1205.5121, doi:10.1016/j.physletb.2012.09.055.
- [20] C. Adolph et al. II - Experimental investigation of transverse spin asymmetries in muon-p SIDIS processes: Sivers asymmetries. *Phys. Lett.*, B717:383–389, 2012. arXiv:1205.5122, doi:10.1016/j.physletb.2012.09.056.
- [21] C. Adolph et al. Collins and Sivers asymmetries in muonproduction of pions and kaons off transversely polarised protons. *Phys. Lett.*, B744:250–259, 2015. arXiv:1408.4405, doi:10.1016/j.physletb.2015.03.056.
- [22] C Adolph et al. Sivers asymmetry extracted in SIDIS at the hard scales of the Drell-Yan process at COMPASS. *Phys. Lett.*, B770:138–145, 2017. arXiv:1609.07374, doi:10.1016/j.physletb.2017.04.042.
- [23] X. Qian et al. Single Spin Asymmetries in Charged Pion Production from Semi-Inclusive Deep Inelastic Scattering on a Transversely Polarized  $^3\text{He}$  Target. *Phys. Rev. Lett.*, 107:072003, 2011. arXiv:1106.0363, doi:10.1103/PhysRevLett.107.072003.
- [24] K. Allada et al. Single spin asymmetries of inclusive hadrons produced in electron scattering from a transversely polarized  $^3\text{He}$  target. *Phys. Rev.*, C89(4):042201, 2014. arXiv:1311.1866, doi:10.1103/PhysRevC.89.042201.
- [25] G. Bunce et al.  $\Lambda_0$  Hyperon Polarization in Inclusive Production by 300-GeV Protons on Beryllium. *Phys. Rev. Lett.*, 36:1113–1116, 1976. doi:10.1103/PhysRevLett.36.1113.
- [26] P. Skubic et al. Neutral Strange Particle Production by 300-GeV Protons. *Phys. Rev.*, D18:3115–3144, 1978. doi:10.1103/PhysRevD.18.3115.
- [27] R. D. Klem, J. E. Bowers, H. W. Courant, H. Kagan, M. L. Marshak, E. A. Peterson, K. Ruddick, W. H. Dragoset, and J. B. Roberts. Measurement of Asymmetries of Inclusive Pion Production in Proton Proton Interactions at 6-GeV/c and 11.8-GeV/c. *Phys. Rev. Lett.*, 36:929–931, 1976. doi:10.1103/PhysRevLett.36.929.
- [28] W. H. Dragoset, J. B. Roberts, J. E. Bowers, H. W. Courant, H. Kagan, M. L. Marshak, E. A. Peterson, K. Ruddick, and R. D. Klem. Asymmetries in Inclusive Proton-Nucleon Scattering at 11.75-GeV/c. *Phys. Rev.*, D18:3939–3954, 1978. doi:10.1103/PhysRevD.18.3939.
- [29] C. E. Allgower et al. Measurement of analyzing powers of  $\pi^+$  and  $\pi^-$  produced on a hydrogen and a carbon target with a 22-GeV/c incident polarized proton beam. *Phys. Rev.*, D65:092008, 2002. doi:10.1103/PhysRevD.65.092008.
- [30] D. L. Adams et al. Comparison of spin asymmetries and cross-sections in  $\pi^0$  production by 200-GeV polarized anti-protons and protons. *Phys. Lett.*, B261:201–206, 1991. doi:10.1016/0370-2693(91)91351-U.
- [31] D. L. Adams et al. Analyzing power in inclusive  $\pi^+$  and  $\pi^-$  production at high  $x_F$  with a 200-GeV polarized proton beam. *Phys. Lett.*, B264:462–466, 1991. doi:10.1016/0370-2693(91)90378-4.
- [32] Gordon L. Kane, J. Pumplin, and W. Repko. Transverse Quark Polarization in Large  $p_T$  Reactions,  $e^+e^-$  Jets, and Leptoproduction: A Test of QCD. *Phys. Rev. Lett.*, 41:1689, 1978. doi:10.1103/PhysRevLett.41.1689.

- [33] Yuxi Pan. Transverse Single Spin Asymmetries of Forward  $\pi^0$  and Jet-like Events in  $\sqrt{s} = 500$  GeV Polarized Proton Collisions at STAR. *Int. J. Mod. Phys. Conf. Ser.*, 40(01):1660037, 2016. doi:10.1142/S2010194516600375.
- [34] Dennis W. Sivers. Single Spin Production Asymmetries from the Hard Scattering of Point-Like Constituents. *Phys. Rev.*, D41:83, 1990. doi:10.1103/PhysRevD.41.83.
- [35] S. Wandzura and Frank Wilczek. Sum Rules for Spin Dependent Electroproduction: Test of Relativistic Constituent Quarks. *Phys. Lett.*, 72B:195–198, 1977. doi:10.1016/0370-2693(77)90700-6.
- [36] Leonard Gamberg, Zhong-Bo Kang, Daniel Pitonyak, and Alexei Prokudin. Phenomenological constraints on  $A_N$  in  $p^\uparrow p \rightarrow \pi X$  from Lorentz invariance relations. *Phys. Lett.*, B770:242–251, 2017. arXiv:1701.09170, doi:10.1016/j.physletb.2017.04.061.
- [37] Alessandro Bacchetta and Marco Radici. Dihadron interference fragmentation functions in proton-proton collisions. *Phys. Rev.*, D70:094032, 2004. arXiv:hep-ph/0409174, doi:10.1103/PhysRevD.70.094032.
- [38] Umberto D’Alesio, Francesco Murgia, and Cristian Pisano. Azimuthal asymmetries for hadron distributions inside a jet in hadronic collisions. *Phys. Rev.*, D83:034021, 2011. arXiv:1011.2692, doi:10.1103/PhysRevD.83.034021.
- [39] Jin Huang, Zhong-Bo Kang, Ivan Vitev, and Hongxi Xing. Spin asymmetries for vector boson production in polarized p+p collisions. *Phys. Rev.*, D93(1):014036, 2016. arXiv:1511.06764, doi:10.1103/PhysRevD.93.014036.
- [40] Asmita Mukherjee and Werner Vogelsang. Jet production in (un)polarized pp collisions: dependence on jet algorithm. *Phys. Rev.*, D86:094009, 2012. arXiv:1209.1785, doi:10.1103/PhysRevD.86.094009.
- [41] John C. Collins. Leading twist single transverse-spin asymmetries: Drell-Yan and deep inelastic scattering. *Phys. Lett.*, B536:43–48, 2002. arXiv:hep-ph/0204004, doi:10.1016/S0370-2693(02)01819-1.
- [42] Ted C. Rogers and Piet J. Mulders. No Generalized TMD-Factorization in Hadro-Production of High Transverse Momentum Hadrons. *Phys. Rev.*, D81:094006, 2010. arXiv:1001.2977, doi:10.1103/PhysRevD.81.094006.
- [43] Leszek Adamczyk et al. Azimuthal transverse single-spin asymmetries of inclusive jets and charged pions within jets from polarized-proton collisions at  $\sqrt{s} = 500$  GeV. *Phys. Rev.*, D97(3):032004, 2018. arXiv:1708.07080, doi:10.1103/PhysRevD.97.032004.
- [44] R. Angeles-Martinez et al. Transverse Momentum Dependent (TMD) parton distribution functions: status and prospects. *Acta Phys. Polon.*, B46(12):2501–2534, 2015. arXiv:1507.05267, doi:10.5506/APhysPolB.46.2501.
- [45] I. Arsene et al. Single Transverse Spin Asymmetries of Identified Charged Hadrons in Polarized p+p Collisions at  $s^{*(1/2)} = 62.4$ -GeV. *Phys. Rev. Lett.*, 101:042001, 2008. arXiv:0801.1078, doi:10.1103/PhysRevLett.101.042001.
- [46] A. Adare et al. Cross section and transverse single-spin asymmetry of  $\eta$  mesons in  $p^\uparrow + p$  collisions at  $\sqrt{s} = 200$  GeV at forward rapidity. *Phys. Rev.*, D90(7):072008, 2014. arXiv:1406.3541, doi:10.1103/PhysRevD.90.072008.

- [47] H. Li et al. Azimuthal asymmetries of back-to-back  $\pi^\pm - (\pi^0, \eta, \pi^\pm)$  pairs in  $e^+e^-$  annihilation. 2019. [arXiv:1909.01857](#).
- [48] A. Adare et al. Measurement of Transverse Single-Spin Asymmetries for  $J/\psi$  Production in Polarized  $p + p$  Collisions at  $\sqrt{s} = 200$  GeV. *Phys. Rev.*, D82:112008, 2010. [Erratum: *Phys. Rev.*D86,099904(2012)]. [arXiv:1009.4864](#), doi:10.1103/PhysRevD.82.112008, 10.1103/PhysRevD.86.099904.
- [49] C. Aidala et al. Nuclear dependence of the transverse single-spin asymmetry in the production of charged hadrons at forward rapidity in polarized  $p + p$ ,  $p + \text{Al}$ , and  $p + \text{Au}$  collisions at  $\sqrt{s_{NN}} = 200$  GeV. *Phys. Rev. Lett.*, 123(12):122001, 2019. [arXiv:1903.07422](#), doi:10.1103/PhysRevLett.123.122001.
- [50] Sanjin Benic and Yoshitaka Hatta. Single spin asymmetry in forward  $pA$  collisions: Phenomenology at RHIC. *Phys. Rev.*, D99(9):094012, 2019. [arXiv:1811.10589](#), doi:10.1103/PhysRevD.99.094012.
- [51] Elke-Caroline Aschenauer et al. The RHIC Cold QCD Plan for 2017 to 2023: A Portal to the EIC. 2016. [arXiv:1602.03922](#).
- [52] S. D. Drell and Tung-Mow Yan. Massive Lepton Pair Production in Hadron-Hadron Collisions at High-Energies. *Phys. Rev. Lett.*, 25:316–320, 1970. [Erratum: *Phys. Rev. Lett.*25,902(1970)]. doi:10.1103/PhysRevLett.25.316, 10.1103/PhysRevLett.25.902.2.
- [53] M. Anselmino, V. Barone, A. Drago, and N. N. Nikolaev. Accessing transversity via  $J/\psi$  production in  $p^\uparrow p^\uparrow$  interactions. *Phys. Lett.*, B594:97–104, 2004. [arXiv:hep-ph/0403114](#), doi:10.1016/j.physletb.2004.05.029.
- [54] S. Arnold, A. Metz, and M. Schlegel. Dilepton production from polarized hadron hadron collisions. *Phys. Rev.*, D79:034005, 2009. [arXiv:0809.2262](#), doi:10.1103/PhysRevD.79.034005.
- [55] John C. Collins and Davison E. Soper. Angular distribution of dileptons in high-energy hadron collisions. *Phys. Rev. D*, 16:2219–2225, Oct 1977. URL: <https://link.aps.org/doi/10.1103/PhysRevD.16.2219>, doi:10.1103/PhysRevD.16.2219.
- [56] K. Gottfried and John David Jackson. On the Connection between production mechanism and decay of resonances at high-energies. *Nuovo Cim.*, 33:309–330, 1964. doi:10.1007/BF02750195.
- [57] Xiang-dong Ji, Jian-Ping Ma, and Feng Yuan. QCD factorization for spin-dependent cross sections in DIS and Drell-Yan processes at low transverse momentum. *Phys. Lett.*, B597:299–308, 2004. [arXiv:hep-ph/0405085](#), doi:10.1016/j.physletb.2004.07.026.
- [58] C. S. Lam and Wu-Ki Tung. A Systematic Approach to Inclusive Lepton Pair Production in Hadronic Collisions. *Phys. Rev.*, D18:2447, 1978. doi:10.1103/PhysRevD.18.2447.
- [59] Daniel Boer and P. J. Mulders. Time reversal odd distribution functions in lepton production. *Phys. Rev.*, D57:5780–5786, 1998. [arXiv:hep-ph/9711485](#), doi:10.1103/PhysRevD.57.5780.
- [60] M. Aghasyan et al. First measurement of transverse-spin-dependent azimuthal asymmetries in the Drell-Yan process. *Phys. Rev. Lett.*, 119(11):112002, 2017. [arXiv:1704.00488](#), doi:10.1103/PhysRevLett.119.112002.

- [61] Andrew Chen et al. Probing nucleon's spin structures with polarized Drell-Yan in the Fermilab SpinQuest experiment. In *23rd International Symposium on Spin Physics (SPIN 2018) Ferrara, Italy, September 10-14, 2018*, 2019. URL: <http://lss.fnal.gov/archive/2018/conf/fermilab-conf-18-412-e.pdf>, arXiv:1901.09994.
- [62] L. Adamczyk et al. Measurement of the transverse single-spin asymmetry in  $p^\uparrow + p \rightarrow W^\pm/Z^0$  at RHIC. *Phys. Rev. Lett.*, 116(13):132301, 2016. arXiv:1511.06003, doi:10.1103/PhysRevLett.116.132301.
- [63] Leonard Gamberg and Zhong-Bo Kang. Single transverse spin asymmetry of prompt photon production. *Phys. Lett.*, B718:181–188, 2012. arXiv:1208.1962, doi:10.1016/j.physletb.2012.10.002.
- [64] Leonard Gamberg and Zhong-Bo Kang. Process dependent sivers function and implication for single spin asymmetry in inclusive hadron production. *Physics Letters B*, 696(1-2):109–118, Jan 2011. URL: <http://dx.doi.org/10.1016/j.physletb.2010.11.066>, doi:10.1016/j.physletb.2010.11.066.
- [65] Silvia Pisano and Marco Radici. Di-hadron fragmentation and mapping of the nucleon structure. *Eur. Phys. J.*, A52(6):155, 2016. arXiv:1511.03220, doi:10.1140/epja/i2016-16155-5.
- [66] John C. Collins, Steve F. Heppelmann, and Glenn A. Ladinsky. Measuring transversity densities in singly polarized hadron hadron and lepton - hadron collisions. *Nucl. Phys.*, B420:565–582, 1994. arXiv:hep-ph/9305309, doi:10.1016/0550-3213(94)90078-7.
- [67] Alessandro Bacchetta and Marco Radici. Partial wave analysis of two hadron fragmentation functions. *Phys. Rev.*, D67:094002, 2003. arXiv:hep-ph/0212300, doi:10.1103/PhysRevD.67.094002.
- [68] Hrayr H. Matevosyan, Anthony W. Thomas, and Wolfgang Bentz. Dihadron fragmentation functions within the Nambu-Jona-Lasinio jet model. *Phys. Rev.*, D88(9):094022, 2013. arXiv:1310.1917, doi:10.1103/PhysRevD.88.094022.
- [69] Hrayr H. Matevosyan, Aram Kotzinian, and Anthony W. Thomas. Dihadron fragmentation functions in the quark-jet model: Transversely polarized quarks. *Phys. Rev.*, D97(1):014019, 2018. arXiv:1709.08643, doi:10.1103/PhysRevD.97.014019.
- [70] L. Adamczyk et al. Observation of Transverse Spin-Dependent Azimuthal Correlations of Charged Pion Pairs in  $p^\uparrow + p$  at  $\sqrt{s} = 200$  GeV. *Phys. Rev. Lett.*, 115:242501, 2015. arXiv:1504.00415, doi:10.1103/PhysRevLett.115.242501.
- [71] L. Adamczyk et al. Transverse spin-dependent azimuthal correlations of charged pion pairs measured in  $p^\uparrow + p$  collisions at  $\sqrt{s} = 500$  GeV. *Phys. Lett.*, B780:332–339, 2018. arXiv:1710.10215, doi:10.1016/j.physletb.2018.02.069.
- [72] Marco Radici and Alessandro Bacchetta. First Extraction of Transversity from a Global Analysis of Electron-Proton and Proton-Proton Data. *Phys. Rev. Lett.*, 120(19):192001, 2018. arXiv:1802.05212, doi:10.1103/PhysRevLett.120.192001.
- [73] Umberto D'Alesio, Francesco Murgia, and Cristian Pisano. Collins and sivers effects in  $p^\uparrow p \rightarrow$  jet  $\pi X$ : Universality and process dependence. *Phys. Part. Nucl.*, 45(4):676–691, 2014. arXiv:1307.4880, doi:10.1134/S1063779614040054.

- [74] Zhong-Bo Kang, Felix Ringer, and Ivan Vitev. The semi-inclusive jet function in SCET and small radius resummation for inclusive jet production. *JHEP*, 10:125, 2016. arXiv:1606.06732, doi:10.1007/JHEP10(2016)125.
- [75] Feng Yuan. Azimuthal asymmetric distribution of hadrons inside a jet at hadron collider. *Phys. Rev. Lett.*, 100:032003, 2008. arXiv:0709.3272, doi:10.1103/PhysRevLett.100.032003.
- [76] Zhong-Bo Kang, Alexei Prokudin, Felix Ringer, and Feng Yuan. Collins azimuthal asymmetries of hadron production inside jets. *Phys. Lett.*, B774:635–642, 2017. arXiv:1707.00913, doi:10.1016/j.physletb.2017.10.031.
- [77] L. Adamczyk et al. Longitudinal and transverse spin asymmetries for inclusive jet production at mid-rapidity in polarized  $p + p$  collisions at  $\sqrt{s} = 200$  GeV. *Phys. Rev.*, D86:032006, 2012. arXiv:1205.2735, doi:10.1103/PhysRevD.86.032006.
- [78] L. C. Bland et al. Cross Sections and Transverse Single-Spin Asymmetries in Forward Jet Production from Proton Collisions at  $\sqrt{s} = 500$  GeV. *Phys. Lett.*, B750:660–665, 2015. arXiv:1304.1454, doi:10.1016/j.physletb.2015.10.001.
- [79] B. I. Abelev et al. Measurement of transverse single-spin asymmetries for di-jet production in proton-proton collisions at  $s^{*1/2} = 200$ -GeV. *Phys. Rev. Lett.*, 99:142003, 2007. arXiv:0705.4629, doi:10.1103/PhysRevLett.99.142003.
- [80] Daniel Boer, R. Jakob, and P. J. Mulders. Asymmetries in polarized hadron production in  $e^+e^-$  annihilation up to order  $1/Q$ . *Nucl. Phys.*, B504:345–380, 1997. arXiv:hep-ph/9702281, doi:10.1016/S0550-3213(97)00456-2.
- [81] M. Anselmino, M. Boglione, U. D’Alesio, J. O. Gonzalez Hernandez, S. Melis, F. Murgia, and A. Prokudin. Collins functions for pions from SIDIS and new  $e^+e^-$  data: a first glance at their transverse momentum dependence. *Phys. Rev.*, D92(11):114023, 2015. arXiv:1510.05389, doi:10.1103/PhysRevD.92.114023.
- [82] Kazuo Abe et al. Measurement of azimuthal asymmetries in inclusive production of hadron pairs in  $e^+e^-$  annihilation at Belle. *Phys. Rev. Lett.*, 96:232002, 2006. arXiv:hep-ex/0507063, doi:10.1103/PhysRevLett.96.232002.
- [83] R. Seidl et al. Measurement of Azimuthal Asymmetries in Inclusive Production of Hadron Pairs in  $e^+e^-$  Annihilation at  $\sqrt{s} = 10.58$  GeV. *Phys. Rev.*, D78:032011, 2008. [Erratum: *Phys. Rev.*D86,039905(2012)]. arXiv:0805.2975, doi:10.1103/PhysRevD.78.032011, 10.1103/PhysRevD.86.039905.
- [84] J. P. Lees et al. Measurement of Collins asymmetries in inclusive production of charged pion pairs in  $e^+e^-$  annihilation at BABAR. *Phys. Rev.*, D90(5):052003, 2014. arXiv:1309.5278, doi:10.1103/PhysRevD.90.052003.
- [85] J. P. Lees et al. Collins asymmetries in inclusive charged  $KK$  and  $K\pi$  pairs produced in  $e^+e^-$  annihilation. *Phys. Rev.*, D92(11):111101, 2015. arXiv:1506.05864, doi:10.1103/PhysRevD.92.111101.
- [86] M. Ablikim et al. Measurement of azimuthal asymmetries in inclusive charged dipion production in  $e^+e^-$  annihilations at  $\sqrt{s} = 3.65$  GeV. *Phys. Rev. Lett.*, 116(4):042001, 2016. arXiv:1507.06824, doi:10.1103/PhysRevLett.116.042001.

- [87] Andreas Metz and Anselm Vossen. Parton Fragmentation Functions. *Prog. Part. Nucl. Phys.*, 91:136–202, 2016. arXiv:1607.02521, doi:10.1016/j.pnpnp.2016.08.003.
- [88] M. Anselmino, Daniel Boer, U. D’Alesio, and F. Murgia. Lambda polarization from unpolarized quark fragmentation. *Phys. Rev.*, D63:054029, 2001. arXiv:hep-ph/0008186, doi:10.1103/PhysRevD.63.054029.
- [89] M. Anselmino, Daniel Boer, U. D’Alesio, and F. Murgia. Transverse lambda polarization in semi-inclusive DIS. *Phys. Rev.*, D65:114014, 2002. arXiv:hep-ph/0109186, doi:10.1103/PhysRevD.65.114014.
- [90] Daniel Boer and Adrian Dumitru. Polarized hyperons from pA scattering in the gluon saturation regime. *Phys. Lett.*, B556:33–40, 2003. arXiv:hep-ph/0212260, doi:10.1016/S0370-2693(03)00081-9.
- [91] Y. Guan et al. Observation of Transverse  $\Lambda/\bar{\Lambda}$  Hyperon Polarization in  $e^+e^-$  Annihilation at Belle. *Phys. Rev. Lett.*, 122(4):042001, 2019. arXiv:1808.05000, doi:10.1103/PhysRevLett.122.042001.
- [92] John C. Collins, Davison E. Soper, and George Sterman. Transverse Momentum Distribution in Drell-Yan Pair and W and Z Boson Production. *Nucl. Phys.*, B250:199, 1985. doi:10.1016/0550-3213(85)90479-1.
- [93] John C. Collins. Fragmentation of transversely polarized quarks probed in transverse momentum distributions. *Nucl. Phys.*, B396:161–182, 1993.
- [94] John C. Collins and Andreas Metz. Universality of soft and collinear factors in hard-scattering factorization. *Phys. Rev. Lett.*, 93:252001, 2004. arXiv:hep-ph/0408249, doi:10.1103/PhysRevLett.93.252001.
- [95] Xiangdong Ji, Jian-Ping Ma, and Feng Yuan. Qcd factorization for semi-inclusive deep-inelastic scattering at low transverse momentum. *Phys. Rev.*, D71:034005, 2005. arXiv:hep-ph/0404183.
- [96] Xiangdong Ji, Jian-Wei Qiu, Werner Vogelsang, and Feng Yuan. A unified picture for single transverse-spin asymmetries in hard processes. *Phys. Rev. Lett.*, 97:082002, 2006. arXiv:hep-ph/0602239, doi:10.1103/PhysRevLett.97.082002.
- [97] Xiangdong Ji, Jian-wei Qiu, Werner Vogelsang, and Feng Yuan. Single Transverse-Spin Asymmetry in Drell-Yan Production at Large and Moderate Transverse Momentum. *Phys. Rev.*, D73:094017, 2006. arXiv:hep-ph/0604023, doi:10.1103/PhysRevD.73.094017.
- [98] Alessandro Bacchetta, Daniel Boer, Markus Diehl, and Piet J. Mulders. Matches and mismatches in the descriptions of semi-inclusive processes at low and high transverse momentum. *JHEP*, 08:023, 2008. arXiv:0803.0227, doi:10.1088/1126-6708/2008/08/023.
- [99] M. Anselmino et al. Sivers effect in Drell-Yan processes. *Phys. Rev.*, D79:054010, 2009. arXiv:0901.3078, doi:10.1103/PhysRevD.79.054010.
- [100] P. J. Mulders and T. C. Rogers. Gauge Links, TMD-Factorization, and TMD-Factorization Breaking. 2011. arXiv:1102.4569.
- [101] S. Mert Aybat and Ted C. Rogers. TMD Parton Distribution and Fragmentation Functions with QCD Evolution. *Phys. Rev.*, D83:114042, 2011. arXiv:1101.5057, doi:10.1103/PhysRevD.83.114042.

- [102] S. Mert Aybat, John C. Collins, Jian-Wei Qiu, and Ted C. Rogers. The QCD Evolution of the Sivers Function. *Phys. Rev.*, D85:034043, 2012. arXiv:1110.6428, doi:10.1103/PhysRevD.85.034043.
- [103] Alessandro Bacchetta and Alexei Prokudin. Evolution of the helicity and transversity Transverse-Momentum-Dependent parton distributions. *Nucl. Phys.*, B875:536–551, 2013. arXiv:1303.2129, doi:10.1016/j.nuclphysb.2013.07.013.
- [104] Ignazio Scimemi and Alexey Vladimirov. Non-perturbative structure of semi-inclusive deep-inelastic and Drell-Yan scattering at small transverse momentum. 2019. arXiv:1912.06532.
- [105] S. Mert Aybat, Alexei Prokudin, and Ted C. Rogers. Calculation of TMD Evolution for Transverse Single Spin Asymmetry Measurements. *Phys. Rev. Lett.*, 108:242003, 2012. arXiv:1112.4423, doi:10.1103/PhysRevLett.108.242003.
- [106] M. Anselmino, M. Boglione, and S. Melis. A Strategy towards the extraction of the Sivers function with TMD evolution. *Phys. Rev.*, D86:014028, 2012. arXiv:1204.1239, doi:10.1103/PhysRevD.86.014028.
- [107] Zhong-Bo Kang, Alexei Prokudin, Peng Sun, and Feng Yuan. Extraction of Quark Transversity Distribution and Collins Fragmentation Functions with QCD Evolution. *Phys. Rev.*, D93(1):014009, 2016. arXiv:1505.05589, doi:10.1103/PhysRevD.93.014009.
- [108] Alessandro Bacchetta, Filippo Delcarro, Cristian Pisano, Marco Radici, and Andrea Signori. Extraction of partonic transverse momentum distributions from semi-inclusive deep-inelastic scattering, Drell-Yan and Z-boson production. *JHEP*, 06:081, 2017. [Erratum: *JHEP*06,051(2019)]. arXiv:1703.10157, doi:10.1007/JHEP06(2017)081, 10.1007/JHEP06(2019)051.
- [109] M. Boglione, U. D’Alesio, C. Flore, and J. O. Gonzalez-Hernandez. Assessing signals of TMD physics in SIDIS azimuthal asymmetries and in the extraction of the Sivers function. *JHEP*, 07:148, 2018. arXiv:1806.10645, doi:10.1007/JHEP07(2018)148.
- [110] K. Goeke, A. Metz, and M. Schlegel. Parameterization of the quark-quark correlator of a spin-1/2 hadron. *Phys. Lett.*, B618:90–96, 2005. arXiv:hep-ph/0504130, doi:10.1016/j.physletb.2005.05.037.
- [111] John P. Ralston and Davison E. Soper. Production of Dimuons from High-Energy Polarized Proton Proton Collisions. *Nucl. Phys.*, B152:109, 1979. doi:10.1016/0550-3213(79)90082-8.
- [112] R. D. Tangerman and P. J. Mulders. Intrinsic transverse momentum and the polarized Drell-Yan process. *Phys. Rev.*, D51:3357–3372, 1995. arXiv:hep-ph/9403227, doi:10.1103/PhysRevD.51.3357.
- [113] U. D’Alesio and F. Murgia. Private communication. *Unpublished*.
- [114] Dennis W. Sivers. Hard scattering scaling laws for single spin production asymmetries. *Phys. Rev.*, D43:261–263, 1991. doi:10.1103/PhysRevD.43.261.
- [115] Gerald A. Miller. Shapes of the proton. *Phys. Rev.*, C68:022201, 2003. arXiv:nucl-th/0304076, doi:10.1103/PhysRevC.68.022201.
- [116] Gerald A. Miller. Densities, Parton Distributions, and Measuring the Non-Spherical Shape of the Nucleon. *Phys. Rev.*, C76:065209, 2007. arXiv:0708.2297, doi:10.1103/PhysRevC.76.065209.

- [117] Alessandro Bacchetta. Transverse-momentum-dependent parton distributions (TMDs). *AIP Conf. Proc.*, 1374(1):29–34, 2011. arXiv:1012.2315, doi:10.1063/1.3647094.
- [118] P. J. Mulders and J. Rodrigues. Transverse momentum dependence in gluon distribution and fragmentation functions. *Phys. Rev.*, D63:094021, 2001. arXiv:hep-ph/0009343, doi:10.1103/PhysRevD.63.094021.
- [119] M. Anselmino, M. Boglione, U. D’Alesio, E. Leader, S. Melis, and F. Murgia. The general partonic structure for hadronic spin asymmetries. *Phys. Rev.*, D73:014020, 2006. arXiv:hep-ph/0509035, doi:10.1103/PhysRevD.73.014020.
- [120] Daniel Boer, Cédric Lorcé, Cristian Pisano, and Jian Zhou. The gluon Sivers distribution: status and future prospects. *Adv. High Energy Phys.*, 2015:371396, 2015. arXiv:1504.04332, doi:10.1155/2015/371396.
- [121] Daniel Boer, Stanley J. Brodsky, Piet J. Mulders, and Cristian Pisano. Direct Probes of Linearly Polarized Gluons inside Unpolarized Hadrons. *Phys. Rev. Lett.*, 106:132001, 2011. arXiv:1011.4225, doi:10.1103/PhysRevLett.106.132001.
- [122] Cristian Pisano, Daniel Boer, Stanley J. Brodsky, Maarten G. A. Buffing, and Piet J. Mulders. Linear polarization of gluons and photons in unpolarized collider experiments. *JHEP*, 10:024, 2013. arXiv:1307.3417, doi:10.1007/JHEP10(2013)024.
- [123] Asmita Mukherjee and Sangem Rajesh.  $J/\psi$  production in polarized and unpolarized ep collision and Sivers and  $\cos 2\phi$  asymmetries. *Eur. Phys. J.*, C77(12):854, 2017. arXiv:1609.05596, doi:10.1140/epjc/s10052-017-5406-4.
- [124] Raj Kishore and Asmita Mukherjee. Accessing linearly polarized gluon distribution in  $J/\psi$  production at the electron-ion collider. *Phys. Rev.*, D99(5):054012, 2019. arXiv:1811.07495, doi:10.1103/PhysRevD.99.054012.
- [125] Daniel Boer, Wilco J. den Dunnen, Cristian Pisano, Marc Schlegel, and Werner Vogelsang. Linearly Polarized Gluons and the Higgs Transverse Momentum Distribution. *Phys. Rev. Lett.*, 108:032002, 2012. arXiv:1109.1444, doi:10.1103/PhysRevLett.108.032002.
- [126] Daniel Boer, Wilco J. den Dunnen, Cristian Pisano, and Marc Schlegel. Determining the Higgs spin and parity in the diphoton decay channel. *Phys. Rev. Lett.*, 111(3):032002, 2013. arXiv:1304.2654, doi:10.1103/PhysRevLett.111.032002.
- [127] Daniel Boer and Cristian Pisano. Impact of gluon polarization on Higgs boson plus jet production at the LHC. *Phys. Rev.*, D91(7):074024, 2015. arXiv:1412.5556, doi:10.1103/PhysRevD.91.074024.
- [128] M. Diehl. Generalized parton distributions. *Phys. Rept.*, 388:41–277, 2003. arXiv:hep-ph/0307382, doi:10.1016/j.physrep.2003.08.002, 10.3204/DESY-THESIS-2003-018.
- [129] Richard P. Feynman. Very high-energy collisions of hadrons. *Phys. Rev. Lett.*, 23:1415–1417, 1969. doi:10.1103/PhysRevLett.23.1415.
- [130] M. Boglione, J. Collins, L. Gamberg, J. O. Gonzalez-Hernandez, T. C. Rogers, and N. Sato. Kinematics of Current Region Fragmentation in Semi-Inclusive Deeply Inelastic Scattering. *Phys. Lett.*, B766:245–253, 2017. arXiv:1611.10329, doi:10.1016/j.physletb.2017.01.021.

- [131] Aram Kotzinian. Beyond Collins and Sivers: Further measurements of the target transverse spin-dependent azimuthal asymmetries in semi-inclusive DIS from COMPASS. In *Proceedings, 15th International Workshop on Deep-inelastic scattering and related subjects (DIS 2007). Vol. 1 and 2: Munich, Germany, April 16-20, 2007*, pages 647–650, 2007. arXiv:0705.2402, doi:10.3204/proc07-01/107.
- [132] Bakur Parsamyan. Six 'beyond Collins and Sivers' transverse spin asymmetries at COMPASS. *Phys. Part. Nucl.*, 45:158–162, 2014. arXiv:1301.6615, doi:10.1134/S106377961401078X.
- [133] M. Anselmino, M. Boglione, U. D'Alesio, A. Kotzinian, F. Murgia, and A. Prokudin. The Role of Cahn and sivers effects in deep inelastic scattering. *Phys. Rev.*, D71:074006, 2005. arXiv:hep-ph/0501196, doi:10.1103/PhysRevD.71.074006.
- [134] M. Anselmino, M. Boglione, U. D'Alesio, A. Kotzinian, F. Murgia, A. Prokudin, and C. Turk. Transversity and Collins functions from SIDIS and e+ e- data. *Phys. Rev.*, D75:054032, 2007. arXiv:hep-ph/0701006, doi:10.1103/PhysRevD.75.054032.
- [135] Vincenzo Barone, Stefano Melis, and Alexei Prokudin. The Boer-Mulders effect in unpolarized SIDIS: An Analysis of the COMPASS and HERMES data on the  $\cos 2\phi$  asymmetry. *Phys. Rev.*, D81:114026, 2010. arXiv:0912.5194, doi:10.1103/PhysRevD.81.114026.
- [136] E. Christova, D. Kotlorz, and E. Leader. Towards a model independent extraction of the Boer-Mulders function. 2019. arXiv:1909.08218.
- [137] A. Airapetian et al. Azimuthal distributions of charged hadrons, pions, and kaons produced in deep-inelastic scattering off unpolarized protons and deuterons. *Phys. Rev.*, D87(1):012010, 2013. arXiv:1204.4161, doi:10.1103/PhysRevD.87.012010.
- [138] C. Adolph et al. Measurement of azimuthal hadron asymmetries in semi-inclusive deep inelastic scattering off unpolarised nucleons. *Nucl. Phys.*, B886:1046–1077, 2014. arXiv:1401.6284, doi:10.1016/j.nuclphysb.2014.07.019.
- [139] Albi Kerbizi. Interpretation of the unpolarized azimuthal asymmetries in SIDIS. *PoS*, SPIN2018:053, 2018. arXiv:1812.07477, doi:10.22323/1.346.0053.
- [140] Andrea Moretti. Measurement of azimuthal asymmetries in SIDIS on unpolarized protons. *PoS*, SPIN2018:052, 2019. arXiv:1901.01773, doi:10.22323/1.346.0052.
- [141] J. Matouek. Measurement of the azimuthal modulations of hadrons in unpolarised SIDIS. *PoS*, DIS2019:189, 2019. arXiv:1907.08851, doi:10.22323/1.352.0189.
- [142] Stanley J. Brodsky, Dae Sung Hwang, and Ivan Schmidt. Final state interactions and single spin asymmetries in semiinclusive deep inelastic scattering. *Phys. Lett.*, B530:99–107, 2002. arXiv:hep-ph/0201296, doi:10.1016/S0370-2693(02)01320-5.
- [143] Stanley J. Brodsky, Dae Sung Hwang, and Ivan Schmidt. Initial state interactions and single spin asymmetries in Drell-Yan processes. *Nucl. Phys.*, B642:344–356, 2002. arXiv:hep-ph/0206259, doi:10.1016/S0550-3213(02)00617-X.
- [144] Daniel Boer, P. J. Mulders, and F. Pijlman. Universality of T odd effects in single spin and azimuthal asymmetries. *Nucl. Phys.*, B667:201–241, 2003. arXiv:hep-ph/0303034, doi:10.1016/S0550-3213(03)00527-3.

- [145] Stanley J. Brodsky, Dae Sung Hwang, Yuri V. Kovchegov, Ivan Schmidt, and Matthew D. Sievert. Single-Spin Asymmetries in Semi-inclusive Deep Inelastic Scattering and Drell-Yan Processes. *Phys. Rev.*, D88(1):014032, 2013. [arXiv:1304.5237](#), [doi:10.1103/PhysRevD.88.014032](#).
- [146] Zhong-Bo Kang, Xiaohui Liu, Felix Ringer, and Hongxi Xing. The transverse momentum distribution of hadrons within jets. *JHEP*, 11:068, 2017. [arXiv:1705.08443](#), [doi:10.1007/JHEP11\(2017\)068](#).
- [147] A. V. Efremov and O. V. Teryaev. QCD Asymmetry and Polarized Hadron Structure Functions. *Phys. Lett.*, 150B:383, 1985. [doi:10.1016/0370-2693\(85\)90999-2](#).
- [148] Jian-wei Qiu and George F. Sterman. Single transverse spin asymmetries. *Phys. Rev. Lett.*, 67:2264–2267, 1991. [doi:10.1103/PhysRevLett.67.2264](#).
- [149] Jian-wei Qiu and George F. Sterman. Single transverse spin asymmetries in hadronic pion production. *Phys. Rev.*, D59:014004, 1999. [arXiv:hep-ph/9806356](#), [doi:10.1103/PhysRevD.59.014004](#).
- [150] Xiangdong Ji, Jian-Wei Qiu, Werner Vogelsang, and Feng Yuan. Single-transverse spin asymmetry in semi-inclusive deep inelastic scattering. *Phys. Lett.*, B638:178–186, 2006. [arXiv:hep-ph/0604128](#), [doi:10.1016/j.physletb.2006.05.044](#).
- [151] Koichi Kanazawa, Yuji Koike, Andreas Metz, and Daniel Pitonyak. Towards an explanation of transverse single-spin asymmetries in proton-proton collisions: the role of fragmentation in collinear factorization. *Phys. Rev.*, D89(11):111501, 2014. [arXiv:1404.1033](#), [doi:10.1103/PhysRevD.89.111501](#).
- [152] Zhong-Bo Kang, Jian-Wei Qiu, Werner Vogelsang, and Feng Yuan. An Observation Concerning the Process Dependence of the Sivers Functions. *Phys. Rev.*, D83:094001, 2011. [arXiv:1103.1591](#), [doi:10.1103/PhysRevD.83.094001](#).
- [153] Hiroo Beppu, Koichi Kanazawa, Yuji Koike, and Shinsuke Yoshida. Three-gluon contribution to the single spin asymmetry for light hadron production in pp collision. *Phys. Rev.*, D89(3):034029, 2014. [arXiv:1312.6862](#), [doi:10.1103/PhysRevD.89.034029](#).
- [154] Yuji Koike and Tetsuya Tomita. Soft-fermion-pole contribution to single-spin asymmetry for pion production in pp collisions. *Phys. Lett.*, B675:181–189, 2009. [arXiv:0903.1923](#), [doi:10.1016/j.physletb.2009.04.017](#).
- [155] Koichi Kanazawa and Yuji Koike. New Analysis of the Single Transverse-Spin Asymmetry for Hadron Production at RHIC. *Phys. Rev.*, D82:034009, 2010. [arXiv:1005.1468](#), [doi:10.1103/PhysRevD.82.034009](#).
- [156] Koichi Kanazawa and Yuji Koike. A phenomenological study on single transverse-spin asymmetry for inclusive light-hadron productions at RHIC. *Phys. Rev.*, D83:114024, 2011. [arXiv:1104.0117](#), [doi:10.1103/PhysRevD.83.114024](#).
- [157] Umberto D’Alesio and Francesco Murgia. Parton intrinsic motion in inclusive particle production: Unpolarized cross sections, single spin asymmetries and the Sivers effect. *Phys. Rev.*, D70:074009, 2004. [arXiv:hep-ph/0408092](#), [doi:10.1103/PhysRevD.70.074009](#).
- [158] E. C. Aschenauer, U. D’Alesio, and F. Murgia. TMDs and SSAs in hadronic interactions. *Eur. Phys. J.*, A52(6):156, 2016. [arXiv:1512.05379](#), [doi:10.1140/epja/i2016-16156-4](#).

- [159] M. Anselmino, M. Boglione, U. D’Alesio, E. Leader, S. Melis, F. Murgia, and A. Prokudin. On the role of Collins effect in the single spin asymmetry  $A_N$  in  $p^\uparrow p \rightarrow hX$  processes. *Phys. Rev.*, D86:074032, 2012. [arXiv:1207.6529](#), [doi:10.1103/PhysRevD.86.074032](#).
- [160] M. Anselmino, M. Boglione, U. D’Alesio, S. Melis, F. Murgia, and A. Prokudin. Sivers effect and the single spin asymmetry  $A_N$  in  $p^\uparrow p \rightarrow hX$  processes. *Phys. Rev.*, D88(5):054023, 2013. [arXiv:1304.7691](#), [doi:10.1103/PhysRevD.88.054023](#).
- [161] A. Bacchetta, C. J. Bomhof, P. J. Mulders, and F. Pijlman. Single spin asymmetries in hadron-hadron collisions. *Phys. Rev.*, D72:034030, 2005. [arXiv:hep-ph/0505268](#), [doi:10.1103/PhysRevD.72.034030](#).
- [162] Umberto D’Alesio, Leonard Gamberg, Zhong-Bo Kang, Francesco Murgia, and Cristian Pisano. Testing the process dependence of the Sivers function via hadron distributions inside a jet. *Phys. Lett.*, B704:637–640, 2011. [arXiv:1108.0827](#), [doi:10.1016/j.physletb.2011.09.067](#).
- [163] A. Metz and D. Pitonyak. Fragmentation contribution to the transverse single-spin asymmetry in proton-proton collisions. *Phys. Lett.*, B723:365–370, 2013. [Erratum: *Phys. Lett.*B762,549(2016)]. [arXiv:1212.5037](#), [doi:10.1016/j.physletb.2013.05.043](#), [10.1016/j.physletb.2016.10.011](#).
- [164] Chris Kouvaris, Jian-Wei Qiu, Werner Vogelsang, and Feng Yuan. Single transverse-spin asymmetry in high transverse momentum pion production in pp collisions. *Phys. Rev.*, D74:114013, 2006. [arXiv:hep-ph/0609238](#), [doi:10.1103/PhysRevD.74.114013](#).
- [165] K. Kanazawa, Y. Koike, A. Metz, and D. Pitonyak. Transverse single-spin asymmetries in  $p^\uparrow p \rightarrow \gamma X$  from quark-gluon-quark correlations in the proton. *Phys. Rev.*, D91(1):014013, 2015. [arXiv:1410.3448](#), [doi:10.1103/PhysRevD.91.014013](#).
- [166] Jian Zhou and Andreas Metz. Dihadron fragmentation functions for large invariant mass. *Phys. Rev. Lett.*, 106:172001, 2011. [arXiv:1101.3273](#), [doi:10.1103/PhysRevLett.106.172001](#).
- [167] Stephen Gliske, Alessandro Bacchetta, and Marco Radici. Production of two hadrons in semi-inclusive deep inelastic scattering. *Phys. Rev.*, D90(11):114027, 2014. [Erratum: *Phys. Rev.*D91,no.1,019902(2015)]. [arXiv:1408.5721](#), [doi:10.1103/PhysRevD.90.114027](#), [10.1103/PhysRevD.91.019902](#).
- [168] R. L. Jaffe, Xue-min Jin, and Jian Tang. Interference fragmentation functions and the nucleon’s transversity. *Phys. Rev. Lett.*, 80:1166–1169, 1998. [arXiv:hep-ph/9709322](#), [doi:10.1103/PhysRevLett.80.1166](#).
- [169] Marco Radici, Rainer Jakob, and Andrea Bianconi. Accessing transversity with interference fragmentation functions. *Phys. Rev.*, D65:074031, 2002. [arXiv:hep-ph/0110252](#), [doi:10.1103/PhysRevD.65.074031](#).
- [170] Alessandro Bacchetta and Marco Radici. Modeling dihadron fragmentation functions. *Phys. Rev.*, D74:114007, 2006. [arXiv:hep-ph/0608037](#), [doi:10.1103/PhysRevD.74.114007](#).
- [171] Feng Yuan and Jian Zhou. Collins Fragmentation and the Single Transverse Spin Asymmetry. *Phys. Rev. Lett.*, 103:052001, 2009. [arXiv:0903.4680](#), [doi:10.1103/PhysRevLett.103.052001](#).
- [172] Leonard Gamberg, Zhong-Bo Kang, and Alexei Prokudin. Indication on the process-dependence of the Sivers effect. *Phys. Rev. Lett.*, 110(23):232301, 2013. [arXiv:1302.3218](#), [doi:10.1103/PhysRevLett.110.232301](#).

- [173] D. Pitonyak, M. Schlegel, and A. Metz. Polarized hadron pair production from electron-positron annihilation. *Phys. Rev.*, D89(5):054032, 2014. arXiv:1310.6240, doi:10.1103/PhysRevD.89.054032.
- [174] D. Boer. *Ph.D. thesis, Vrije U., Amsterdam, 1998.*
- [175] M. Anselmino, R. Kishore, and A. Mukherjee. Polarizing fragmentation function and the  $\Lambda$  polarization in  $e^+e^-$  processes. *Phys. Rev.*, D100(1):014029, 2019. arXiv:1905.02777, doi:10.1103/PhysRevD.100.014029.
- [176] Umberto D’Alesio, Francesco Murgia, and Marco Zaccheddu. First extraction of the  $\Lambda$  polarising fragmentation function from Belle  $e^+e^-$  data. 2020. arXiv:2003.01128.
- [177] Daniel Callos, Zhong-Bo Kang, and John Terry. Extracting the Transverse Momentum Dependent Polarizing Fragmentation Functions. 2020. arXiv:2003.04828.
- [178] Yuji Koike, Andreas Metz, Daniel Pitonyak, Kenta Yabe, and Shinsuke Yoshida. Twist-3 fragmentation contribution to polarized hyperon production in unpolarized hadronic collisions. *Phys. Rev.*, D95(11):114013, 2017. arXiv:1703.09399, doi:10.1103/PhysRevD.95.114013.
- [179] Leonard Gamberg, Zhong-Bo Kang, Daniel Pitonyak, Marc Schlegel, and Shinsuke Yoshida. Polarized hyperon production in single-inclusive electron-positron annihilation at next-to-leading order. *JHEP*, 01:111, 2019. arXiv:1810.08645, doi:10.1007/JHEP01(2019)111.
- [180] M. Anselmino, M. Boglione, U. D’Alesio, A. Kotzinian, F. Murgia, A. Prokudin, and S. Melis. Update on transversity and Collins functions from SIDIS and  $e^+e^-$  data. *Nucl. Phys. Proc. Suppl.*, 191:98–107, 2009. arXiv:0812.4366, doi:10.1016/j.nuclphysbps.2009.03.117.
- [181] M. Anselmino, M. Boglione, U. D’Alesio, S. Melis, F. Murgia, and A. Prokudin. Simultaneous extraction of transversity and Collins functions from new SIDIS and  $e^+e^-$  data. *Phys. Rev.*, D87:094019, 2013. arXiv:1303.3822, doi:10.1103/PhysRevD.87.094019.
- [182] J. C. Collins, A. V. Efremov, K. Goeke, S. Menzel, A. Metz, and P. Schweitzer. Sivers effect in semi-inclusive deeply inelastic scattering. *Phys. Rev.*, D73:014021, 2006. arXiv:hep-ph/0509076, doi:10.1103/PhysRevD.73.014021.
- [183] P. Schweitzer, T. Teckentrup, and A. Metz. Intrinsic transverse parton momenta in deeply inelastic reactions. *Phys. Rev.*, D81:094019, 2010. arXiv:1003.2190, doi:10.1103/PhysRevD.81.094019.
- [184] M. R. Adams et al. Perturbative QCD effects observed in 490-GeV deep inelastic muon scattering. *Phys. Rev.*, D48:5057–5066, 1993. doi:10.1103/PhysRevD.48.5057.
- [185] M. Arneodo et al. Measurement of Hadron Azimuthal Distributions in Deep Inelastic Muon Proton Scattering. *Z. Phys.*, C34:277, 1987. doi:10.1007/BF01548808.
- [186] A. Airapetian et al. Measurement of single spin azimuthal asymmetries in semiinclusive electroproduction of pions and kaons on a longitudinally polarized deuterium target. *Phys. Lett.*, B562:182–192, 2003. arXiv:hep-ex/0212039, doi:10.1016/S0370-2693(03)00566-5.
- [187] H. Mkrtchyan et al. Transverse momentum dependence of semi-inclusive pion production. *Phys. Lett.*, B665:20–25, 2008. arXiv:0709.3020, doi:10.1016/j.physletb.2008.05.047.
- [188] M. Osipenko et al. Measurement of unpolarized semi-inclusive  $\pi^+$  electroproduction off the proton. *Phys. Rev.*, D80:032004, 2009. arXiv:0809.1153, doi:10.1103/PhysRevD.80.032004.

- [189] A. Airapetian et al. Transverse momentum broadening of hadrons produced in semi-inclusive deep-inelastic scattering on nuclei. *Phys. Lett.*, B684:114–118, 2010. arXiv:0906.2478, doi:10.1016/j.physletb.2010.01.020.
- [190] C. Adolph et al. Hadron Transverse Momentum Distributions in Muon Deep Inelastic Scattering at 160 GeV/c. *Eur. Phys. J.*, C73:2531, 2013. arXiv:1305.7317, doi:10.1140/epjc/s10052-013-2531-6.
- [191] M. Aghasyan et al. Transverse-momentum-dependent Multiplicities of Charged Hadrons in Muon-Deuteron Deep Inelastic Scattering. *Phys. Rev.*, D97(3):032006, 2018. arXiv:1709.07374, doi:10.1103/PhysRevD.97.032006.
- [192] A. Airapetian et al. Multiplicities of charged pions and kaons from semi-inclusive deep-inelastic scattering by the proton and the deuteron. *Phys. Rev.*, D87:074029, 2013. arXiv:1212.5407, doi:10.1103/PhysRevD.87.074029.
- [193] Andrea Signori, Alessandro Bacchetta, Marco Radici, and Gunar Schnell. Investigations into the flavor dependence of partonic transverse momentum. *JHEP*, 11:194, 2013. arXiv:1309.3507, doi:10.1007/JHEP11(2013)194.
- [194] M. Anselmino, M. Boglione, J. O. Gonzalez Hernandez, S. Melis, and A. Prokudin. Unpolarised Transverse Momentum Dependent Distribution and Fragmentation Functions from SIDIS Multiplicities. *JHEP*, 04:005, 2014. arXiv:1312.6261, doi:10.1007/JHEP04(2014)005.
- [195] M. Anselmino, M. Boglione, U. D’Alesio, F. Murgia, and A. Prokudin. Study of the sign change of the Sivers function from STAR Collaboration W/Z production data. *JHEP*, 04:046, 2017. arXiv:1612.06413, doi:10.1007/JHEP04(2017)046.
- [196] J. Matouek. Weighted transverse spin asymmetries in 2015 COMPASS Drell-Yan data. *PoS, SPIN2018:038*, 2018. arXiv:1812.08505, doi:10.22323/1.346.0038.
- [197] M. Anselmino et al. Comparing extractions of Sivers functions. In *Transversity. Proceedings, Workshop, Como, Italy, September 7-10, 2005*, pages 236–243, 2005. arXiv:hep-ph/0511017, doi:10.1142/9789812773272\_0028.
- [198] M. Anselmino, M. Boglione, U. D’Alesio, A. Kotzinian, F. Murgia, and A. Prokudin. Extracting the Sivers function from polarized SIDIS data and making predictions. *Phys. Rev.*, D72:094007, 2005. [Erratum: *Phys. Rev.*D72,099903(2005)]. arXiv:hep-ph/0507181, doi:10.1103/PhysRevD.72.094007, 10.1103/PhysRevD.72.099903.
- [199] Werner Vogelsang and Feng Yuan. Single-transverse spin asymmetries: From DIS to hadronic collisions. *Phys. Rev.*, D72:054028, 2005. arXiv:hep-ph/0507266, doi:10.1103/PhysRevD.72.054028.
- [200] J. C. Collins, A. V. Efremov, K. Goeke, M. Grosse Perdekamp, S. Menzel, B. Meredith, A. Metz, and P. Schweitzer. Sivers effect in semi-inclusive deeply inelastic scattering and Drell-Yan. In *Transversity. Proceedings, Workshop, Como, Italy, September 7-10, 2005*, pages 212–219, 2005. arXiv:hep-ph/0510342, doi:10.1142/9789812773272\_0025.
- [201] M. Anselmino, M. Boglione, U. D’Alesio, A. Kotzinian, S. Melis, F. Murgia, A. Prokudin, and C. Turk. Sivers Effect for Pion and Kaon Production in Semi-Inclusive Deep Inelastic Scattering. *Eur. Phys. J.*, A39:89–100, 2009. arXiv:0805.2677, doi:10.1140/epja/i2008-10697-y.

- [202] Alessandro Bacchetta and Marco Radici. Constraining quark angular momentum through semi-inclusive measurements. *Phys. Rev. Lett.*, 107:212001, 2011. arXiv:1107.5755, doi:10.1103/PhysRevLett.107.212001.
- [203] M. Anselmino, M. Boglione, U. D’Alesio, F. Murgia, and A. Prokudin. Role of transverse momentum dependence of unpolarized parton distribution and fragmentation functions in the analysis of azimuthal spin asymmetries. *Phys. Rev.*, D98(9):094023, 2018. arXiv:1809.09500, doi:10.1103/PhysRevD.98.094023.
- [204] Matthias Burkardt. Sivers mechanism for gluons. *Phys. Rev.*, D69:091501, 2004. arXiv:hep-ph/0402014, doi:10.1103/PhysRevD.69.091501.
- [205] M. Anselmino, U. D’Alesio, S. Melis, and F. Murgia. Constraints on the gluon Sivers distribution via transverse single spin asymmetries at mid-rapidity in  $p^\uparrow p \rightarrow \pi^0 X$  processes at RHIC. *Phys. Rev.*, D74:094011, 2006. arXiv:hep-ph/0608211, doi:10.1103/PhysRevD.74.094011.
- [206] Stanley J. Brodsky and Susan Gardner. Evidence for the Absence of Gluon Orbital Angular Momentum in the Nucleon. *Phys. Lett.*, B643:22–28, 2006. arXiv:hep-ph/0608219, doi:10.1016/j.physletb.2006.10.024.
- [207] U. D’Alesio, F. Murgia, and C. Pisano. Towards a first estimate of the gluon Sivers function from  $A_N$  data in pp collisions at RHIC. *JHEP*, 09:119, 2015. arXiv:1506.03078, doi:10.1007/JHEP09(2015)119.
- [208] M. Anselmino, M. Boglione, U. D’Alesio, E. Leader, and F. Murgia. Accessing Sivers gluon distribution via transverse single spin asymmetries in  $p^\uparrow p \rightarrow D + X$  processes at RHIC. *Phys. Rev.*, D70:074025, 2004. arXiv:hep-ph/0407100, doi:10.1103/PhysRevD.70.074025.
- [209] Umberto D’Alesio, Francesco Murgia, Cristian Pisano, and Pieter Taels. Probing the gluon Sivers function in  $p^\uparrow p \rightarrow J/\psi X$  and  $p^\uparrow p \rightarrow D X$ . *Phys. Rev.*, D96(3):036011, 2017. arXiv:1705.04169, doi:10.1103/PhysRevD.96.036011.
- [210] Umberto D’Alesio, Francesco Murgia, Cristian Pisano, and Sangem Rajesh. Single-spin asymmetries in  $p^\uparrow p \rightarrow J/\psi + X$  within a TMD approach: role of the color octet mechanism. 2019. arXiv:1910.09640.
- [211] Umberto D’Alesio, Carlo Flore, Francesco Murgia, Cristian Pisano, and Pieter Taels. Unraveling the Gluon Sivers Function in Hadronic Collisions at RHIC. *Phys. Rev.*, D99(3):036013, 2019. arXiv:1811.02970, doi:10.1103/PhysRevD.99.036013.
- [212] Dennis Sivers. Single-Spin Observables and Orbital Structures in Hadronic Distributions. *Phys. Rev.*, D74:094008, 2006. arXiv:hep-ph/0609080, doi:10.1103/PhysRevD.74.094008.
- [213] Dennis Sivers. Chiral dynamics and single-spin asymmetries. In *Proceedings, XII Advanced Research Workshop on High Energy Spin Physics, DSPIN-07, Dubna, Russia, 3-7 Sep, 2007*, pages 161–165, 2007. arXiv:0711.3185.
- [214] M. Anselmino, M. Boglione, U. D’Alesio, S. Melis, F. Murgia, and A. Prokudin. New insight on the Sivers transverse momentum dependent distribution function. *J. Phys. Conf. Ser.*, 295:012062, 2011. arXiv:1012.3565, doi:10.1088/1742-6596/295/1/012062.
- [215] Jacques Soffer. Positivity constraints for spin dependent parton distributions. *Phys. Rev. Lett.*, 74:1292–1294, 1995. arXiv:hep-ph/9409254, doi:10.1103/PhysRevLett.74.1292.

- [216] Marco Radici, A. Courtoy, Alessandro Bacchetta, and Marco Guagnelli. Improved extraction of valence transversity distributions from inclusive dihadron production. *JHEP*, 05:123, 2015. arXiv:1503.03495, doi:10.1007/JHEP05(2015)123.
- [217] M. Alekseev et al. Collins and Sivers asymmetries for pions and kaons in muon-deuteron DIS. *Phys. Lett.*, B673:127–135, 2009. arXiv:0802.2160, doi:10.1016/j.physletb.2009.01.060.
- [218] Anna Martin. COMPASS results on Collins and Sivers asymmetries for charged hadrons. *Phys. Part. Nucl.*, 45:141–145, 2014. arXiv:1303.2076, doi:10.1134/S1063779614010079.
- [219] A. Bianconi, S. Boffi, R. Jakob, and M. Radici. Two hadron interference fragmentation functions. Part 1. General framework. *Phys. Rev.*, D62:034008, 2000. arXiv:hep-ph/9907475, doi:10.1103/PhysRevD.62.034008.
- [220] Alessandro Bacchetta, Aurore Courtoy, and Marco Radici. First glances at the transversity parton distribution through dihadron fragmentation functions. *Phys. Rev. Lett.*, 107:012001, 2011. arXiv:1104.3855, doi:10.1103/PhysRevLett.107.012001.
- [221] Alessandro Bacchetta, A. Courtoy, and Marco Radici. First extraction of valence transversities in a collinear framework. *JHEP*, 03:119, 2013. arXiv:1212.3568, doi:10.1007/JHEP03(2013)119.
- [222] A. Vossen et al. Observation of transverse polarization asymmetries of charged pion pairs in  $e^+e^-$  annihilation near  $\sqrt{s} = 10.58$  GeV. *Phys. Rev. Lett.*, 107:072004, 2011. arXiv:1104.2425, doi:10.1103/PhysRevLett.107.072004.
- [223] Marco Radici, Alessandro M. Ricci, Alessandro Bacchetta, and Asmita Mukherjee. Exploring universality of transversity in proton-proton collisions. *Phys. Rev.*, D94(3):034012, 2016. arXiv:1604.06585, doi:10.1103/PhysRevD.94.034012.
- [224] R. L. Jaffe and Xiang-Dong Ji. Chiral odd parton distributions and polarized Drell-Yan. *Phys. Rev. Lett.*, 67:552–555, 1991. doi:10.1103/PhysRevLett.67.552.
- [225] Tanmoy Bhattacharya, Vincenzo Cirigliano, Saul Cohen, Rajan Gupta, Huey-Wen Lin, and Boram Yoon. Axial, Scalar and Tensor Charges of the Nucleon from 2+1+1-flavor Lattice QCD. *Phys. Rev.*, D94(5):054508, 2016. arXiv:1606.07049, doi:10.1103/PhysRevD.94.054508.
- [226] C. Alexandrou et al. Nucleon scalar and tensor charges using lattice QCD simulations at the physical value of the pion mass. *Phys. Rev.*, D95(11):114514, 2017. [erratum: *Phys. Rev.* D96,no.9,099906(2017)]. arXiv:1703.08788, doi:10.1103/PhysRevD.96.099906, 10.1103/PhysRevD.95.114514.
- [227] Rajan Gupta, Boram Yoon, Tanmoy Bhattacharya, Vincenzo Cirigliano, Yong-Chull Jang, and Huey-Wen Lin. Flavor diagonal tensor charges of the nucleon from (2+1+1)-flavor lattice QCD. *Phys. Rev.*, D98(9):091501, 2018. arXiv:1808.07597, doi:10.1103/PhysRevD.98.091501.
- [228] Marco Radici. First extraction of transversity from data on lepton-hadron scattering and hadronic collisions. *PoS*, SPIN2018:044, 2019. arXiv:1810.00496, doi:10.22323/1.346.0044.
- [229] Marco Radici. Update on phenomenological extraction of the proton tensor charge. *PoS*, DIS2019:199, 2019. doi:10.22323/1.352.0199.
- [230] Umberto D’Alesio, Carlo Flore, and Alexei Prokudin. Role of the Soffer bound in determination of transversity and the tensor charge. 2020. arXiv:2001.01573.

- [231] J. Benel, A. Courtoy, and R. Ferro-Hernandez. Constrained fit of the valence transversity distributions from dihadron production. 2019. [arXiv:1912.03289](#).
- [232] Justin Cammarota, Leonard Gamberg, Zhong-Bo Kang, Joshua A. Miller, Daniel Pitonyak, Alexei Prokudin, Ted C. Rogers, and Nobuo Sato. The origin of single transverse-spin asymmetries in high-energy collisions. 2020. [arXiv:2002.08384](#).
- [233] Vincenzo Barone et al. Antiproton-proton scattering experiments with polarization. 2005. [arXiv:hep-ex/0505054](#).
- [234] Matthias Burkardt. Impact parameter dependent parton distributions and off forward parton distributions for  $\zeta \rightarrow 0$ . *Phys. Rev.*, D62:071503, 2000. [Erratum: *Phys. Rev.*D66,119903(2002)]. [arXiv:hep-ph/0005108](#), [doi:10.1103/PhysRevD.62.071503](#), [10.1103/PhysRevD.66.119903](#).
- [235] Markus Diehl. Introduction to GPDs and TMDs. *Eur. Phys. J.*, A52(6):149, 2016. [arXiv:1512.01328](#), [doi:10.1140/epja/i2016-16149-3](#).
- [236] Eugene P. Wigner. On the quantum correction for thermodynamic equilibrium. *Phys. Rev.*, 40:749–760, 1932. [doi:10.1103/PhysRev.40.749](#).
- [237] N. L. Balazs and B. K. Jennings. Wigner’s Function and Other Distribution Functions in Mock Phase Spaces. *Phys. Rept.*, 104:347, 1984. [doi:10.1016/0370-1573\(84\)90151-0](#).
- [238] M. Hillery, R. F. O’Connell, M. O. Scully, and Eugene P. Wigner. Distribution functions in physics: Fundamentals. *Phys. Rept.*, 106:121–167, 1984. [doi:10.1016/0370-1573\(84\)90160-1](#).
- [239] H. W. Lee. *Phys. Rep.*, 259:147, 1985.
- [240] K. Vogel and H. Risken. Determination of quasiprobability distributions in terms of probability distributions for the rotated quadrature phase. *Phys. Rev.*, A40:2847–2849, 1989. [doi:10.1103/PhysRevA.40.2847](#).
- [241] D. T. Smithey, M. Beck, M. G. Raymer, and A. Faridani. Measurement of the Wigner distribution and the density matrix of a light mode using optical homodyne tomography: Application to squeezed states and the vacuum. *Phys. Rev. Lett.*, 70:1244–1247, 1993. [doi:10.1103/PhysRevLett.70.1244](#).
- [242] K. Banaszek, C. Radzewicz, K. Wodkiewicz, and J. S. Krasinski. Direct measurement of the Wigner function by photon counting. *Phys. Rev.*, A60:674–677, 1999. [arXiv:quant-ph/9903027](#), [doi:10.1103/PhysRevA.60.674](#).
- [243] Yoshikazu Hagiwara and Yoshitaka Hatta. Use of the Husimi distribution for nucleon tomography. *Nucl. Phys.*, A940:158–166, 2015. [arXiv:1412.4591](#), [doi:10.1016/j.nuclphysa.2015.04.005](#).
- [244] Xiang-dong Ji. Viewing the proton through ‘color’ filters. *Phys. Rev. Lett.*, 91:062001, 2003. [arXiv:hep-ph/0304037](#), [doi:10.1103/PhysRevLett.91.062001](#).
- [245] Andrei V. Belitsky, Xiang-dong Ji, and Feng Yuan. Quark imaging in the proton via quantum phase space distributions. *Phys. Rev.*, D69:074014, 2004. [arXiv:hep-ph/0307383](#), [doi:10.1103/PhysRevD.69.074014](#).
- [246] M. Diehl. Generalized parton distributions in impact parameter space. *Eur. Phys. J.*, C25:223–232, 2002. [Erratum: *Eur. Phys. J.*C31,277(2003)]. [arXiv:hep-ph/0205208](#), [doi:10.1007/s10052-002-1016-9](#).

- [247] S. J. Brodsky, D. Chakrabarti, A. Harindranath, A. Mukherjee, and J. P. Vary. Hadron optics in three-dimensional invariant coordinate space from deeply virtual compton scattering. *Phys. Rev.*, D75:014003, 2007. [arXiv:hep-ph/0611159](#), [doi:10.1103/PhysRevD.75.014003](#).
- [248] S. J. Brodsky, D. Chakrabarti, A. Harindranath, A. Mukherjee, and J. P. Vary. Hadron optics: Diffraction patterns in deeply virtual Compton scattering. *Phys. Lett.*, B641:440–446, 2006. [arXiv:hep-ph/0604262](#), [doi:10.1016/j.physletb.2006.08.061](#).
- [249] C. Lorcé and B. Pasquini. Quark Wigner Distributions and Orbital Angular Momentum. *Phys. Rev.*, D84:014015, 2011. [arXiv:1106.0139](#), [doi:10.1103/PhysRevD.84.014015](#).
- [250] Stephan Meissner, Andreas Metz, and Marc Schlegel. Generalized parton correlation functions for a spin-1/2 hadron. *JHEP*, 08:056, 2009. [arXiv:0906.5323](#), [doi:10.1088/1126-6708/2009/08/056](#).
- [251] C. Lorcé and B. Pasquini. Structure analysis of the generalized correlator of quark and gluon for a spin-1/2 target. *JHEP*, 09:138, 2013. [arXiv:1307.4497](#), [doi:10.1007/JHEP09\(2013\)138](#).
- [252] Alan D. Martin, M. G. Ryskin, and T. Teubner.  $Q^{*2}$  dependence of diffractive vector meson electroproduction. *Phys. Rev.*, D62:014022, 2000. [arXiv:hep-ph/9912551](#), [doi:10.1103/PhysRevD.62.014022](#).
- [253] Valery A. Khoze, Alan D. Martin, and M. G. Ryskin. Can the Higgs be seen in rapidity gap events at the Tevatron or the LHC? *Eur. Phys. J.*, C14:525–534, 2000. [arXiv:hep-ph/0002072](#), [doi:10.1007/s100520000359](#).
- [254] Tianbo Liu and Bo-Qiang Ma. Quark Wigner distributions in a light-cone spectator model. *Phys. Rev.*, D91:034019, 2015. [arXiv:1501.07690](#), [doi:10.1103/PhysRevD.91.034019](#).
- [255] Cedric Lorcé, Barbara Pasquini, Xiaonu Xiong, and Feng Yuan. The quark orbital angular momentum from Wigner distributions and light-cone wave functions. *Phys. Rev.*, D85:114006, 2012. [arXiv:1111.4827](#), [doi:10.1103/PhysRevD.85.114006](#).
- [256] Yoshitaka Hatta. Notes on the orbital angular momentum of quarks in the nucleon. *Phys. Lett.*, B708:186–190, 2012. [arXiv:1111.3547](#), [doi:10.1016/j.physletb.2012.01.024](#).
- [257] E. Leader and C. Lorcé. The angular momentum controversy: What’s it all about and does it matter? *Phys. Rept.*, 541(3):163–248, 2014. [arXiv:1309.4235](#), [doi:10.1016/j.physrep.2014.02.010](#).
- [258] R. L. Jaffe and Aneesh Manohar. The G(1) Problem: Fact and Fantasy on the Spin of the Proton. *Nucl. Phys.*, B337:509–546, 1990. [doi:10.1016/0550-3213\(90\)90506-9](#).
- [259] Xiang-Dong Ji. Deeply virtual Compton scattering. *Phys. Rev.*, D55:7114–7125, 1997. [arXiv:hep-ph/9609381](#), [doi:10.1103/PhysRevD.55.7114](#).
- [260] Masashi Wakamatsu. Is gauge-invariant complete decomposition of the nucleon spin possible? *Int. J. Mod. Phys.*, A29:1430012, 2014. [arXiv:1402.4193](#), [doi:10.1142/S0217751X14300129](#).
- [261] P. Hagler, A. Mukherjee, and A. Schafer. Quark orbital angular momentum in the Wandzura-Wilczek approximation. *Phys. Lett.*, B582:55–63, 2004. [arXiv:hep-ph/0310136](#), [doi:10.1016/j.physletb.2003.11.076](#).

- [262] C. Lorcé and B. Pasquini. Multipole decomposition of the nucleon transverse phase space. *Phys. Rev.*, D93(3):034040, 2016. [arXiv:1512.06744](#), [doi:10.1103/PhysRevD.93.034040](#).
- [263] D. Chakrabarti, T. Maji, C. Mondal, and A. Mukherjee. Quark Wigner distributions and spin-spin correlations. *Phys. Rev.*, D95(7):074028, 2017. [arXiv:1701.08551](#), [doi:10.1103/PhysRevD.95.074028](#).
- [264] D. Chakrabarti, T. Maji, C. Mondal, and A. Mukherjee. Wigner distributions and orbital angular momentum of a proton. *Eur. Phys. J.*, C76(7):409, 2016. [arXiv:1601.03217](#), [doi:10.1140/epjc/s10052-016-4258-7](#).
- [265] A. Courtoy and A. S. Miramontes. Quark Orbital Angular Momentum in the MIT Bag Model. *Phys. Rev.*, D95(1):014027, 2017. [arXiv:1611.03375](#), [doi:10.1103/PhysRevD.95.014027](#).
- [266] Yoshikazu Hagiwara, Yoshitaka Hatta, and Takahiro Ueda. Wigner, Husimi, and generalized transverse momentum dependent distributions in the color glass condensate. *Phys. Rev.*, D94(9):094036, 2016. [arXiv:1609.05773](#), [doi:10.1103/PhysRevD.94.094036](#).
- [267] Asmita Mukherjee, Sreeraj Nair, and Vikash Kumar Ojha. Quark Wigner Distributions and Orbital Angular Momentum in Light-front Dressed Quark Model. *Phys. Rev.*, D90(1):014024, 2014. [arXiv:1403.6233](#), [doi:10.1103/PhysRevD.90.014024](#).
- [268] Asmita Mukherjee, Sreeraj Nair, and Vikash Kumar Ojha. Wigner distributions for gluons in a light-front dressed quark model. *Phys. Rev.*, D91(5):054018, 2015. [arXiv:1501.03728](#), [doi:10.1103/PhysRevD.91.054018](#).
- [269] Jai More, Asmita Mukherjee, and Sreeraj Nair. Quark Wigner Distributions Using Light-Front Wave Functions. *Phys. Rev.*, D95(7):074039, 2017. [arXiv:1701.00339](#), [doi:10.1103/PhysRevD.95.074039](#).
- [270] Jai More, Asmita Mukherjee, and Sreeraj Nair. Wigner Distributions For Gluons. *Eur. Phys. J.*, C78(5):389, 2018. [arXiv:1709.00943](#), [doi:10.1140/epjc/s10052-018-5858-1](#).
- [271] K. Kanazawa, C. Lorcé, A. Metz, B. Pasquini, and M. Schlegel. Twist-2 generalized transverse-momentum dependent parton distributions and the spin/orbital structure of the nucleon. *Phys. Rev.*, D90(1):014028, 2014. [arXiv:1403.5226](#), [doi:10.1103/PhysRevD.90.014028](#).
- [272] Dipankar Chakrabarti, Narindar Kumar, Tanmay Maji, and Asmita Mukherjee. Sivers and Boer-Mulders GTMDs in Light-front Holographic Quark-diquark Model. 2019. [arXiv:1902.07051](#).
- [273] Niklas Mueller and Raju Venugopalan. Constructing phase space distributions with internal symmetries. *Phys. Rev.*, D99(5):056003, 2019. [arXiv:1901.10492](#), [doi:10.1103/PhysRevD.99.056003](#).
- [274] Shohini Bhattacharya, Andreas Metz, and Jian Zhou. Generalized TMDs and the exclusive double Drell-Yan process. *Phys. Lett.*, B771:396–400, 2017. [arXiv:1702.04387](#), [doi:10.1016/j.physletb.2017.05.081](#).
- [275] Shohini Bhattacharya, Andreas Metz, Vikash Kumar Ojha, Jeng-Yuan Tsai, and Jian Zhou. Exclusive double quarkonium production and generalized TMDs of gluons. 2018. [arXiv:1802.10550](#).

- [276] Yoshitaka Hatta, Bo-Wen Xiao, and Feng Yuan. Probing the Small- $x$  Gluon Tomography in Correlated Hard Diffractive Dijet Production in Deep Inelastic Scattering. *Phys. Rev. Lett.*, 116(20):202301, 2016. [arXiv:1601.01585](#), [doi:10.1103/PhysRevLett.116.202301](#).
- [277] Yoshitaka Hatta, Yuya Nakagawa, Feng Yuan, Yong Zhao, and Bowen Xiao. Gluon orbital angular momentum at small- $x$ . *Phys. Rev.*, D95(11):114032, 2017. [arXiv:1612.02445](#), [doi:10.1103/PhysRevD.95.114032](#).
- [278] Xiangdong Ji, Feng Yuan, and Yong Zhao. Hunting the Gluon Orbital Angular Momentum at the Electron-Ion Collider. *Phys. Rev. Lett.*, 118(19):192004, 2017. [arXiv:1612.02438](#), [doi:10.1103/PhysRevLett.118.192004](#).
- [279] Yoshikazu Hagiwara, Yoshitaka Hatta, Roman Pasechnik, Marek Tasevsky, and Oleg Teryaev. Accessing the gluon Wigner distribution in ultraperipheral  $pA$  collisions. *Phys. Rev.*, D96(3):034009, 2017. [arXiv:1706.01765](#), [doi:10.1103/PhysRevD.96.034009](#).